



ATLANTIC ZONE MONITORING PROGRAM

AZMP Bulletin PMZA

PROGRAMME DE MONITORAGE DE LA ZONE ATLANTIQUE

ISSN 1916-6362

http://www.meds-sdmm.dfo-mpo.gc.ca/zmp/main_zmp_e.html

Contents / Table des matières

The Atlantic Zone Monitoring Program / Le Programme de Monitorage de la Zone Atlantique	p.2
A Message From the Editors / Un message de la rédaction.....	p.2
Environmental Review / Revue Environnementale .	p.3
Physical, Chemical and Biological Status of the Labrador Sea.....	p.12
Seasonal Cycles of Calanus finmarchicus Abundance at Fixed Time-Series Stations on the Scotian and Newfoundland Shelves (1999–2006)	p.17
Understanding Copepod Life History Patterns Through Inter-Regional Comparison of AZMP Zooplankton Data	p.21
Quality Control of Bottle Data at Maurice Lamontagne Institute / Contrôle de qualité des données bouteilles à l'Institut Maurice-Lamontagne	p.27
Estimation of Mixed Layer Depth at the AZMP Fixed Stations	p.37
A Preliminary Assessment of the Performance of an Automated System for the Analysis of Zooplankton Samples from the Gulf of St. Lawrence, Northwest Atlantic.....	p.42
Temperature, Salinity and Oxygen Measurements From Argo Profiling Floats in the Slope Water Region.	p.47
Monitoring Seabirds at Sea in Eastern Canada ..	p.52
AZMP Personnel / Personnel du PMZA	p.59
Publications	p.59

Edited by / Rédigé par

Patrick Ouellet¹, Laure Devine¹, & Brian Petrie²
 Layout by / Mis en page par Claude Nozères¹
¹Institut Maurice-Lamontagne
 850, route de la Mer, Mont-Joli, QC, G5H 3Z4
²Bedford Institute of Oceanography
 Box 1006, Dartmouth, NS, B2Y 4A2
 BulletinPMZA-AZMP@dfo-mpo.gc.ca

Le Bulletin du PMZA

Le bulletin annuel du PMZA publie des articles anglais, français ou bilingues afin de fournir aux océanographes et aux chercheurs des pêches, aux gestionnaires de l'habitat et de l'environnement, ainsi qu'au public en général les plus récentes informations concernant le Programme de Monitorage de la Zone Atlantique (PMZA). Le bulletin présente une revue annuelle des conditions océanographiques générales pour la région nord-ouest de l'Atlantique, incluant le golfe du Saint-Laurent, ainsi que de l'information reliée au PMZA concernant des événements particuliers, des études ou des activités qui ont eu lieu au cours de l'année précédente.

The AZMP Bulletin

The AZMP annual bulletin publishes English, French, and bilingual articles to provide oceanographers and fisheries scientists, habitat and environment managers, and the general public with the latest information concerning the Atlantic Zone Monitoring Program (AZMP). The bulletin presents an annual review of the general oceanographic conditions in the Northwest Atlantic region, including the Gulf of St. Lawrence, as well as AZMP-related information concerning particular events, studies, or activities that took place during the previous year.

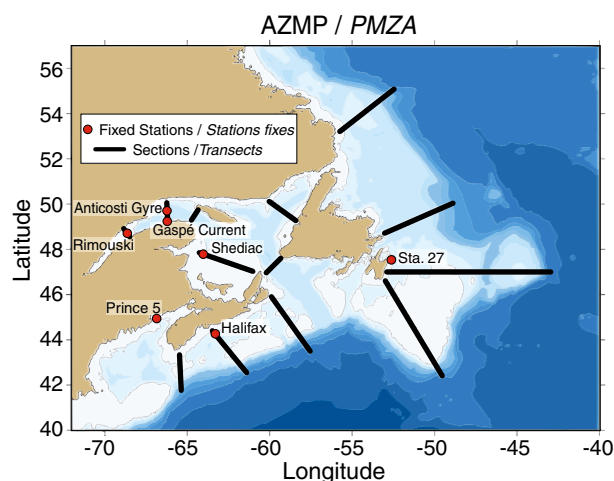


Fig. 1 Locations of sections and fixed stations.

Position des transects et des stations fixes.

The Atlantic Zone Monitoring Program

The AZMP was implemented in 1998 with the aim of collecting and analyzing the biological, chemical, and physical field data that are necessary to (1) characterize and understand the causes of oceanic variability at the seasonal, interannual, and decadal scales, (2) provide multidisciplinary data sets that can be used to establish relationships among the biological, chemical, and physical variables, and (3) provide adequate data to support the sound development of ocean activities. AZMP involves the Gulf, Québec, Maritimes, and Newfoundland regions of DFO. Its sampling strategy is based on (1) seasonal and opportunistic sampling along sections to quantify the oceanographic variability in the Canadian NW Atlantic shelf region, (2) higher-frequency temporal sampling at more accessible fixed sites to monitor the shorter time scale dynamics in representative areas, (3) fish survey and remote sensing data to provide broader spatial coverage and a context to interpret other data, and (4) data from other existing monitoring programs such as CPR (Continuous Plankton Recorder) lines, Sea Level Network, nearshore Long-Term Temperature Monitoring, Toxic Algae monitoring, or from other external organizations (e.g., winds and air temperatures from Environment Canada) to complement AZMP data.

The key element of the AZMP sampling strategy is the oceanographic sampling at fixed stations and along sections. The fixed stations are occupied about every two weeks, conditions permitting, and the sections are sampled from one to three times during the year. The location of the regular sections and the fixed stations are shown in Figure 1. Temperature, salinity, fluorescence, oxygen, chl *a*, nitrates, silicates, and phosphates are measured, and phytoplankton and zooplankton samples are collected. These measurements are carried out following well-established common protocols.

A Message From the Editors

In 2001, members of the Atlantic Zone Monitoring Program (AZMP) published the first annual bulletin. Since then, many articles have been published, from short descriptions of new technologies to sophisticated scientific analyses using monitoring data.

With this seventh issue, we think it is time to evaluate to what degree the objectives have been met, particularly in providing a broad description of the oceanographic environment, and demonstrating the role of the monitoring activities in furthering our understanding of the ecosystem. We would like feedback from our readers and therefore invite your comments (e-mail address below). Are the type, scientific content, and length of the articles and reviews appropriate? Are there other issues that could be addressed or other aspects of the bulletin that merit change?

In addition, although the editorial team strives to assure the quality of the information presented in each issue of the bulletin, we remind our readers that it is still essential to seek out the authors' permission before using or citing information or specific contents from their articles.

We hope that you find the bulletin useful and will appreciate receiving your suggestions that will lead to its improvement.

BulletinPMZA-AZMP@dfo-mpo.gc.ca

Le Programme de Monitorage de la Zone Atlantique

Le PMZA a été mis en œuvre en 1998 et vise à collecter et analyser l'information biologique, chimique et physique recueillie sur le terrain afin de (1) caractériser et comprendre les causes de la variabilité océanique aux échelles saisonnières, inter-annuelles et décennales, (2) fournir les ensembles de données pluridisciplinaires qui sont nécessaires pour établir des relations entre les variables biologiques, chimiques et physiques et (3) fournir les données pour le développement durable des activités océaniques. Le PMZA implique les régions du Golfe, du Québec, des Maritimes et de Terre-Neuve du MPO. Sa stratégie d'échantillonnage est fondée sur (1) l'échantillonnage saisonnier et opportuniste le long de transects afin de quantifier la variabilité biologique, chimique et physique de l'environnement, (2) l'échantillonnage à plus haute fréquence à des stations fixes plus accessibles pour moniter la dynamique à plus fine échelle de temps dans des régions représentatives, (3) l'utilisation des données provenant des missions d'évaluation de stocks et de la télédétection pour fournir une couverture spatiale plus vaste et le contexte pour l'interprétation des autres données et (4) l'utilisation de données provenant d'autres programmes de monitorage comme les transects CPR (*Continuous Plankton Recorder*), les réseaux côtiers de niveau d'eau et de température, le monitroge des algues toxiques, ou provenant d'autres organismes externes (ex. vents et température de l'air de Environnement Canada) pour compléter les données du PMZA.

L'élément clé de la stratégie d'échantillonnage est la collecte de mesures océanographiques aux stations fixes et le long de transects. Les stations fixes sont occupées à toutes les deux semaines, dépendant des conditions, et les sections sont échantillonées de 1 à 3 fois durant l'année. La localisation des transects et des stations fixes est illustrée à la Figure 1. L'échantillonnage régulier comprend des mesures de température, salinité, fluorescence, oxygène, chl *a*, nitrates, silicates et phosphates, ainsi que la collecte d'échantillons de phytoplancton et de zooplancton. Ces mesures sont effectuées suivant des protocoles communs bien établis.

Un message de la rédaction

En 2001, les membres du Programme de Monitorage de la Zone Atlantique (PMZA) publiaient un premier bulletin annuel. Depuis, plusieurs articles ont paru dans le bulletin, allant de brèves descriptions de nouvelles technologies à des analyses scientifiques sophistiquées produites à partir des données de monitorage.

Dans ce septième numéro nous pensons qu'il est temps d'évaluer jusqu'à quel point les objectifs ont été atteints, en particulier de fournir une description générale de l'état de l'environnement océanographique, ainsi que le rôle du monitroge pour notre compréhension de l'écosystème. Nous désirons connaître l'opinion de nos lecteurs et nous vous invitons à nous faire parvenir vos commentaires (voir l'adresse courriel plus bas). Est-ce que le genre, le contenu scientifique et la longueur des articles et des revues sont appropriés ? Est-ce qu'il y a d'autres sujets qui pourraient être traités ou d'autres aspects du bulletin qui devraient être modifiés ?

De plus, bien que l'équipe de rédaction s'efforce d'assurer la qualité de l'information présentée dans chaque numéro, nous tenons à rappeler qu'il demeure essentiel de rechercher la permission des auteurs avant d'utiliser ou de citer l'information ou des faits spécifiques contenus dans leurs articles.

Nous espérons que vous trouvez utile notre bulletin et nous aimerions recevoir vos suggestions pour améliorer son contenu.

BulletinPMZA-AZMP@dfo-mpo.gc.ca

Physical, Chemical and Biological Status of the Environment¹

État de l'environnement physique, chimique et biologique¹

AZMP Monitoring Group

Northwest Atlantic Fisheries Centre, Box 5667, St. John's, NL, A1C 5X1

Institut Maurice-Lamontagne, B.P. 1000, Mont-Joli, QC, G5H 3Z4

Bedford Institute of Oceanography, Box 1006, Dartmouth, NS, B2Y 4A2

Integrated Science Data Management, 200 Kent St., Ottawa, ON, K1A 0E6

Michel.Mitchell@mar.dfo-mpo.gc.ca (AZMP Chairman / Président PMZA)

Physical Environment

Cold (<0°C) surface water prevailed over the Labrador and Newfoundland shelves, the Gulf of St. Lawrence, and the inshore half of the Scotian Shelf in late winter 2007 (Fig. 1A). The offshore branch of the Labrador Current on the eastern edge of the Grand Banks is clearly indicated as a stream of cold water; the inshore branch is seen in Avalon Channel. Cold water and some ice from the Gulf of St. Lawrence mark

Environnement physique

L'eau froide (<0°C) dominait en surface à la fin de l'hiver 2007 sur les plateaux du Labrador et de Terre-Neuve, dans le golfe du Saint-Laurent et sur la portion côtière du plateau Néo-Écossais (Fig. 1A). La branche hauturière du courant du Labrador sur le bord est des Grands Bancs est clairement identifiée comme un écoulement d'eau froide, la branche côtière se situant au dessus du chenal Avalon. De l'eau froide et un peu de glace

provenant du golfe du Saint-Laurent identifient le courant de la Nouvelle-Écosse entre le détroit de Cabot et le sud-ouest de la Nouvelle-Écosse. Des températures chaudes (~20°C) en surface sont en évidence en août dans le sud du golfe du Saint-Laurent (Fig. 1B), tout comme les eaux froides du courant du Labrador au large de la marge est du Grand Banc et vers le nord au large du Labrador, les zones de remontée des eaux au large du sud-ouest de la Nouvelle-Écosse, à la tête du chenal Laurentien et le long de la Basse-Côte-Nord dans le golfe du Saint-Laurent, et les eaux du mélange maréal sur le banc Georges.

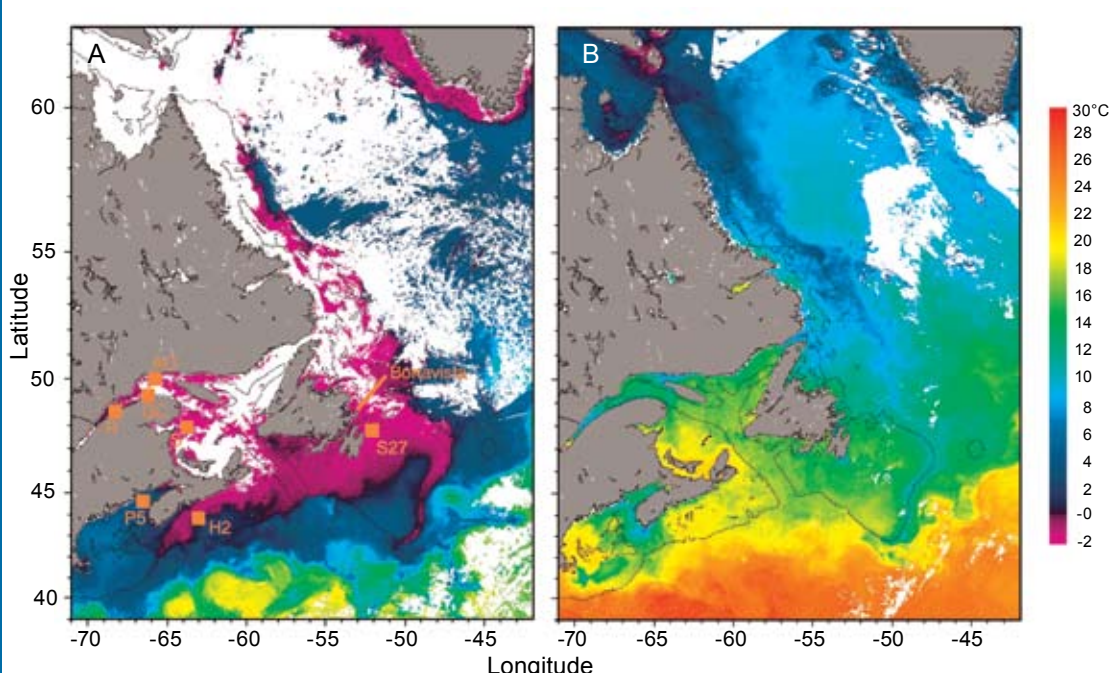


Fig. 1 Sea-surface temperature in the AZMP region during (A) March and (B) August 2007. The locations of fixed stations (squares; Rimouski [R], Anticosti Gyre [AG], Gaspé Current [GC], Sheddac Valley [S], Station 27 [S27], Halifax 2 [H2], Prince 5 [P5]) and the Bonavista section (line) are shown. White areas indicate sea ice or clouds.

Température à la surface de la mer dans la région couverte par le PMZA en (A) mars et (B) août 2007. Les positions des stations fixes (carrés : Rimouski [R], gyre Anticosti [AG], courant de Gaspé [GC], vallée de Sheddac [S], Station 27 [S27], Halifax 2 [H2], Prince 5 [P5]) et de la section Bonavista (ligne) sont illustrées. Les zones blanches indiquent la présence de glace ou de nuages.

the Nova Scotia Current from Cabot Strait to SW Nova Scotia. Warm surface temperatures (~20°C) are evident in the southern Gulf of St. Lawrence in August (Fig. 1B), as are the cooler waters of the Labrador Current off the eastern edge of Grand Bank and northward off the coast of Labrador, the upwelling zones off SW Nova Scotia, at the head of Laurentian Channel

élevés record observés en 2006. Cette diminution a ramené les températures près de la normale dans la plupart des secteurs en 2007 à l'exception des températures au-dessus de la normale au centre et au nord du plateau du Labrador (de 0,8°C), du Grand Banc (de 1°C) et à l'est et au sud du golfe du Saint-Laurent (de 0,5°C). Des températures de surface de

¹ The environmental overviews are presented in greater detail as research documents and science advisory reports available at:

http://www.dfo-mpo.gc.ca/csas/csas/Publications/Pub_Index_e.htm

¹ Les revues environnementales sont présentées plus en détail dans les documents de recherche et les avis scientifiques disponibles sur le site : http://www.dfo-mpo.gc.ca/csas/csas/Publications/Pub_Index_f.htm

and along the lower north shore of the Gulf of St. Lawrence, and the tidally mixed waters over Georges Bank.

In 2007, there was an almost uniform decrease of the annual average sea-surface temperature by $\sim 1^{\circ}\text{C}$ from Hudson Strait to the Gulf of Maine, including the Gulf of St. Lawrence, from record highs observed in 2006. This decrease led to near-normal temperatures in most areas during 2007 except for above-normal values on the northern and central Labrador Shelf (by 0.8°C), the Grand Bank (by 1°C), and the eastern and southern Gulf of St. Lawrence (by 0.5°C); lower-than-normal annual SST prevailed on the western Scotian Shelf and Georges Bank (by 0.6°C).

A number of atmospheric (air temperature, the North Atlantic Oscillation [NAO], freshwater runoff at Québec City), ice, and oceanographic variables are summarized as time series (1980–2007) in matrix form in Figure 2. When possible, the variables are displayed as differences (anomalies) relative to 1971–2000 average values; furthermore, because these series have different units ($^{\circ}\text{C}$, m^3 , m^2 , etc.), each anomaly time series is normalized by dividing by its standard deviation (SD), which is also calculated using data from 1971–2000. This allows a more direct comparison of the various series. Missing data are represented by grey cells, values within 0.5 SD of the average as white cells, and conditions corresponding to warmer than normal (higher temperatures, reduced ice volumes, reduced cold water volumes or areas, negative NAO index) by more than 0.5 SD as red cells, with more intense reds corresponding to increasingly warmer conditions. Similarly, blue represents colder-than-normal conditions. Higher-than-normal freshwater inflow and stratification anomalies are shown as red but are not necessarily indicative of warmer-than-normal conditions.

Air temperatures are an indication of the amount of heat that can be transferred from the atmosphere to the ocean. The air temperature pattern across the region is highly coherent, generally cooling from the early 1980s to 1993–94, followed by a warm period marked by strong peaks in 1999 and 2006. In 2007, temperatures were above normal at Cartwright and the Îles de la Madeleine and within the normal range (i.e., within 0.5 SD of the long-term mean) at the other four locations.

Freshwater runoff in the Gulf of St. Lawrence, particularly within the St. Lawrence Estuary, strongly influences the circulation, salinity, and stratification (and hence upper-layer temperatures) in the Gulf and, through the Nova Scotia Current, on the Scotian Shelf. For example, the average 0–20 m salinity in the Magdalen Shallows for the low runoff period of 1999–2007 is ~ 0.5 more than the average for high runoff years in the 1970s, 80s, and 90s. This represents approximately an extra 17 km^3 of freshwater in the upper 20 m of the Shallows. In fact, during the past 16 of 21 years, freshwater inflow at Québec City has been below normal by more than 0.5 SD; in 2007 the inflow was substantially below normal (by 1.5 SD) but higher than the record low conditions observed from 1962–65 (2.5 to 3.1 SD below normal).

The NAO is an index of the dominant atmospheric forcing over the North Atlantic Ocean. It affects winds, air tempera-

0.6 $^{\circ}\text{C}$ sous la moyenne annuelle dominaient à l'ouest du plateau Néo-Écossais et sur le banc Georges.

Plusieurs variables atmosphériques (température de l'air, oscillation nord Atlantique [NAO], débit d'eau douce à Québec), océanographiques et relatives à la glace sont présentées sous forme de séries temporelles (1980 à 2007) dans un tableau synoptique (Fig. 2). Lorsque possible, les variables sont présentées en tant que différences (anomalies) relatives par rapport aux moyennes de la période 1971 à 2000. De plus, comme les séries ont des unités différentes ($^{\circ}\text{C}$, m^3 , m^2 , etc.), chaque série temporelle d'anomalies a été réduite par division par son écart-type calculé sur les données de la période 1971 à 2000. Ceci afin de permettre une comparaison directe des différentes séries. Une donnée manquante est indiquée par une cellule grise, les valeurs entre 0 et 0,5 écart-type de la moyenne sont représentées par des cellules blanches, alors que les conditions plus chaudes que la normale (températures élevées, volumes de glace réduits, surfaces ou volumes d'eau froide réduits, un indice NAO négatif) par plus de 0,5 écart-type sont en rouge, avec une gamme d'intensités correspondant à des conditions de réchauffement croissantes. De manière semblable, les tons de bleu représentent des conditions plus froides que la normale. Les anomalies du débit d'eau douce et de stratification plus élevées que la normale sont en rouge mais elles n'indiquent pas nécessairement des conditions plus chaudes que la normale.

Les températures de l'air sont une indication de la quantité de chaleur qui peut être transmise de l'atmosphère vers l'océan. Les températures de l'air montrent une image cohérente sur toute la région, un refroidissement général entre le début des années 1980 jusqu'en 1993–94, suivi d'une période de réchauffement marquée par des sommets élevés en 1999 et 2006. En 2007, les températures étaient au-dessus de la normale à Cartwright et aux îles de la Madeleine et normales (soit jusqu'à 0,5 écart-type de la moyenne à long terme) aux quatre autres localités.

Le débit d'eau douce dans le golfe du Saint-Laurent, en particulier dans l'estuaire du Saint-Laurent, influence fortement la circulation, la salinité et la stratification (donc les températures dans les couches supérieures) dans le golfe et, par le courant de la Nouvelle-Écosse, sur le plateau Néo-Écossais. Par exemple, la salinité moyenne entre 0 et 20 m sur le plateau madelinien pour la période de faibles débits de 1999 à 2007 est supérieure de $\sim 0,5$ unité par rapport à la moyenne des années de forts débits des décennies 1970, 1980 et 1990. Cela représente approximativement un surplus de 17 km^3 d'eau douce dans les 20 m supérieurs du plateau. En fait, pour 16 des 21 dernières années, le débit d'eau douce à Québec a été sous la normale par plus de 0,5 écart-type. En 2007, le débit a été de beaucoup sous la normale (de 1,5 écart-types), mais plus élevé que les basses conditions record observées de 1962 à 1965 (de 2,5 à 3,1 écart-types sous la normale).

Le NAO est un indice des forces atmosphériques dominantes sur l'océan Atlantique Nord. Il influence les vents, les températures de l'air, les précipitations et les caractéristiques hydrographiques de la côte est canadienne, soit directement ou par le biais des courants océaniques. Les effets directs se font sentir surtout sur les eaux de la mer du Labrador et des plateaux du Labrador et de Terre-Neuve où un NAO négatif

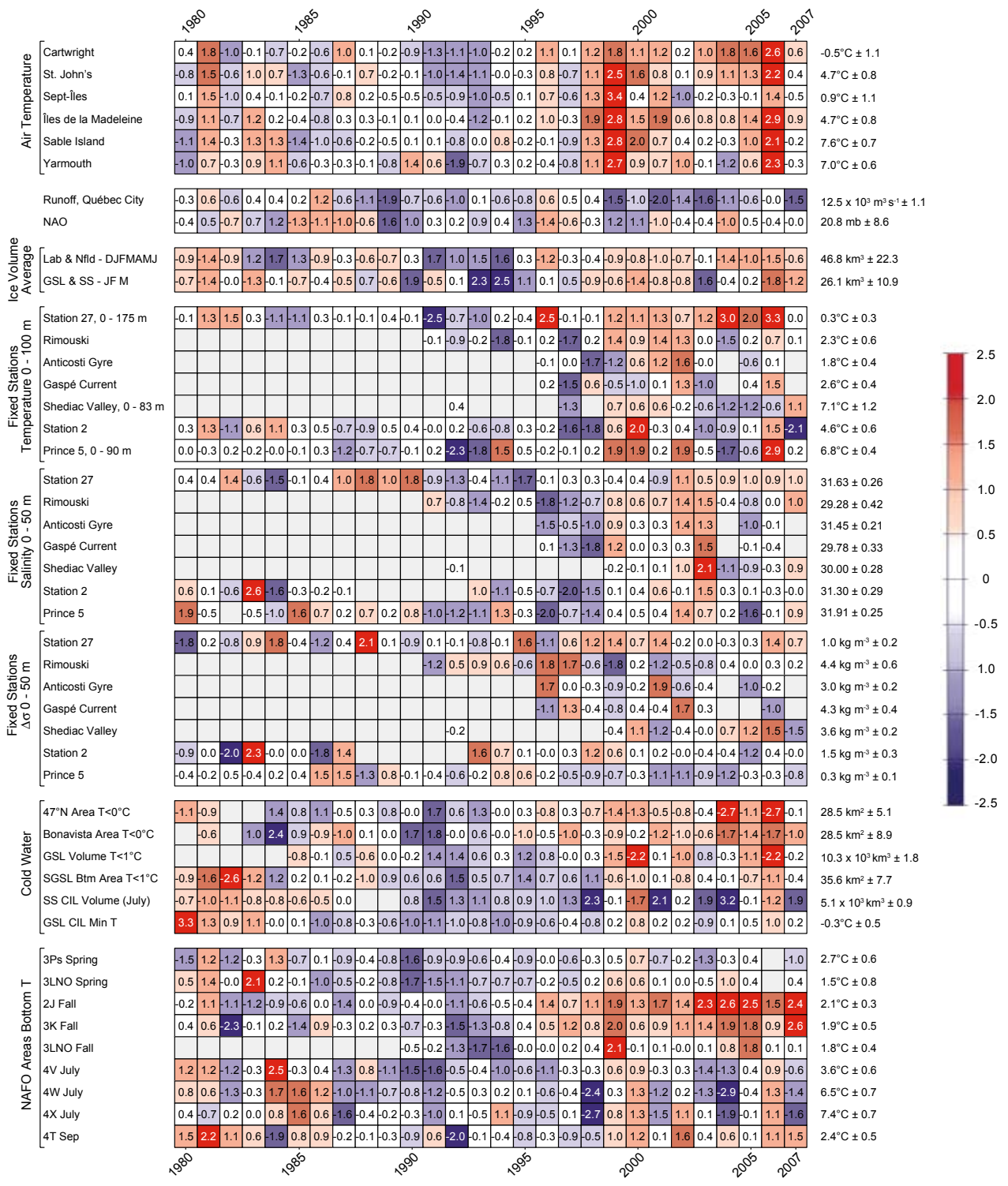


Fig. 2 Time series of atmospheric and oceanographic variables, 1980–2007. A grey cell indicates missing data; a white cell is a value within 0.5 SD of the long-term mean based on data from 1971–2000 when possible. For air temperature, NAO index, ice volumes, fixed station depth-averaged temperature, cold water volumes and areas, and bottom temperatures of NAFO areas, a red cell indicates warmer-than-normal conditions and a blue cell colder than normal. More intense colours indicate larger anomalies. For the freshwater inflow, salinity, and stratification, red corresponds to above-normal conditions. The numbers in cells are the differences from the long-term means divided by the standard deviations. Long-term means and standard deviations are shown on the right hand side of the figure. (North Atlantic Oscillation [NAO], Gulf of St. Lawrence [GSL], southern Gulf of St. Lawrence [SGSL], cold intermediate layer [CIL], Scotian Shelf [SS].

Séries temporelles (de 1980 à 2007) des variables atmosphériques et océanographiques. Une cellule grise indique une donnée manquante et une cellule blanche une valeur entre 0 et 0,5 écart-type de la moyenne à long terme calculée, lorsque possible, sur les données de 1971 à 2000. Pour la température de l'air, l'indice NAO, les volumes de glace, la température moyenne sur la profondeur aux stations fixes, surfaces et volumes d'eau froide, et la température au fond dans les divisions de l'OPANO, les cellules rouges indiquent des conditions plus chaudes que la normale et les cellules bleues plus froides que la normale. Les teintes plus fortes correspondent aux plus grandes anomalies. Pour le débit d'eau douce, la salinité et la stratification, le rouge correspond aux conditions au-dessus de la normale. Les chiffres à l'intérieur des cellules sont les différences par rapport aux moyennes à long terme divisées par les écart-types. Les moyennes et les écarts-types sont présentées à droite de la figure. (Oscillation nord Atlantique [NAO], golfe du Saint-Laurent [GSL], sud du golfe du Saint-Laurent [SGSL], couche intermédiaire froide [CIL], plateau Néo-Écossais [SS]).

ture, precipitation, and the hydrographic properties on the eastern Canadian seaboard either directly or through ocean currents. Direct effects occur predominantly to waters of the Labrador Sea and the Labrador and Newfoundland shelves, where a negative NAO corresponds to warmer-than-average conditions. The tendency of the ocean currents to move from north to south spreads the NAO's influence into the Gulf of St. Lawrence and onto the Scotian Shelf. For the past seven years, the NAO has generally been negative, though the index was normal in 2007.

With the exceptions of 1983–85 and 1991–92, ice volumes on the Newfoundland-Labrador Shelf and the Gulf of St. Lawrence-Scotian Shelf have been strongly positively correlated over the past 28 years. The exceptional years featured large ice volumes on the Newfoundland-Labrador Shelf but small volumes in the Gulf. On average, the ice volumes for the shelf area and the Gulf appear to be related to the NAO. Since 1980, there have been nine years when the NAO has been more than 0.5 SD below (generally milder winters) or above (generally colder winters) normal. The difference in the ice volumes between these two groups of years (colder - milder) is 4 km³ (monthly average for Jan.-Mar.) for the Gulf of St. Lawrence-Scotian Shelf and 16 km³ (monthly average for Dec.-June) for the Newfoundland-Labrador Shelf. For the past decade, ice volumes on the Newfoundland-Labrador Shelf and the Gulf of St. Lawrence-Scotian Shelf have generally been lower than normal. This continued during 2007, when the ice volumes were significantly below normal.

There are sufficient data to estimate annual 0–100 m (or 0-bottom) temperature anomalies for Station 27, Prince 5, and Halifax 2; however, the four series from the Gulf are only 35–60% complete. Though the fixed stations are not strongly coherent, sorting the annual anomalies based on whether average air temperature anomalies are greater or less than 0.5 SD from normal produces consistent results: water temperature differences (warm – cold air temperature years) were 1.6°C for Rimouski and Station 27, 1.2°C for Prince 5, and 0.7°C for Halifax 2. In 2007, temperatures at Rimouski, Station 27, and Prince 5 were near normal, 1.3°C above normal at Shédiac and 1.3°C below normal at Halifax 2.

The salinity anomalies at Rimouski, Shédiac, Station 27, and Prince 5 were about 1 SD above normal in 2007; on the other hand, salinity was near normal at Halifax 2. Stratification was weaker than normal at Shédiac and Prince 5, normal at Halifax 2 and Rimouski, and stronger than normal at Station 27.

The measures of cold water volumes and areas are quite coherent over the region, with a single function able to capture about 60% of the overall variance. The strongest relationship is within the Gulf of St. Lawrence (cold intermediate layer [CIL] volume and SGSL area) and the weakest between the Scotian and Newfoundland shelves. In 2007, the Gulf CIL volume, the southern Gulf bottom area ($T < 1^\circ\text{C}$), and the 47°N cross section ($T < 1^\circ\text{C}$) were nearly normal with slightly negative tendencies; the Bonavista section had a CIL area that was significantly less than normal. The Scotian Shelf CIL volume on the other hand was significantly greater than normal.

correspond à des conditions plus chaudes que la normale. La tendance des courants océaniques d'aller du nord au sud étend l'influence du NAO à l'intérieur du golfe du Saint-Laurent et sur le plateau Néo-Écossais. Au cours des sept dernières années, en général le NAO a été négatif, bien qu'en 2007 l'indice était normal.

À l'exception des périodes de 1983 à 1985 et de 1991 à 1992, les volumes de glace sur les plateaux du Labrador et de Terre-Neuve ainsi que dans le golfe du Saint-Laurent et sur le plateau Néo-Écossais ont été fortement positivement corrélés au cours des 28 dernières années. Les années d'exception sont marquées par des volumes de glace importants sur les plateaux du Labrador et de Terre-Neuve mais de petits volumes dans le golfe. En moyenne, les volumes de glace sur le plateau et dans le golfe semblent reliés au NAO. Depuis 1980, il y a eu neuf années où le NAO a été plus de 0,5 écart-type en-dessous (généralement des hivers doux) et au-dessus (généralement des hivers froids) de la normale. La différence des volumes de glace entre ces groupes d'années (plus froides – plus douces) est de 4 km³ (moyenne mensuelle de janvier à mars) pour le golfe du Saint-Laurent et le plateau Néo-Écossais et de 16 km³ (moyenne mensuelle de décembre à juin) pour les plateaux du Labrador et de Terre-Neuve. Pour la dernière décennie, les volumes de glace sur les plateaux du Labrador et de Terre-Neuve ainsi que dans le golfe du Saint-Laurent et sur le plateau Néo-Écossais ont été plus bas que la normale. La situation s'est poursuivie en 2007 alors que les volumes de glace étaient de beaucoup sous la normale.

Il y a suffisamment de données pour l'estimation d'anomalies annuelles des températures de 0 à 100 m (ou de 0 jusqu'au fond) pour la Station 27, Prince 5 et Halifax 2; cependant pour le golfe les quatre séries ne sont complètes qu'à 35 à 60 %. Malgré la faible cohérence entre les stations fixes, un classement des anomalies annuelles basé sur le fait que les anomalies des températures moyennes de l'air sont plus grandes ou plus petites que 0,5 écart-type produit des résultats fiables : les différences de température de l'eau (années de températures de l'air chaudes – froides) étaient de 1,6°C à Rimouski et Station 27, 1,2°C à Prince 5 et 0,2°C à Halifax 2. En 2007, les températures à Rimouski, Station 27 et Prince 5 étaient près de la normale, de 1,3°C au-dessus de la normale à Shédiac et étaient 1,3°C sous la normale à Halifax 2.

Les anomalies de salinité à Rimouski, Shédiac, Station 27 et Prince 5 étaient environ 1 écart-type au-dessus de la normale en 2007 alors qu'elles étaient près de la normale à Halifax 2. La stratification était plus faible que la normale à Shédiac et Prince 5, normale à Halifax 2 et Rimouski et plus forte que la normale à la Station 27.

Les mesures de volumes d'eau froide sont très cohérentes pour toute la région où une seule fonction explique environ 60 % de la variance totale. La relation la plus forte est à l'intérieur du golfe du Saint-Laurent (entre le volume de la couche intermédiaire froide [CIL] et la surface d'eau froide dans le SGSL) et la plus faible entre les plateaux Néo-Écossais et de Terre-Neuve. En 2007, le volume de CIL dans le golfe, la surface ($T < 1^\circ\text{C}$) au fond dans le sud du golfe et la surface effective ($T < 1^\circ\text{C}$) suivant la ligne 47°N étaient près de la normale avec de faibles tendances négatives. Le transect de Bonavista avait

Bottom temperatures divided the region in two: NAFO areas 2J, 3K, and 4T had above-normal bottom temperatures by as much as 2.6 SD, areas 3LNO and 4RS (quantified by the Gulf CIL minimum temperature) were within 0.5 SD of normal but slightly positive, whereas bottom temperatures for areas 3Ps, 4V, 4W, and 4X featured below-normal temperatures by -0.6 to -1.6 SD.

In summary, for 2007, the average value of the 22 indexes of water temperature, bottom temperature, and cold water volumes or areas (Fig. 2) was 0.3, the eighth highest during the 1980–2007 period; 9 were more than 0.5 SD above normal, 6 within 0.5 SD of normal, and 7 more than 0.5 SD below normal. This is a considerable change from 2006, when the average of the 22 indexes was 1.3, the highest value for the 1980–2007 period.

Chemical and Biological Environment

Nutrient (nitrate) inventories in surface waters (0–50 m) at Station 27 in 2007 were slightly above average but the inventories below the thermocline (50–150 m) were nearly as high

une surface effective de CIL beaucoup plus faible que la normale. Par contre, le volume de la CIL du plateau Néo-Écossais était de beaucoup supérieur à la normale.

Les températures au fond divisent la région en deux : les divisions de l'OPANO 2J, 3K, et 4T avaient des températures au fond jusqu'à 2,6 écart-types au-dessus de la normale, elles étaient à l'intérieur de 0,5 écart-type mais légèrement positives pour les divisions 3LNO et 4RS (définies par la minimum de température de la CIL du golfe), alors que les températures au fond des divisions 3Ps, 4V, 4W et 4X montraient des températures sous la normale de -0,6 à -1,6 écart-types.

En résumé, pour 2007 la valeur moyenne des 22 indices de température de l'eau, température au fond et volumes ou surfaces d'eau froide (Fig. 2) était 0,3, la huitième plus élevée de la période de 1980 à 2007; 9 indices étaient plus de 0,5 écart-type au-dessus de la normale, 6 entre 0 et 0,5 écart-type de la normale et 7 plus de 0,5 écart-type sous la normale. Il s'agit d'un changement considérable par rapport à 2006, alors que la moyenne des 22 indices était 1,5, la valeur la plus élevée de la période 1980–2007.

Environnement chimique et biologique

À la station 27, les concentrations en sels nutritifs (nitrates) en surface (0 à 50 m) étaient légèrement au-dessus de la moyenne en 2007 mais les concentrations sous la thermocline (50 à 150 m) étaient tout près des niveaux élevés record observés en 2000. Il y a des indices d'une augmentation de l'intensité de la floraison printanière de phytoplancton en 2007 par rapport aux années précédentes et la durée de la floraison a été la plus longue jamais observée (Fig. 3A). Les images de la couleur de l'océan en 2007 ont montré que le moment des floraisons de phytoplancton en surface était en accord avec les années passées. Toutefois, selon les images satellites et les stations océanographiques du PMZA l'amplitude de la floraison printanière sur les Grands Bancs et sur le plateau au nord-est de Terre-Neuve a eu tendance à augmenter en 2006 et 2007, comparativement aux années précédentes. Outre la période de floraison printanière, l'abondance de phytoplancton a été généralement plus faible que la moyenne pour le reste de l'année. Nous avons détecté des indices de floraisons de phytoplancton sous la surface en été (juillet-août) mais il y a eu peu d'indication d'une floraison automnale à la Station 27 en 2007, comparativement aux années précédentes.

En 2007, les concentrations en sels nutritifs dans le golfe du Saint-Laurent (GSL), particulièrement en hiver, ont continué à augmenter, notamment au centre et dans le nord-ouest du golfe (NOGSL) où les niveaux étaient beaucoup plus élevés comparativement à la période de 2001 à 2006. Les

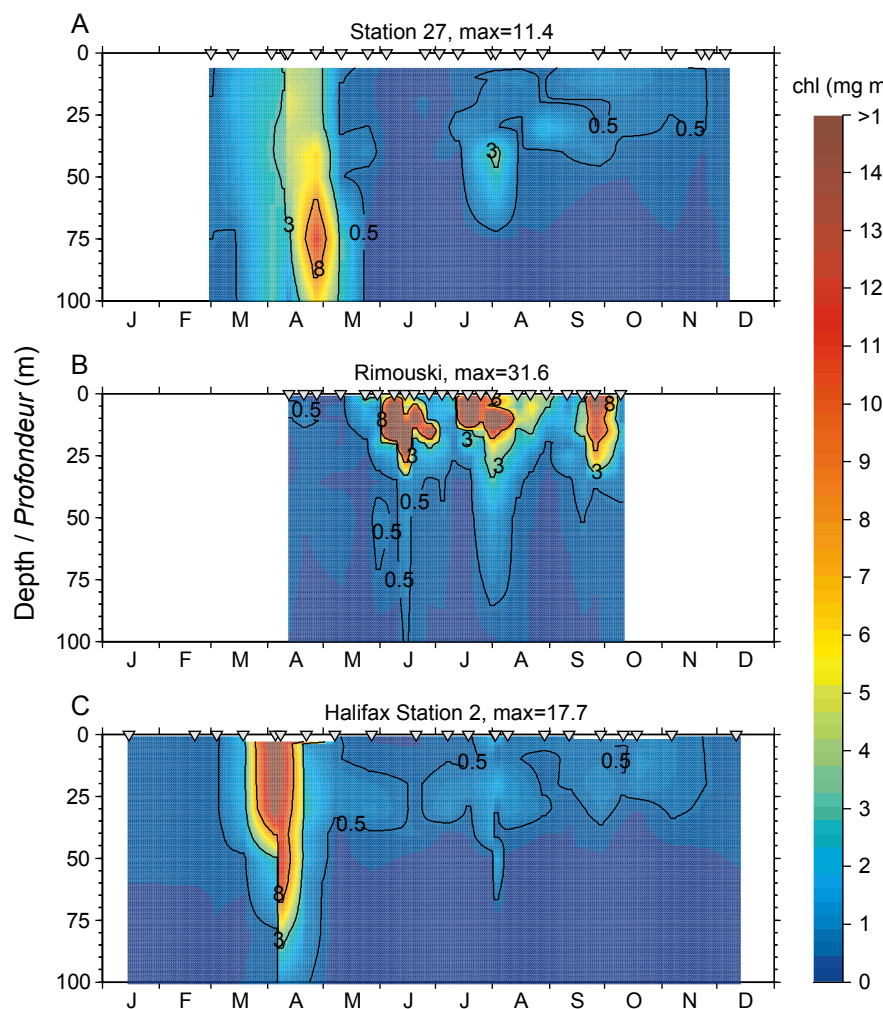


Fig. 3 Evolution of the vertical phytoplankton chlorophyll concentration for the fixed stations: (A) Station 27, (B) Rimouski Station, and (C) Halifax Station 2. The gray triangles indicate sampling points. White areas are data gaps.

Évolution des concentrations en chlorophylle du phytoplancton pour les stations fixes : (A) Station 27, (B) station de Rimouski et (C) Station 2 de Halifax. Les triangles gris indiquent les moments d'échantillonnage. Les zones blanches indiquent une absence de données.

as the record levels observed in 2000. There are some indications of an increase in the magnitude of the spring phytoplankton bloom in 2007 compared to previous years and the duration was the longest on record (Fig. 3A). Ocean colour imagery in 2007 indicated the timing of surface phytoplankton blooms to be consistent with earlier years. However, the magnitude of the spring bloom on the Grand Banks and northeast Newfoundland Shelf tended to be higher in 2006 and 2007 in contrast to previous years, as inferred from both satellite imagery and the AZMP oceanographic sections. Other than during the spring bloom, phytoplankton abundance was generally lower than average throughout the remainder of the year. We detected evidence of subsurface phytoplankton blooms during the summer (July–August), but there was little evidence of an autumn bloom at Station 27 in 2007 compared to previous years.

In 2007, the surface nutrient inventories in the Gulf of St. Lawrence (GSL), particularly in winter, continued to increase, notably in the centre and northwestern Gulf (NW GSL), where levels were significantly higher compared to the 2001–2006 period. Ocean colour imagery indicated that the spring phytoplankton bloom in these regions was more intense but of shorter duration in 2007 compared to the 1998–2006 average. An increase in the magnitude and duration of the spring phytoplankton bloom was also observed in some areas of the southern Gulf of St. Lawrence including the Cabot Strait in 2007. The phytoplankton growth cycle in the Lower St. Lawrence Estuary (LSLE) returned to the normal condition in 2007, showing several major pulses during summer and a small bloom of short duration during fall (Fig. 3B). The invasive North Pacific diatom *Neodenticula seminae*, which was observed in the Gulf over the previous six years, was not detected in 2007.

Nutrient inventories in winter off Halifax were at normal levels in 2007; however, summer levels were lower than the long-term average, especially in bottom waters where nitrate concentrations were the lowest seen since systematic observations began in 1999. The magnitude of the spring phytoplankton bloom was at record high levels at the fixed station (Fig. 3C). Although the timing of the bloom was near normal, its duration was short relative to earlier years in the time series. In addition, biomass levels outside the spring bloom period continued to decline in 2007. Ocean colour imagery indicated that the intense spring bloom seen at the Halifax Station was widespread in 2007, extending over the entire Scotian Shelf in April.

Large calanoid copepods continued to make up the bulk (60–90%) of the mesozooplankton biomass at the three fixed stations in 2007 (Fig. 4). Smaller species (*Para-* and *Pseudocalanus* spp. and *Oithona* spp.) contributed (10–20%) to the biomass at Station 27 and off Halifax but were of minor importance in the LSLE. Deep, cold-water species (*Calanus glacialis* and *Calanus hyperboreus*) made up a large part of the total biomass at all of the fixed stations as well and contributed to the seasonal biomass peaks; *C. hyperboreus* dominated the biomass at the Rimouski (LSLE) station year-round. *Calanus finmarchicus* was a key species at all sites, representing almost half of the biomass over the year at Station 27 and off Halifax and 30% at the Rimouski station. Total biomass

images de la couleur de l'océan ont montré que la floraison printanière de phytoplancton dans ces régions a été plus forte mais de plus courte durée en 2007 comparativement à la moyenne de 1998 à 2006. Une augmentation de l'amplitude et de la durée de la floraison printanière de phytoplancton a aussi été observée en 2007 dans certains secteurs du sud du golfe du Saint-Laurent incluant le détroit de Cabot. Le cycle de croissance du phytoplancton dans l'estuaire maritime du Saint-Laurent (EMSL) est revenu à la normale en 2007 avec plusieurs épisodes importants pendant l'été et une petite floraison de courte durée pendant l'automne (Fig. 3B). La diatomée envahissante *Neodenticula seminae*, observé dans le golfe au cours des six dernières années, n'a pas été détecté en 2007.

Les concentrations en sels nutritifs en hiver au large de Halifax étaient à des niveaux normaux en 2007; toutefois, les niveaux en été étaient plus faibles que la moyenne à long terme, particulièrement dans les eaux près du fond où les nitrates étaient à leur plus bas depuis le début des observations systématiques en 1999. L'amplitude de la floraison printanière de phytoplancton était à un niveau élevé record à la station fixe (Fig. 3C). Malgré que le moment de la floraison était quasi normal, la durée a été courte relativement aux années antérieures de la série temporelle. De plus, les niveaux de biomasse en dehors de la période de floraison ont continué à décliner en 2007. Les images de la couleur de l'océan ont montré que la floraison printanière à la Station Halifax était étendue en 2007, s'étendant sur tout le plateau Néo-Écossais en avril.

Les grands copépodes formaient toujours la majeure partie (60 à 90 %) de la biomasse de mesozooplankton aux trois stations fixes en 2007 (Fig. 4). Les petites espèces (*Para-* et *Pseudocalanus* spp. et *Oithona* spp.) comptaient pour 10 à 20 % de la biomasse à la Station 27 et au large de Halifax mais elles sont peu importantes dans l'EMSL. Les espèces d'eau froide et profonde (*Calanus glacialis* et *Calanus hyperboreus*) comptent également pour une grande partie de la biomasse à toutes les stations fixes et contribuent aux sommets saisonniers de biomasse; *C. hyperboreus* a dominé la biomasse à Rimouski (EMSL) toute l'année. À toutes les stations, *Calanus finmarchicus* était une espèce clé comptant pour presque la moitié de la biomasse pour toute l'année à la Station 27 et au large de Halifax et pour 30 % de la biomasse à la station de Rimouski. En 2007, la biomasse totale montrait un maximum très net au printemps au large de Halifax mais avait une distribution plus étendue (été-automne) à la Station 27 et à la station de Rimouski.

En 2007, à la Station 27 la biomasse totale des copépodes dominants était de 40 % plus élevée qu'en 2006, et seulement 20 % plus faible que le maximum de la série observé en 2002. L'abondance en nombre de *C. finmarchicus* à la Station 27 a diminué légèrement (20 %) relativement à l'année précédente et était légèrement plus faible que la moyenne pour 1999 à 2006. L'abondance de *C. glacialis*, *Centropages* spp. et *Temora longicornis* était au niveau ou tout près de la valeur la plus faible enregistrée depuis 1999. Par contre, les abondances de *C. hyperboreus*, *Acartia* spp., *Metridia* spp., *Microcalanus* spp., *Oithona* spp., *Pseudocalanus* spp., *Sagitta* spp., des larvacés, des gastropodes et des euphausiacés ont augmenté en 2007. Les abondances totales de zooplancton estimées pour les Grands Bancs et le plateau de Terre-Neuve

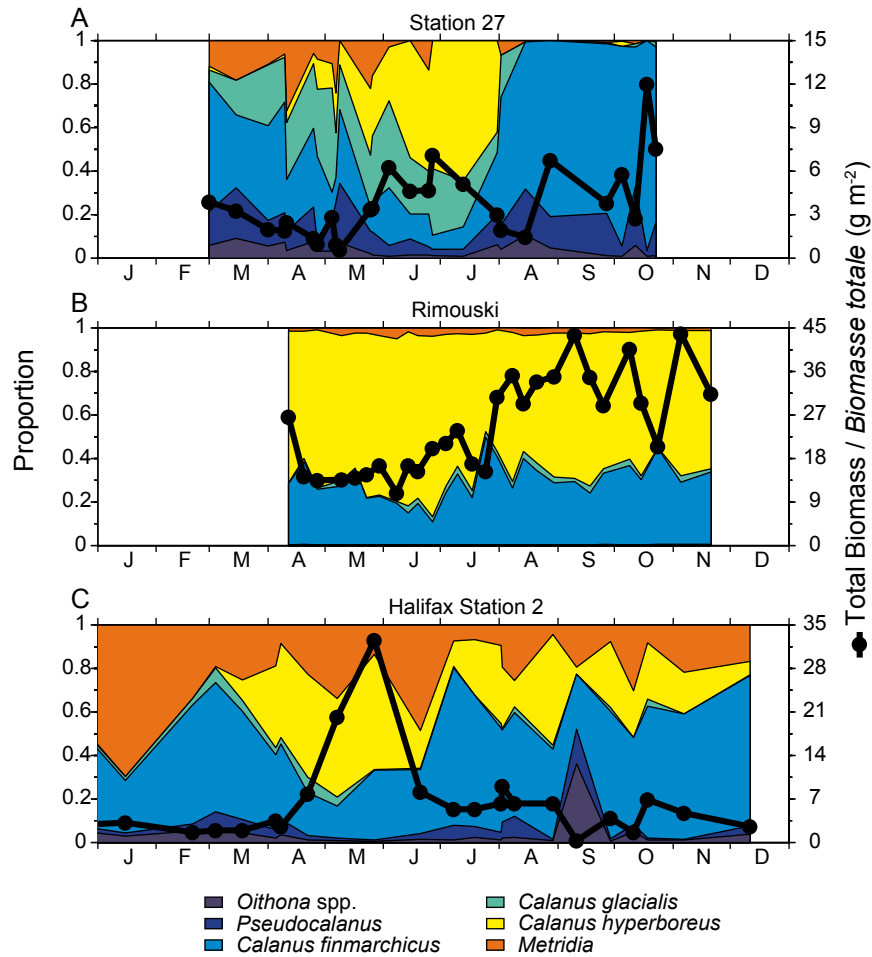


Fig. 4 Relative importance of the dominant copepod species for the fixed stations: (A) Station 27, (B) Rimouski Station, and (C) Halifax Station 2. The solid line shows the total integrated (surface-bottom) biomass of the dominant copepods. White areas are data gaps.

Importance relative de quelques espèces dominantes de copépodes pour les stations fixes : (A) Station 27, (B) station de Rimouski et (C) Station 2 de Halifax. La ligne noire épaisse indique la biomasse intégrée (surface-fond) de copépodes. Les zones blanches indiquent une absence de données.

in 2007 showed a pronounced spring peak off Halifax but was more broadly distributed (summer-fall) at Station 27 and the Rimouski station.

In 2007, the overall biomass of the dominant copepods at Station 27 was 40% higher than in 2006 and only 20% lower than the time-series maximum observed in 2002. The numerical abundance of *C. finmarchicus* at Station 27 decreased slightly (20%) relative to the previous year and was only slightly lower than the 1999–2006 average. The abundances of *C. glacialis*, *Centropages* spp., and *Temora longicornis* were at or near the lowest value recorded since 1999. In contrast, the abundances of *C. hyperboreus*, *Acartia* spp., *Metridia* spp., *Microcalanus* spp., *Oithona* spp., *Pseudocalanus* spp., *Sagitta* spp., larvaceans, gastropods, and euphausiids increased in 2007. The overall abundance estimates of zooplankton on the Grand Banks and Newfoundland Shelf in 2007 were close to average on the former and slightly below average on the latter. The abundance of *C. finmarchicus* decreased slightly throughout the region while the abundance of *C. glacialis* continued to decline on the Grand Banks. In contrast, *Metridia* spp. reached its highest level in

en 2007 étaient près de la moyenne pour les Grands Bancs et légèrement sous la moyenne pour le plateau. L'abondance de *C. finmarchicus* a diminué légèrement dans toute la région alors que l'abondance de *C. glacialis* a diminué sur les Grands Bancs. Par contre, *Metridia* spp. a atteint un maximum d'abondance dans la région à l'exception du nord du plateau de Terre-Neuve où son abondance était près de la moyenne à long terme. En 2007, dans toute la région l'abondance de la plupart du zooplancton carnivore a montré un déclin par rapport à 2006 pour tous les groupes. Dans la plus grande partie de la région, la biomasse relative de *C. finmarchicus* et de *Metridia* spp. était généralement plus grande que la moyenne à long terme au détriment des deux espèces sœurs de *Calanus*. Ce patron a persisté de l'automne 2006 jusqu'à l'été 2007.

La biomasse de mésozooplancton dans l'EMSL et le NOGSL en novembre 2007 était la quatrième plus forte observée au cours des 14 dernières années. Par contre, la biomasse de macrozooplancton, l'abondance de l'euphausiacé *Thysanoessa raschii* et l'abondance de l'amphipode hypéride *Themisto libellula* étaient au même niveau qu'en 2006 et pour les deux années correspondaient aux plus faibles valeurs observées au cours des 14 dernières années dans l'EMSL et le NOGSL.

En 2007, la biomasse de zooplancton et l'abondance de *C. finmarchicus* à la Station Halifax étaient plus élevées qu'en 2006 et près de la moyenne à long terme. L'année 2007 a été aussi remarquable pour

l'abondance quasi record des jeunes stades de développement de *C. finmarchicus* (stades CI-CIII) pendant le maximum au printemps. Comme cela a été le cas pour les deux années précédentes, en 2007 la biomasse de *C. glacialis* était faible ou absente au large de Halifax (Fig. 4C). La biomasse d'autres espèces (*Metridia* spp., *Pseudocalanus* spp.) était également sous les niveaux observés auparavant. Par contre, la biomasse de *C. hyperboreus* a augmenté pour atteindre un niveau record en 2007; le double de la moyenne à long terme. Cependant, des relevés plus étendus de la biomasse et de l'abondance de zooplancton dans le golfe du Maine/baie de Fundy et sur le plateau Néo-Écossais en 2007 indiquent qu'en général le zooplancton était à des niveaux sous la normale sur le banc Georges (en hiver) et sur le plateau Néo-Écossais (printemps, été et automne).

La série temporelle de plus de 40 ans du *Continuous Plankton Recorder* a montré que l'abondance de phytoplancton au cours de la dernière décennie, estimée par l'indice de couleur de phytoplancton, a été bien au-dessus des niveaux observés au cours des années 1960 et 1970 sur les Grands Bancs et sur le plateau Néo-Écossais (Fig. 5A). Les niveaux de phytoplancton

all areas with the exception of the northern Newfoundland Shelf, where its abundance was near the long-term average. The abundance of most carnivorous zooplankton in 2007 showed a decrease from 2006 levels in all taxa and areas. Throughout much of the region, the relative biomasses of *C. finmarchicus* and *Metridia* spp. were generally greater than the long-term averages at the expense of the two sister species of *Calanus*. This pattern persisted from the autumn of 2006 into the summer of 2007.

Mesozooplankton biomass in the LSLE and in the NWGSL in November 2007 was the fourth highest observed over the last 14 years. In contrast, macrozooplankton biomass, the mean abundance of the euphausiid *Thysanoessa raschii*, and the mean abundance of the hyperiid amphipod *Themisto libellula* were at the same levels as seen in 2006 and both years corresponded to the lowest value observed over the last 14 years in the LSLE and in the NWGSL.

Zooplankton biomass and *C. finmarchicus* abundance in 2007 at the Halifax Station were higher than the levels seen in 2006 and close to the long-term average. The year 2007 was also notable for its near record high numbers of early developmental stages of *C. finmarchicus* (stages CI-CIII) during the spring maximum. As was the case for the previous two years, the biomass of *C. glacialis* in 2007 was low or absent off Halifax (Fig. 4C). The biomasses of other species (*Metridia* spp., *Pseudocalanus* spp.) were also below levels seen previously. In contrast, *C. hyperboreus* biomass increased to record high levels in 2007, at twice the long-term average. However, broader surveys of zooplankton biomass and abundance in the Gulf of Maine/Bay of Fundy and on the Scotian Shelf during 2007 indicated that zooplankton overall were below normal levels on Georges Bank (winter) and on the Scotian Shelf (spring, summer, and fall).

The >40-year time series from the Continuous Plankton Recorder showed that phytoplankton abundance over the last decade, as estimated by the phytoplankton colour index, has been well above levels observed in the 1960s and 1970s on both the Grand Banks and the Scotian Shelf (Fig. 5A). Phytoplankton levels on the Grand Banks have consistently exceeded those on the Scotian Shelf and there has been strong coherence in interannual variability between the two regions. In contrast to phytoplankton, zooplankton (*Para- /Pseudocalanus* spp., *C. finmarchicus*, total euphausiids) abundance in recent years, particularly that of the larger species (*C. finmarchicus* and euphausiids) that make up the bulk of the biomass, has generally been at or below levels seen during the early decades of the time series in both regions (Fig. 5B, C, D). As seen for phytoplankton, zooplankton abundances have generally been higher on the Grand Banks than on the Scotian Shelf; however, interannual variability has been less coherent between the regions. Over the past few years, abundances of both phytoplankton and zooplankton have been converging on long-term mean levels. Most notably, phytoplankton levels have been declining and euphausiid levels have been increasing.

Highlight 2007

In 2007, one of the outstanding features of the biological environment was the widespread occurrence of a record high

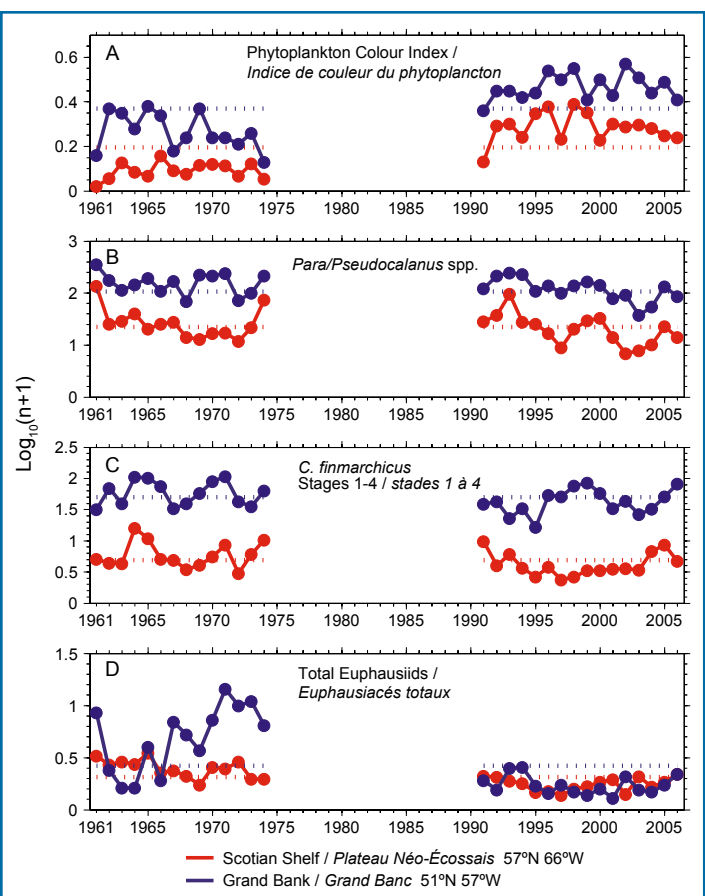


Fig. 5 Data from the Continuous Plankton Recorder (CPR) showing the annual average phytoplankton colour index (A) and annual average abundances of dominant zooplankton taxa (B,C,D) from the Scotian Shelf (red) and Grand Bank (blue) regions. Horizontal dotted lines represent the long-term means.

Données CPR (Continuous Plankton Recorder) montrant l'indice annuel de couleur du phytoplancton (A) et les abondances annuelles moyennes de certains taxons dominants du zooplancton (B, C, D) pour les régions du plateau Néo-Écossais (rouge) et du Grand Banc (bleu). Les lignes pointillées indiquent les moyennes à long terme.

sur les Grands Bancs ont continuellement excédé ceux du plateau Néo-Écossais et il y a avait une forte cohérence de la variabilité interannuelle entre les deux régions. Contrairement au phytoplancton, au cours des dernières années, l'abondance de zooplancton (*Para- /Pseudocalanus* spp., *C. finmarchicus*, euphausiacés totaux), en particulier celle des grandes espèces (*C. finmarchicus* et euphausiacés) qui constituent la plus grande partie de la biomasse, était en général au niveau ou sous les niveaux observés au cours des premières décennies de la série temporelle dans les deux régions (Fig. 5B, C, D). Comme pour le phytoplancton, les abondances de zooplankton ont été en général plus élevées sur les Grands Bancs que sur le plateau Néo-Écossais; cependant, il y avait moins de cohérence dans la variabilité interannuelle entre les régions. Pour ces dernières années les abondances de phytoplancton et de zooplankton ont convergé vers les niveaux moyens à long terme; particulièrement, les niveaux de phytoplancton ont décliné et les euphausides ont augmenté.

Faits saillants pour 2007

En 2007, un évènement remarquable de l'environnement biologique a été l'étendue d'une floraison record de phytoplankton au printemps, dans certains cas plus de 4 fois plus de

spring phytoplankton bloom, in some cases >4-fold more biomass than observed over the previous 10 years from satellite ocean colour observations (Fig. 6). The magnitude of the spring bloom is thought to be related to the winter/spring inventory of nutrients in surface waters; however, winter/spring nutrient inventories were not sufficiently elevated in any of the Atlantic zone areas in 2007 to account for this remarkable spring event, nor were characteristics of the physical environment (e.g., winter mixing) exceptional. Clearly, a simple cause-effect relationship does not explain this event.

One might also expect to see some manifestation of the record high bloom in the biomass or abundance of the primary consumers of phytoplankton, the mesozooplankton. In all regions, some component of zooplankton biomass or the abundance of dominant species was above average, possibly reflecting a direct response to an increased food supply during the important early life stages.

While local air temperatures and winds play the major role in the annual cycle of water temperatures throughout the region, Canadian east coast waters are also strongly influenced by flow from the arctic. Currents from the north bring not only cold water but also northern species of plankton. For example, we continue to observe cold-water copepods such as *C. glacialis* and *C. hyperboreus* in all regions. In addition, the arctic hyperiid amphipod *T. libellula* has continued to be a component of the macrozooplankton in the Gulf of St. Lawrence. In the last few years, however, the relative importance of some of these cold water species (e.g., *C. glacialis* off Halifax and on the Grand Banks, *T. libellula* in the LSLE, NWGSL, and Grand Banks) have diminished, presumably as a result of the warming ocean conditions and reduction in the CIL. In 2007, this trend reversed on the Scotian Shelf: the CIL increased, bottom water nitrates decreased, and *C. hyperboreus* biomass increased, all indicators of increased influence of Labrador Slope Water in the area.

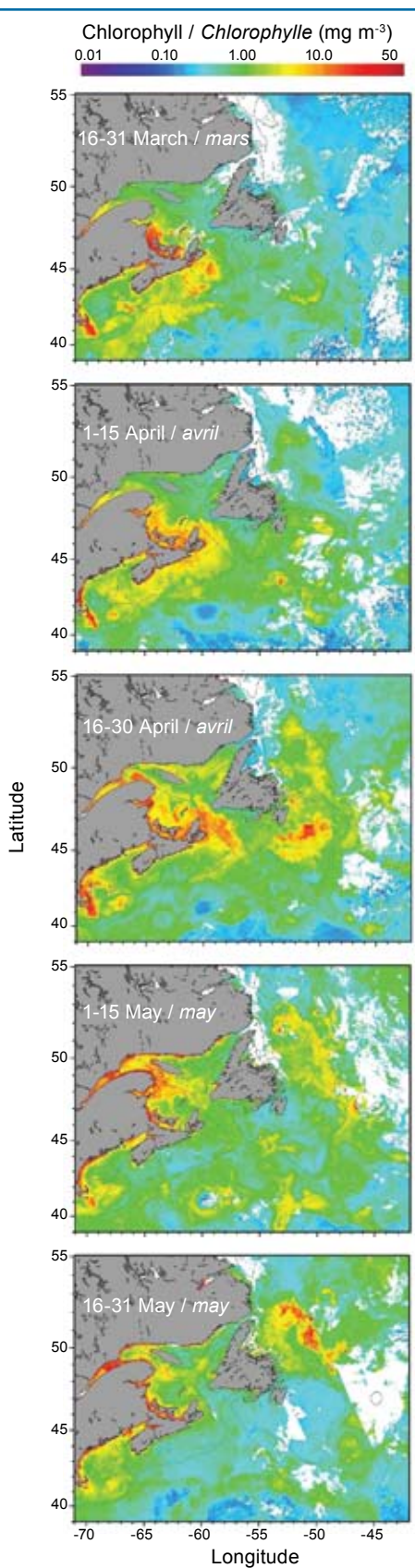


Fig. 6 Time-sequence of satellite composite images of phytoplankton chlorophyll in the Atlantic zone showing the magnitude and extent of the record-high spring bloom in 2007.

Série temporelle d'images satellitaires composites de la chlорophylle phytoplanctonique dans la zone Atlantique montrant l'amplitude et l'étendue de la floraison printanière record de 2007.

biomasse qu'il en a été observé au cours des dix dernières années à partir des images satellites de la couleur de l'océan (Fig. 6). L'amplitude de la floraison printanière est sensée être reliée à la concentration de sels nutritifs dans les eaux de surface en hiver et au printemps; cependant, les concentrations de sels nutritifs en hiver et au printemps n'étaient pas suffisamment élevées dans aucun des secteurs de la zone Atlantique en 2007 pour expliquer ce remarquable événement, non plus que d'exceptionnelles conditions de l'environnement physique (ex. mélange hivernal). Il est clair qu'une simple relation cause-effet de la sorte n'est pas satisfaisante ici.

On pourrait s'attendre à ce que le niveau élevé record de la floraison se soit reflété dans la biomasse ou l'abondance des consommateurs primaires de phytoplancton, le mésozooplancton. Dans toutes les régions, certains composants de la biomasse ou l'abondance des espèces dominantes de zooplancton étaient au-dessus de la moyenne, reflétant probablement une réponse directe à l'augmentation des ressources alimentaires au cours des importants premiers stades de développement.

Bien que les températures locales de l'air et les vents jouent un rôle important dans le cycle annuel des températures de l'eau dans toute la région, les eaux de l'Est canadien sont également fortement influencées par les écoulements provenant de l'Arctique. Les courants provenant du nord ne transportent pas uniquement de l'eau froide mais aussi des espèces nordiques de plancton. Par exemple, nous continuons d'observer des copépodes d'eau froide tels que *C. glacialis* et *C. hyperboreus* dans toutes les régions. De plus, l'amphipode hypéride arctique *T. libellula* a continué à être une composante du macrozooplankton dans le golfe du Saint-Laurent. Au cours des dernières années cependant, l'importance relative de quelques unes de ces espèces d'eau froide (ex. *C. glacialis* au large de Halifax et sur les Grands Bancs, *T. libellula* dans l'EMSL, NOGSL et les Grands Bancs) a diminué, vraisemblablement un résultat des conditions de réchauffement océanique et la réduction de la CIL. En 2007, cette tendance s'est inversée sur le plateau Néo-Écossais : la CIL a augmenté, les nitrates dans les eaux près du fond ont diminué et la biomasse de *C. hyperboreus* a augmenté, tous des indices d'une augmentation de l'influence des eaux du talus continental du Labrador dans la région.

Physical, Chemical and Biological Status of the Labrador Sea

Labrador Sea Monitoring Group¹

Bedford Institute of Oceanography, Box 1006, Dartmouth, NS, B2Y 4A2
ross.hendry@mar.dfo-mpo.gc.ca, glen.harrison@mar.dfo-mpo.gc.ca

Sommaire

Il s'agit du deuxième rapport annuel sur les conditions physiques, chimiques, et biologiques dans la mer du Labrador produit par la direction des Sciences de la région des Maritimes, MPO, à l'Institut océanographique de Bedford. La majorité de l'information présentée provient des visites annuelles à la section AR7W, du banc Hamilton sur le plateau continental du Labrador à cap Désolation sur le plateau continental du Groenland. En 2007, le relevé s'est déroulé du 10 au 27 mai. L'information sur l'historique de la section AR7W peut être consultée dans le rapport d'état initial publié dans le bulletin du PMZA numéro 6. En général, les températures de l'air près de la surface et de l'eau dans la mer du Labrador sont demeurées plus chaudes que la normale en 2007 mais elles montraient un léger refroidissement par rapport aux valeurs record de la période 2002 à 2006. Les moyennes annuelles de la température de l'air près de la surface dans la partie ouest de la mer du Labrador et dans l'est de l'Arctique canadien étaient jusqu'à 2 °C plus froides que les niveaux record élevés de 2006. Les températures à la surface de la mer étaient jusqu'à 1 °C plus chaudes que la normale au centre-ouest de la mer du Labrador mais près ou sous la normale sur le plateau continental et la pente continentale supérieure du Labrador. Les couches supérieures de la mer du Labrador sont demeurées chaudes et salées. L'augmentation de la température et de la salinité des eaux qui n'ont pas été aérées récemment par la convection hivernale se poursuit, suggérant une augmentation de l'apport d'eaux de l'Atlantique en provenance du sud. Les tendances récentes de la température et de la salinité dans les 500 m supérieurs au centre de la mer du Labrador sont moins évidentes. Ces couches moins profondes sont demeurées exceptionnellement chaudes et salées au cours des 4 à 5 dernières années. Les concentrations totales de carbone inorganique dans les couches supérieures au centre de la mer du Labrador ont continué à augmenter, accompagnées d'une décroissance correspondante du pH. Les concentrations en oxygène dissous dans la même masse d'eau montrent une tendance à la baisse. L'état des sels nutritifs poursuit les tendances récentes, à la baisse pour les silicates et à la hausse pour les nitrates résultant en l'augmentation des ratios nitrate:silicate. La grande variabilité observée pour toutes les propriétés biologiques rend la détection de tendances multi annuelles incertaine. Les concentrations de chlorophylle et de bactéries dans la couche supérieure sont demeurées stables au cours de la dernière décennie, mais les tendances montrent une légère pente négative au centre de la mer du Labrador.

Introduction

DFO Maritimes Region Science Branch at the Bedford Institute of Oceanography monitors physical, chemical, and biological conditions in the Labrador Sea with annual occupations of the AR7W section from Hamilton Bank on the Labrador Shelf to Cape Desolation on the Greenland Shelf. This is the second annual Labrador Sea status report. Background material on the history of the AR7W section can be found in the initial status report published in AZMP Bulletin 6.

The AR7W Section

Figure 1 shows a map of the Labrador Sea and the locations of the standard hydrographic and selected meteorological stations discussed below. Ice conditions permitting, 28 stations are sampled annually between Hamilton Bank on the Labrador Shelf and Cape Desolation on the Greenland Shelf. The surveys measure temperature, salinity, and a comprehensive suite of chemical variables including dissolved oxygen, nutrients, and dissolved inorganic carbon. Since 1994, biological variables such as dissolved and particulate biogenic (organic) carbon, bacteria, phytoplankton, and zooplankton have been an integral part of the measurement program.

The 2007 survey took place from 10–27 May 2007. Most of the planned Labrador Sea AR7W work was completed but ice conditions prevented the occupation of the four most inshore stations on the Labrador Shelf and the most inshore station on the West Greenland Shelf.

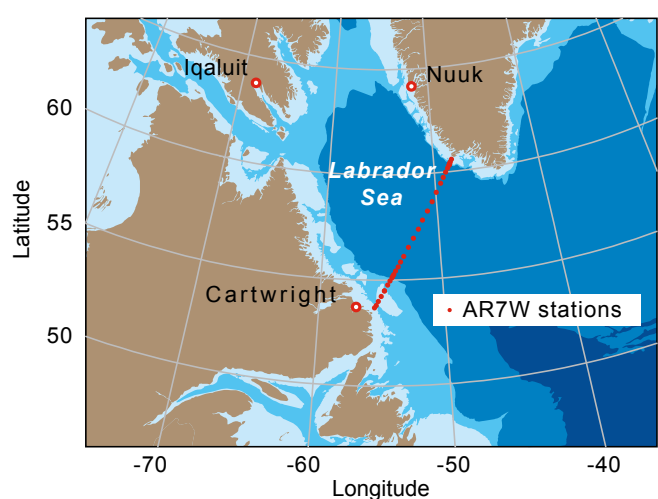


Fig. 1 Map of the Labrador Sea showing the AR7W section and selected meteorological stations.

Carte de la mer du Labrador montrant le transect AR7W ainsi que quelques stations météorologiques.

¹ The Labrador Sea Monitoring Group includes scientists and technicians from Ocean Sciences Division <http://www.mar.dfo-mpo.gc.ca/science/ocean/osd/osd-e.html> and Ecosystem Research Division <http://www.mar.dfo-mpo.gc.ca/science/ocean/erd/erd-e.html>. For further information, please contact Ross Hendry (OSD) ross.hendry@mar.dfo-mpo.gc.ca or Glen Harrison (ERD) glen.harrison@mar.dfo-mpo.gc.ca.

Physical Environment

Air Temperature

Air temperatures in 2007 over the eastern Canadian Arctic and the Labrador Sea were 0.5 to 3.0°C warmer than normal (1971–2000 normal period) with maximum observed annual mean temperature anomalies in the northern sector near Davis Strait (Fig. 2). Surface air temperatures in 2007 in the Canadian Arctic and western Labrador Sea were slightly warmer than normal but up to 2°C cooler than the record high conditions observed in 2006. Surface air temperatures for 2007 at Iqaluit (Nunavut) were about 0.8°C warmer than normal based on January–September station data, compared with the record-high 2.3°C anomaly recorded in 2006.

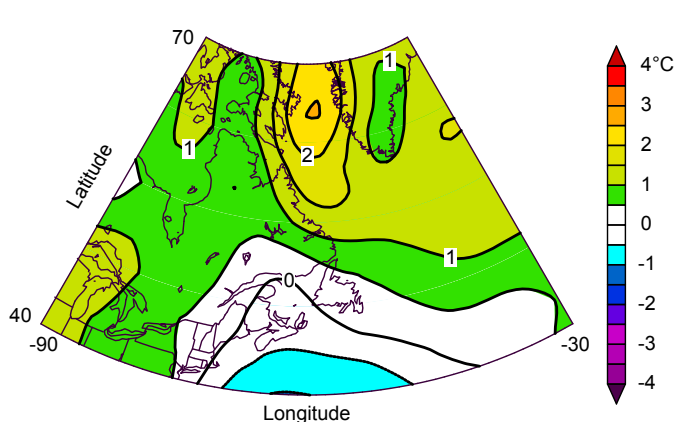


Fig. 2 Annual mean 1000 mb air temperature anomalies for 2007 relative to 1971–2000 from NCEP (National Centers for Environmental Prediction) Reanalysis data.

Anomalies annuelles moyennes de la température de l'air à 1000 mb pour 2007 par rapport aux années 1971–2000 provenant des données de réanalyse des NCEP (National Centers for Environmental Prediction).

Cartwright (Labrador) air temperatures in 2007 were about 0.9°C warmer than normal based on January–November station data, compared with a record-high 2.7°C anomaly in 2006. Annual average air temperatures over the eastern Labrador Sea continued to be warmer than normal but were nearly unchanged from 2006. Nuuk (Greenland) annual mean surface air temperatures based on station data were about 1.3°C warmer than normal in 2007, compared with a 1.6°C anomaly in 2006.

Sea-Surface Temperature

Annual mean sea-surface temperatures (SST) for 2007 from the UK Hadley Centre HadISST product were 0.8 to 1°C above normal over much of the interior of the Labrador Sea (Fig. 3), similar to conditions reported for 2006. Conditions on the Labrador Shelf in 2007 were near normal but notably cooler than seen in 2006. Waters to the south of Greenland including the southern part of the West Greenland Shelf saw annual mean surface temperature anomalies greater than 1°C, i.e., 0.5 to 1°C warmer than observed in 2006.

SST along the AR7W transect has generally increased since the cold period in the early 1990s and was exceptionally

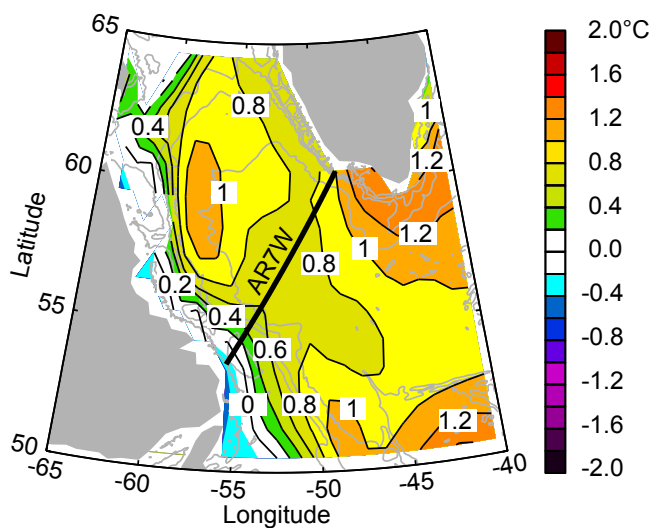


Fig. 3 Sea-surface temperature anomalies for 2007 relative to 1971–2000 (from the U.K. Hadley Centre HadISST climatology). The line marks the AR7W section.

Anomalies annuelles moyennes de la température de surface de la mer pour 2007 par rapport aux années 1971 – 2000 (provenant de la climatologie HadISST du Hadley Centre, Royaume-Uni). La ligne montre le transect AR7W.

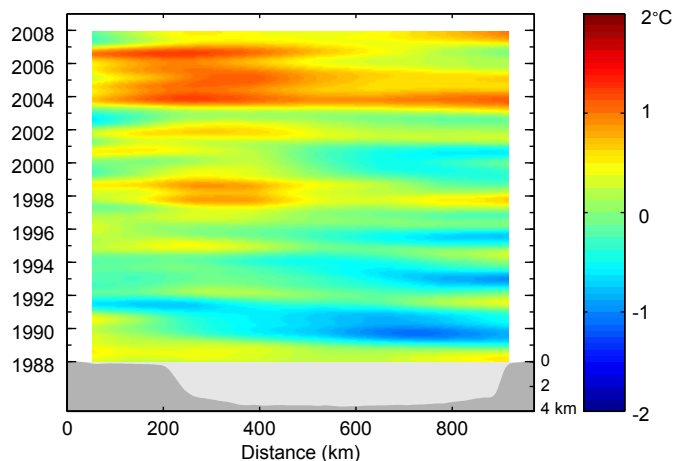


Fig. 4 Low-pass filtered 1988–2007 HadISST sea-surface temperature anomalies relative to 1971–2000 interpolated to the AR7W line. The bathymetry along the AR7W line is shown at the bottom of the figure.

Anomalies de la température de surface de la mer HadISST observées pour 1988 – 2007 par rapport aux années 1971 – 2000; ces données ont été filtrées par un filtre passe-bas et interpolées au transect AR7W. Le profil bathymétrique du transect est illustré au bas de la figure.

warm during the 2003–2006 period (Fig. 4). The annual mean section-averaged SST for each year from 2003–2006 was higher than any other time during the past 75 years of the HadISST record. The 2007 section-averaged SST was the tenth highest during this 75-year period, just lower than that observed in 1997. The SST data along the AR7W line show a recent cooling trend on the Labrador Shelf and a warming trend on the West Greenland Shelf, as was noted in the comparison of conditions in 2006 and 2007 above.

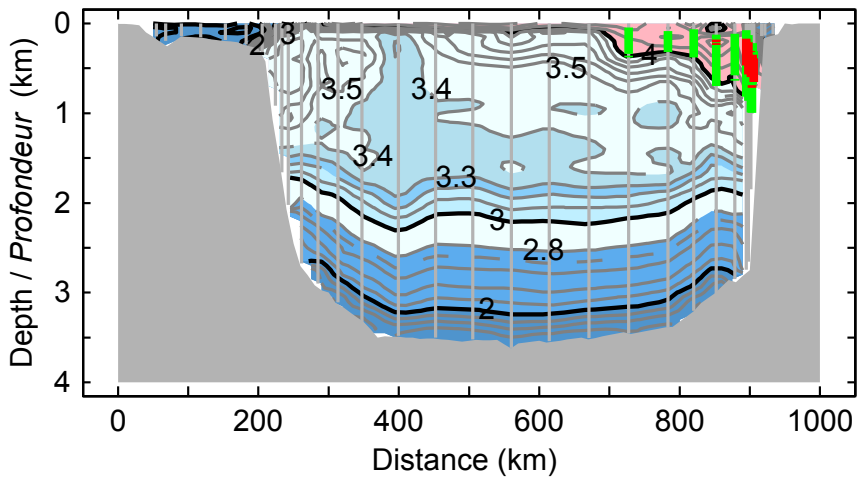


Fig. 5 Section plot of potential temperature from the 2007 occupation of AR7W. Station positions are marked by vertical lines. Waters with potential temperatures in the range 4–6°C are highlighted for salinities in the range 34.95–35.10 (red) or 34.85–34.95 (green).

Profils verticaux de la température potentielle au cours de la campagne AR7W 2007. Les lignes verticales montrent les positions des stations. Les régions colorées indiquent des eaux avec températures potentielles dans l'intervalle 4 – 6°C dont la salinité est dans l'intervalle 34,95 – 35,10 (en rouge) ou 34,85 – 34,95 (en vert).

AR7W Hydrography

The 2007 AR7W survey of the Labrador Sea took place from 12–18 May 2007, the earliest occupation of AR7W since annual observations began in the early 1990s. Heavier ice conditions than in recent years prevented the occupation of inshore stations on the Labrador Shelf. The survey also encountered an unusual band of sea ice on the outer West Greenland Shelf. Nevertheless, the 2007 survey found a continuation of the warm conditions at intermediate depths that have been observed in recent years (Fig. 5). Waters warmer than 4°C were abundant in the upper 500 m on the West Greenland side in 2007, as has been found in recent years. Figure 5 highlights the warm and saline Atlantic waters from the Irminger Current that enter the Labrador Sea as an offshore branch of the West Greenland Current and play an important role in the regional heat and salt balance.

During the early 1990s, deep winter convection in the Labrador Sea filled the upper 2 km with cold and fresh water. Milder conditions in later years have seen winter overturning to depths of 500 to 1000 m. There has been at least a partial annual renewal by winter convection in

the upper 500 m, but the deeper layers have been more isolated from direct surface inputs of heat and fresh water. Steady increases in temperature and salinity of the 500–1500 m layer in the central Labrador Basin (Fig. 6) since the end of deep convection in 1994 indicate increasing proportions of Atlantic water from the south. The 100–500 m layer shows a more variable recent trend to warmer and saltier conditions. This layer is subject to the effects of surface heat and freshwater forcing and freshwater input from ice melt in addition to horizontal exchanges. In both layers, the past four years show the warmest and saltiest conditions of the AR7W record.

Chemical Environment

Deep mixed layers formed in the Labrador Sea during winter convection exchange oxygen, carbon dioxide (CO_2), and other gases with the overlying atmosphere. The Labrador Sea acts as a net sink of atmospheric CO_2 as the surface waters absorb it during winter overturning and rapidly transport it to depth.

Dissolved CO_2 reported as total inorganic carbon (TIC) has increased steadily in recent years in the upper layers (100–500 m) of the central Labrador Sea (Fig. 7). Increasing levels of dissolved CO_2 lead to ocean acidification through corresponding increases in the concentration of carbonic acid, which has potential impacts on marine ecosystems. The concentration of total inorganic carbon in this newly ventilated Labrador Sea water has increased by about 12 $\mu\text{mol kg}^{-1}$ from 1996 to 2007, with a corresponding decrease of about 0.04 pH units (Fig. 7).

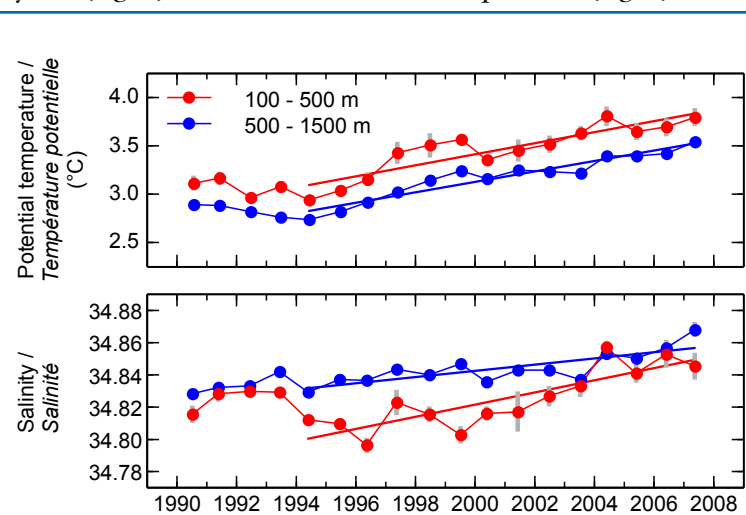


Fig. 6 Time series of potential temperature (top) and salinity (bottom) in the 100–500 m and 500–1500 m depth ranges for the period 1990–2007 and corresponding regression lines for the period 1994–2007 for stations in the central Labrador Basin.

Séries temporelles de la température potentielle (panneau du haut) et de la salinité (panneau du bas) pour les intervalles de profondeurs 100 – 500 m et 500 – 1500 m pour la période 1990 – 2007, et les lignes de régression correspondantes pour la période 1994 – 2007 pour les stations au centre du bassin du Labrador.

Dissolved oxygen shows a negative trend in this same central Labrador Sea water mass (Fig. 8). As much as half of this decrease could be due to decreases in oxygen solubility associated with warmer water temperatures. Decreased air-sea exchanges of oxygen and a reduction in the transport of oxygen to depth are expected in the milder conditions of the past decade. Under these conditions, biological oxygen consumption (respiration) will decrease oxygen concentration. Any decrease in dissolved oxygen associated with increased respiration will increase TIC. The observed increases

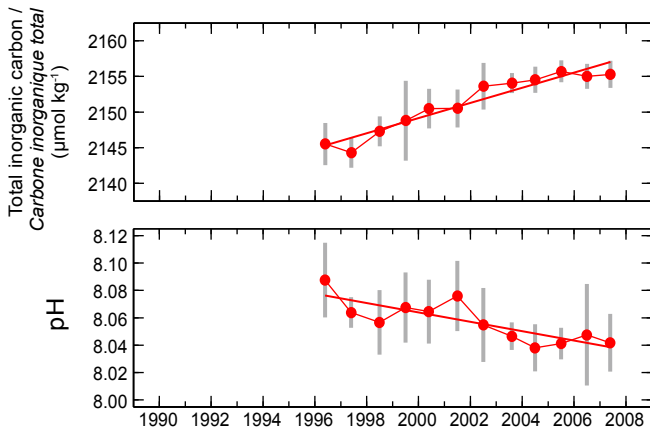


Fig. 7 Total inorganic carbon (top) and pH (bottom) in the 100–500 m depth range and corresponding regression lines for stations in the central part of the Labrador Basin for the period 1996–2007.

Concentrations de carbone inorganique total (panneau du haut) et pH (panneau du bas) dans l'intervalle de profondeur 100 – 500 m et les lignes de régression correspondantes pour des stations au centre du bassin du Labrador pour la période 1996 – 2007.

in TIC (Fig. 7) are a reflection of increases in atmospheric CO₂ related to global change, but biology plays a role.

Changes have also been observed in the inventories of nutrients needed for primary production. Silicate is essential to most diatoms for shell construction and to silicoflagellates for skeletal structure. While other phytoplankton, many of which are smaller in size, do not need silicate, nitrate is used by virtually all phytoplankton species for protein synthesis. Nutrients in the 60–200 m depth range reflect the surface water concentrations after winter mixing and drive the annual plankton growth. Nutrient climatologies at 200 m (Fig. 9) suggest that exports from Baffin Bay provide the main source of upper-layer silicate in the Labrador Sea, leading to relatively high values on the Labrador Shelf and Slope, while North Atlantic waters provide the main source of upper-layer nitrate, leading to relatively high values in the interior of the Labrador Sea. For 2007, section averages for silicate and nitrate in the 60–200 m depth range indicate a continuation of the trends observed for the 1990 to 2006 period: a general increase in nitrate concentrations and decrease in silicate concentrations, consistent with a decrease in the relative importance of Arctic source waters

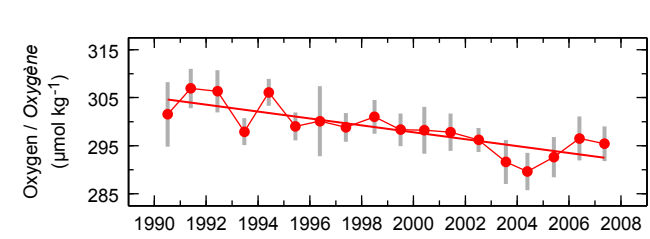


Fig. 8 Dissolved oxygen concentration in the 150–500 m depth range and corresponding regression lines for stations in the central part of the Labrador Basin for the period 1990–2007.

Concentration d'oxygène dissous dans l'intervalle de profondeur 150 – 500 m et la ligne de régression correspondante pour des stations au centre du bassin du Labrador pour la période 1990 – 2007.

compared to Atlantic source waters. These trends in nitrate and silicate concentrations generate increases in nitrate to silicate ratios across the entire AR7W section (Fig. 10). The largest changes in ratio are seen on the Greenland Shelf. Increases in the nitrate:silicate ratio have the potential to influence phytoplankton growth and community structure. Differential nutrient availability is a selective force that may influence species composition and thereby the size structure of phytoplankton communities in the Labrador Sea.

Biological Environment

Time series of 0–100 m mean chlorophyll concentration and bacterial abundance for station groups on the Labrador Shelf, the central Labrador Basin, and the Greenland Shelf show large scatter partly caused by sampling issues related to seasonal variability (Fig. 11). Although both biogenic carbon pools have remained relatively stable for the last decade,

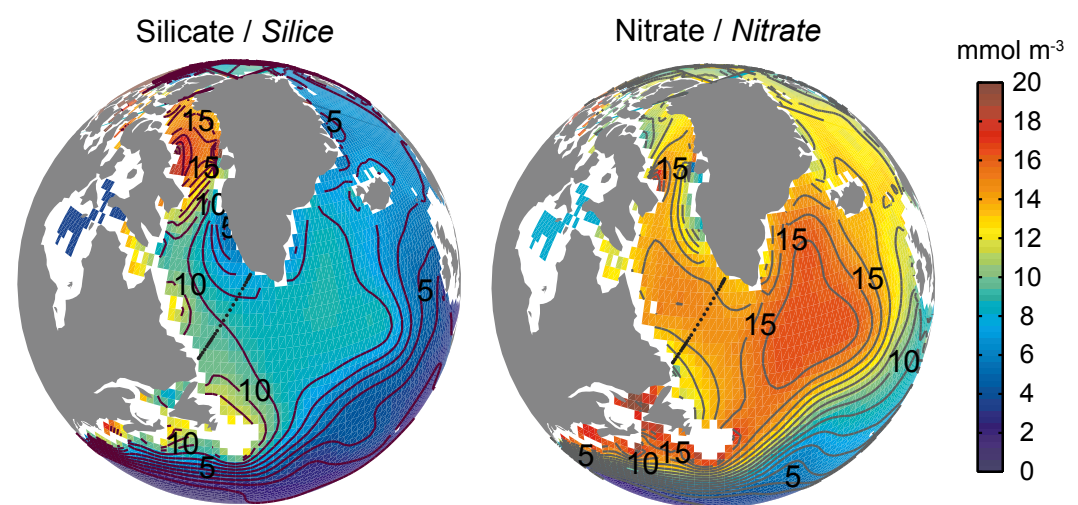


Fig. 9 Climatological distributions of silicate (left) and nitrate (right) at 200 m depth in the Northwest Atlantic from the World Ocean Atlas 2005. Dots mark the positions of the standard AR7W stations.

Concentration de la silice (à gauche) et de nitrate (à droite) à 200 m de profondeur dans l'Atlantique Nord-Ouest selon le World Ocean Atlas 2005. Les positions des stations standards AR7W sont illustrées par les points noirs.

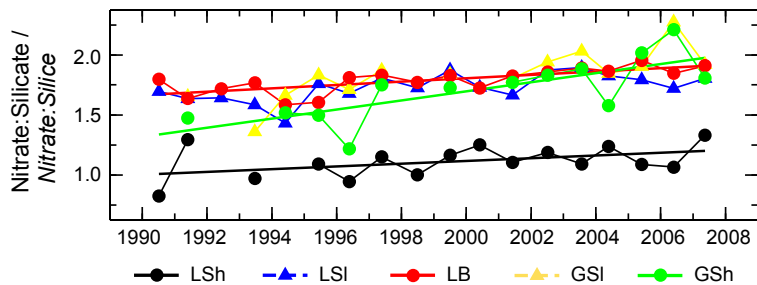


Fig. 10 Nitrate:silicate concentration ratios (60–200 m) and corresponding regression lines for groups of stations for the Labrador Shelf (LSh), the Labrador Slope (LSI), the central Labrador Basin (LB), the West Greenland Slope (GSI), and the West Greenland Shelf (GSh).

Les rapports des concentrations nitrate:silice (60 – 200 m) et les lignes de régression correspondantes pour des groupes de stations sur le plateau continental du Labrador (LSh), sur le talus continental du Labrador (LSI), dans le bassin du Labrador (LB), sur le talus continental de l'ouest du Groenland (GSI), et sur le plateau continental de l'ouest du Groenland (GSh).

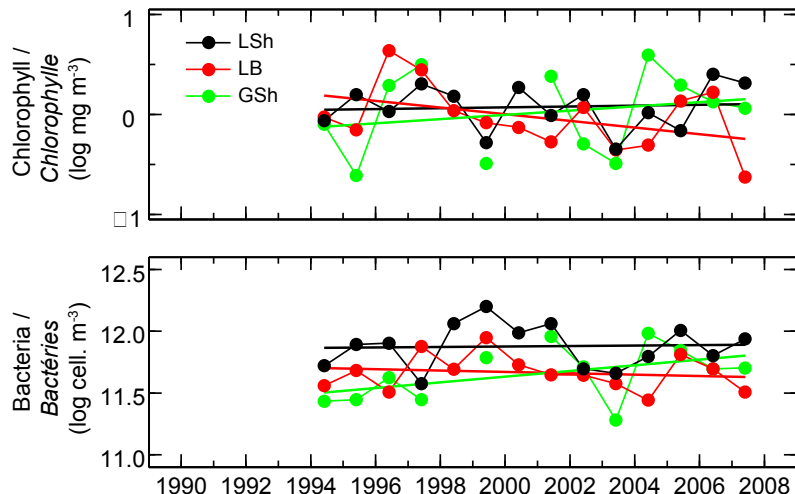


Fig. 11 Chlorophyll concentration (top) and bacterial abundance (bottom) in the 0–100 m depth range and corresponding regression lines for groups of stations for the Labrador Shelf (LSh), the central Labrador Basin (LB), and the Greenland Shelf (GSh).

Concentration de la chlorophylle (panneau du haut) et l'abondance des bactéries (panneau du bas) dans l'intervalle de profondeur 0–100 m et les lignes de régression correspondantes pour des groupes de stations sur le plateau continental du Labrador (LSh), dans le bassin du Labrador (LB), et sur le plateau continental de l'ouest du Groenland (GSh).

they both show slight negative trends in the central Labrador Basin. Increasing temperatures and shifts in nutrient levels might be expected to affect biological processes. These signals could be propagated through plankton food webs from the bottom up, starting at the level of phytoplankton, which are the primary producers. The issue of changes in species composition is under active investigation and is something to look for in future AR7W surveys.

The copepod *Calanus finmarchicus* makes up a large proportion of the total mesozooplankton biomass sampled on AR7W surveys. The 2007 survey took place from 12–18 May 2007, the earliest occupation of AR7W since annual observations began in the early 1990s. The spring

bloom had not yet begun on the Labrador Shelf and Slope, and reproductive success was correspondingly low in the western Labrador Sea. In West Greenland waters, the spring bloom was well underway and there was a corresponding increase in reproductive success. More detailed analyses of the zooplankton measurements on the 2007 AR7W survey will follow when all of the samples have been processed.

Highlights 2007

Overall, Labrador Sea surface air and sea temperatures remained warmer than normal in 2007 but showed a slight cooling relative to record-high values during 2002–2006. Annual mean surface air temperatures over the western Labrador Sea and eastern Canadian Arctic were up to 2°C cooler than record-high conditions observed in 2006. Sea-surface temperatures were up to 1°C warmer than normal in the west-central Labrador Sea but near or below normal on the Labrador Shelf and inner Labrador Slope.

The upper layers of the Labrador Sea remained warm and saline. Waters that have not recently been ventilated by winter convection continue to become warmer and saltier, indicating an increasing fraction of Atlantic waters from the south. Recent temperature and salinity trends in the upper 500 m of the central Labrador Sea are less obvious. These shallower levels have remained exceptionally warm and saline during the past 4–5 years.

Total inorganic carbon concentrations in the upper levels of the central Labrador Sea continued to increase with a corresponding decrease in pH. Dissolved oxygen concentrations in the same water mass show a downward trend. Nutrient conditions followed recent trends—downward in silicate and upward in nitrate—resulting in increasing nitrate:silicate ratios.

High variability in all biological properties makes multi-year trends uncertain. Upper-layer chlorophyll and bacteria concentrations have remained relatively stable for the last decade, but both show slight negative trends in the central Labrador Sea.

Acknowledgements

Figure 2 was provided by the NOAA/ESRL Physical Sciences Division from their Web site at <http://www.cdc.noaa.gov>. The HadISST 1.1 global sea-surface temperature data were provided by the Hadley Centre for Climate Prediction and Research (<http://www.metoffice.com>). Climatological hydrographic and nutrient data from the World Ocean Atlas 2005 were provided by the U.S. National Oceanographic Data Center (<http://www.nodc.noaa.gov/>). Many staff and associates of Ocean Sciences Division and Ecosystem Research Division at BIO have contributed to the Labrador Sea program. The efforts of the officers and crew of CCGS *Hudson* in support of this work in recent years are gratefully acknowledged.

Seasonal Cycles of *Calanus finmarchicus* Abundance at Fixed Time-Series Stations on the Scotian and Newfoundland Shelves (1999–2006)

Erica Head¹ and Pierre Pepin²

¹Bedford Institute of Oceanography, Box 1006, Dartmouth, NS, B2Y 4A2

²Northwest Atlantic Fisheries Centre, Box 5667, St. John's, NL, A1C 5X1

erica.head@mar.dfo-mpo.gc.ca

Sommaire

Les cycles saisonniers moyens de 1999 à 2006 de l'abondance bimensuelle de *Calanus finmarchicus* montrent que les jeunes stades copépodites (CI-CIII) apparaissent en avril-mai et juin-août aux stations des séries temporelles du PMZA Halifax (HL2) et St John's (Stn 27) respectivement. Les cycles saisonniers de la concentration intégrée de chlorophylle montrent que la floraison printanière débute en mars et atteint son maximum en avril aux deux stations. Par contre, les températures sont de 0,3 à 3,3°C plus froides à Stn 27 tout le long de l'année. Puisque les augmentations de la température et de la concentration de nourriture accroissent les taux de reproduction et de développement de *C. finmarchicus* et que les concentrations de phytoplancton sont comparables aux deux stations, il s'ensuit de l'apparition plus hâtive des jeunes stades à HL2 que la température a une plus grande influence pour déterminer le moment de l'apparition de la nouvelle génération. Un regroupement des années selon le moment de la floraison printanière et des conditions de température montre dans le cas de HL2 que pour les années chaudes quand la floraison de phytoplancton débute plus tôt, le maximum d'abondance de CI était plus tôt (début avril) que lors des années froides quand la floraison débute plus tard (début mai). À Stn 27, les CI apparaissent aussi plus tôt (début mai plutôt que début juin) et la floraison printanière débute plus tôt durant les années chaudes par rapport aux années froides. Un plus grand nombre d'œufs et de nauplii de *C. finmarchicus* produit en février et au début de mars à HL2 pourraient survivre jusqu'aux stades copépodites les années de floraisons hâtives par rapport aux années de floraisons tardives parce que les concentrations de phytoplancton dans le premier cas seraient suffisamment élevées au bon moment pour fournir une nourriture alternative aux prédateurs potentiels, lesquels peuvent inclure les femelles de *C. finmarchicus*. À Stn 27, la ponte et le développement des nauplii se font pendant la floraison printanière de sorte que la prédation, incluant par les femelles, serait moins importante.

Introduction

Sampling of hydrographic, chemical, and biological variables at fixed time-series stations is an important part of the Atlantic Zone Monitoring Program (AZMP). One of the goals of this sampling is to characterize the seasonal cycles of abundance of the dominant members of the zooplankton and how they vary from year to year with changes in environmental conditions. Variations in the reproductive timing of the dominant copepod zooplankton, *Calanus finmarchicus*, are important because its eggs and nauplii are preferred food sources for larval fish. In northern Norway, delays in *C. finmarchicus* reproduction, induced by low temperatures, have caused “mismatches” in the timing of the emergence of larval cod and their prey, which in turn resulted in poor cod recruitment (Ellertsen et al. 1989). In contrast, early reproduction of *C. finmarchicus* on Western Bank (outer central Scotian Shelf) in 1999 coincided with an exceptionally large year class of haddock (Head et al. 2005). These latter phenomena were accompanied by unusually high bottom temperatures in the waters surrounding the Bank and an unusually early spring bloom. Early blooms in other years have also coincided with years of high haddock recruitment (Platt et al. 2003).

The sampling undertaken for the AZMP at the fixed time-series stations off Halifax and St. John's (Fig. 1; HL2 and Stn 27) since 1999 has allowed us to describe the climatological seasonal cycles of abundance and stage distribution of *C. finmarchicus* at these locations and to explore how they are influenced by environmental changes.

Sampling and Analysis

Zooplankton samples were collected by vertical net hauls between the bottom (150 m at HL2, 170 m at Stn 27) and the surface using ring nets fitted with a 200 µm mesh, which collects all copepodite stages of *C. finmarchicus* with 100% effi-

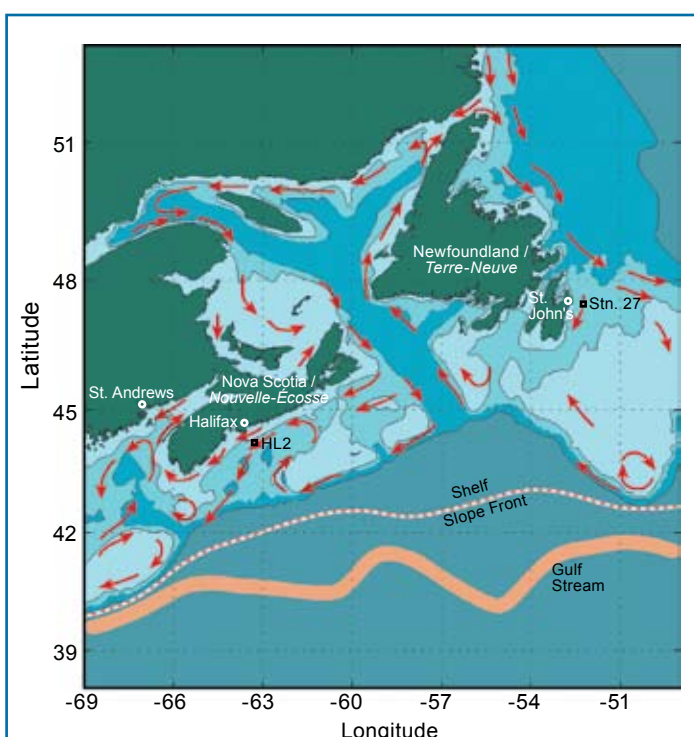


Fig. 1 Locations of fixed time series stations off Halifax (HL2) and St. John's (Stn 27). The dominant, long-term mean circulation over the Scotian and Newfoundland shelves is shown by red arrows.

Positions des stations fixes des séries temporelles au large de Halifax (HL2) et de St. John's (Stn 27). Les flèches rouges montrent le patron dominant de la circulation moyenne à long terme sur le plateau continental de la Nouvelle-Écosse et de Terre-Neuve.

cency. Zooplankton samples were preserved in 5% formalin. Three species of *Calanus* (*C. finmarchicus*, *C. glacialis*, and *C. hyperboreus*) are found at HL2 and Stn 27. In the AZMP samples, *Calanus* are identified and enumerated to the level

of stage and species in subsamples that contain at least 100 *Calanus* (Mitchell et al. 2002).

For the determination of chlorophyll *a* concentration, water samples were collected using Niskin bottles at fixed depths of 0, 5, 10, 20, 30, 40, and 50 m. The water was filtered through glass fibre filters and the chlorophyll was extracted and quantified fluorometrically using the method of Holm-Hansen et al. (1965) at HL2 and Welschmeyer (1994) at Stn 27. Temperature profiles were collected whenever biological sampling was carried out.

Calanus counts from the samples collected between January 1999 and December 2006 were used to generate average abundances for twice-monthly periods for each stage. Some two-week periods of the year were only sampled in a few years because of poor weather or logistical problems. In the worst case, there was only one sample for early March at Stn 27, and in general few samples were collected there during the winter months (Jan.-Mar.). The same twice-monthly averaging procedure was used for the chlorophyll *a* and temperature data. Chlorophyll *a* and temperature data collected in 1999 at Stn 27 were excluded because of the poor quality of the former.

Results and Discussion

All *C. finmarchicus* copepodite stages were found in high numbers at both stations, with the young stages (CI-III) dominant during the annual abundance peaks, which were in April-May at HL2 and June-early August at Stn 27 (Fig. 2). CVs were dominant during the late summer and fall. Adult CVI females were less abundant and males even less so. The life cycle of *C. finmarchicus* is annual over much of its range (Conover 1988). The general view is that mating occurs in early spring, the males then die and the females go on to lay eggs in the near-surface layers for 1-2 months, before they too die or are eaten. The eggs develop through six naupliar and four copepodite stages over spring and early summer, reaching the pre-adult CV stage by mid to late summer. The CVs descend from the surface layers to overwinter at depth in a resting, non-feeding state known as diapause, returning to the surface as adults to mate and reproduce the following year. This appears to be what happens at HL2, where there is one main peak of young stages (CI-III) in April-May. Using experimentally derived temperature-dependent development rates (Corkett et al. 1986), we can estimate that these CIs came from eggs laid during February-March.

At Stn 27, the peak abundance of young stages (CI-CIII) occurs in June-early August, and we can estimate that these individuals would have developed from eggs laid in April-late May. Young stages are present at Stn 27 from late August to February, however, indicating a prolonged reproductive period. This situation is akin to what is seen in the Lower St. Lawrence Estuary, where egg-laying persists until at least August (Plourde and Runge 1993), and in Cabot Strait, where young stages are present in October (Head and Pepin 2007).

Increases in temperature and food concentration lead to increases in female egg production rates (Campbell and Head 2000) and in growth and development rates of *C. finmarchicus* copepodites (Campbell et al. 2001). In addition, increased

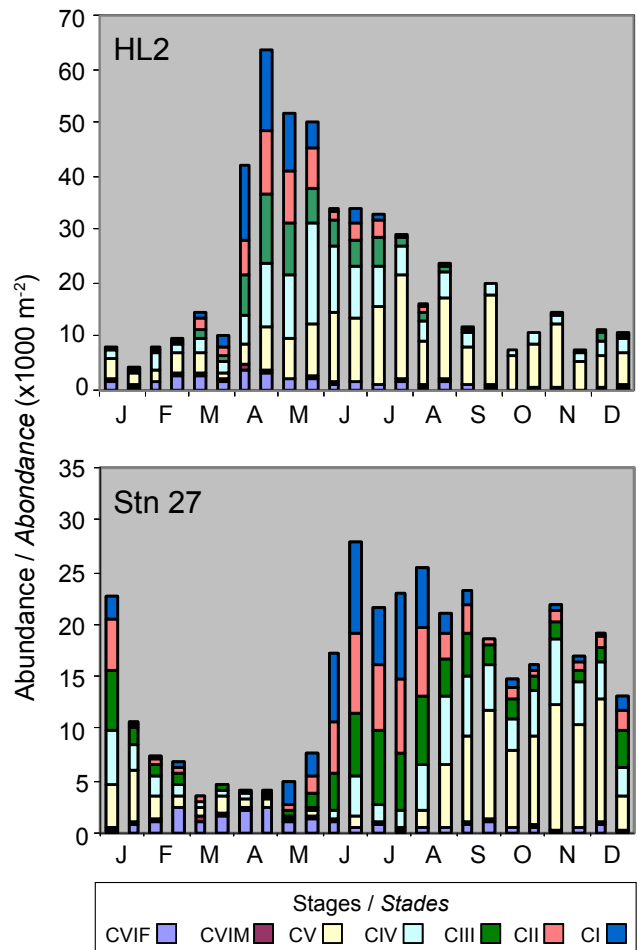


Fig. 2. Seasonal cycle of abundance of *Calanus finmarchicus* by stage at HL2 and Stn 27 averaged over two-week periods between January 1999 and December 2006.

Cycle d'abondance saisonnière de *Calanus finmarchicus*, moyennes bimensuelles pour chaque stade pour la période de janvier 1999 à décembre 2006 à HL2 et Stn 27.

food concentrations also promote development to egg-laying capacity in immature females (Plourde and Runge 1993). Thus, we would expect regional and inter-annual changes in temperature conditions and the dynamics of the phytoplankton bloom to influence the timing of the appearance of the year's new generation of *Calanus*. If we consider first the regional differences between HL2 and Stn 27, then we see that temperatures at HL2 are 0.3-2.3°C higher than at Stn 27 between February and June, while the chlorophyll peaks are at more or less the same time at both stations and are of comparable magnitude (Fig. 3). Although the temperature differences are not large, they are occurring over the range (-0.3 to 6.3°C) where changes in development rates with temperature are greatest (Corkett et al. 1986). Under these conditions, the new generation of CIs appears 2-3 months later at Stn 27, suggesting that temperature is having a greater effect on the timing of reproduction than is the timing or magnitude of the spring phytoplankton bloom.

An analysis of year-to-year differences in temperature and chlorophyll conditions at the individual stations was also carried out. In order to maximize the effects of differences in temperature and food concentration among years, we looked

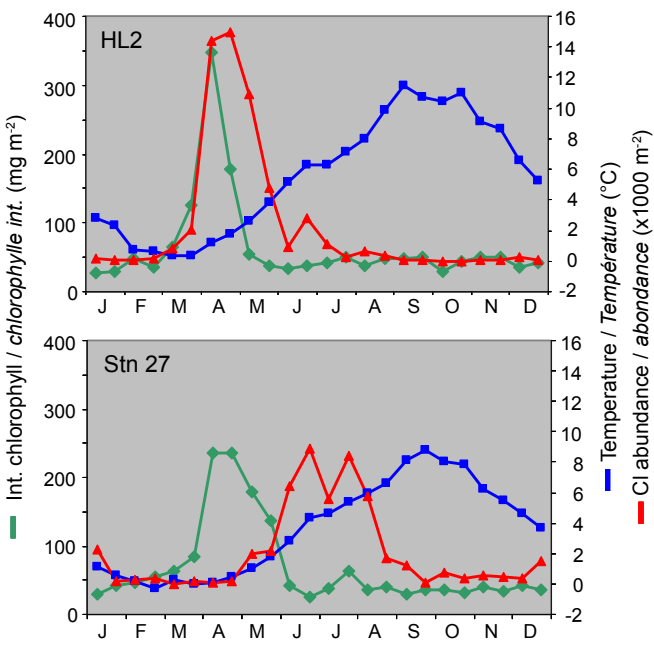


Fig. 3 Seasonal cycles of temperature (0–50 m average), chlorophyll concentration (integrated from 0 to 50 m), and stage CI *C. finmarchicus* abundance averaged over two-week periods between January 1999 and December 2006 at HL2 and January 2000 and December 2006 at Stn 27.

*Cycles saisonniers de la température (moyenne de 0 à 50 m), de la concentration de chlorophylle (intégrée entre 0 et 50 m) et de l'abondance du stade CI de *C. finmarchicus*, moyennes bimensuelles pour la période de janvier 1999 à décembre 2006 à HL2 et janvier 2000 à décembre 2006 à Stn 27.*

to see when chlorophyll concentrations reached a certain threshold level and what the average 0–50 m temperatures were during the two months prior to the appearance of the young stages, when egg-laying and growth through the naupliar stages would have occurred (Feb.–Mar. at HL2; Apr.–May at Stn 27). At HL2, years were classified as “early-warm” years if 0–50 m integrated chlorophyll concentrations reached 100 mg m⁻² before or during the first half of March and if average Feb.–Mar. temperatures were >0.4°C. These conditions were met in 1999 and 2002, when the Feb.–Apr. average 0–50 m temperature was 0.93°C. “Late-cool” years were years when chlorophyll concentrations reached 100 mg m⁻² during or after the second half of March and when average Feb.–Mar. temperatures were <0.4°C (2003–2005, average 0–50 m temperature was -0.29°C). This chlorophyll threshold was chosen because

maximal egg production rates are observed at concentrations above 100 mg m⁻² (E. Head, unpubl. data). Chlorophyll concentrations and CI abundances were then averaged over twice-monthly periods during these two groups of years. This analysis showed that peak abundance of CIs was higher and occurred one month earlier (early April versus early May) in early-warm years than in late-cool years (Fig. 4). In addition, in early-warm years, a second peak in CI abundance in late June became more distinct than the one seen in the seven-year climatology (Figures 3, 4). This second peak suggests that some CVs from the year's first generation matured to adulthood and produced a second generation. McLaren and Corkett (1984) and McLaren et al. (2001) have also reported seeing two generations of *C. finmarchicus* on Browns and Western banks, respectively. Finally, this analysis shows that the peak in CI abundance occurred after the peak in chlorophyll concentration rather than at the same time, as was seen in the seven-year climatology.

At Stn 27, sampling in the Feb.–Mar. period was too infrequent to allow grouping of the years according to the timing of the chlorophyll increase. It was, however, adequate in Apr.–May to allow us to group years into warm and cool years with average 0–50 m temperatures >0.4°C (2000 and 2004–2006; average 0–50 m temperature was 0.66°C) or <0.4°C (2001–2003; average 0–50 m temperature was -0.23°C). Interestingly, when the years were grouped this way, the resulting chlorophyll concentrations in February and March increased earlier in years that were warm in Apr.–May (Fig. 4). In fact, however, average 0–50 m temperatures in Apr.–May co-varied with those in Feb.–Mar. taken from the BIO Climate database,

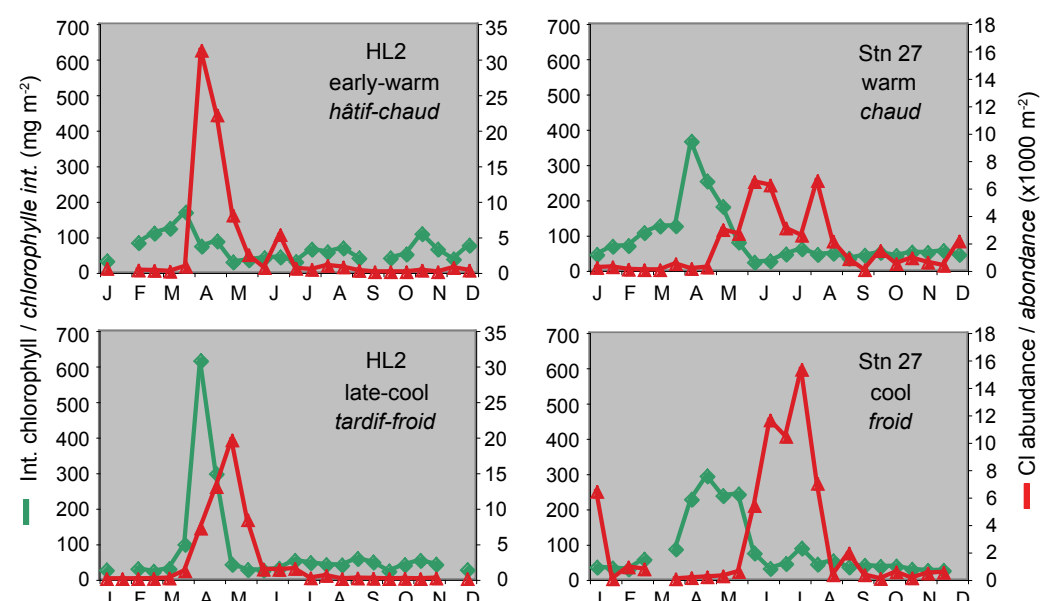


Fig. 4 Seasonal cycles of integrated chlorophyll concentration (0–50 m) and stage CI *C. finmarchicus* abundance in years with different temperature (0–50 m average) conditions in Feb.–Mar. (HL2) or Apr.–May (Stn 27) and with different bloom dynamics at HL2. HL2: early bloom, warm years (1999 and 2002); late bloom, cool years (2003–2005). Stn 27: warm years (2000 and 2004–2006); cool years (2001–2003).

*Cycles saisonniers de la concentration intégrée de chlorophylle (0–50 m) et de l'abondance du stade CI de *C. finmarchicus* selon les années de différentes conditions de températures (moyenne de 0–50 m) en février – mars (HL2) ou avril – mai (Stn 27) et selon différentes dynamiques de floraisons à HL2. HL2 : floraison hâtive, années chaudes (1999 et 2002); floraison tardive, années froides (2003–2005). Stn 27 : années chaudes (2000 et 2004–2006); années froides (2001–2003).*

which included some temperature profiles collected when there was no biological sampling. Thus, the bloom was earlier when Feb.-May temperatures were warmer. High numbers of CIs appeared earlier in warm years, although here, in contrast to HL2, the maximum abundance was higher in the cool years. As in the seven-year climatology, it is unclear whether there was more than one distinct generation, although there may have been a second production peak in the warm years.

One interesting point at HL2 is that the peak in chlorophyll concentration was much lower in early-warm years than in late-cool years. One reason for this difference may be that the mixed-layer depth is deeper in cool years (78 versus 44 m; G. Harrison, pers. comm.), so that the input of nutrients to the surface layers is probably greater. As well, however, because the CI peak occurs earlier and is larger in early-warm years, grazing by these and the late naupliar stages might have had more of an impact on the magnitude of the spring bloom peak than in late-cool years. At Stn 27, the grazing impact of the new generation would have been after the peak of the bloom in warm and cool years and so would not have differentially influenced the magnitude of the bloom. At HL2, the fact that the CI abundance peak is higher in warm years suggests that phytoplankton concentration is probably not an important factor in limiting *C. finmarchicus* growth. Instead, we suspect that in early bloom years it is the survival of the eggs and nauplii that may be enhanced by the early presence of high phytoplankton levels. In the absence of alternative foods, filter feeding copepods, including the female *C. finmarchicus* themselves, may feed on eggs and early nauplii. Cannibalistic behaviour has been suggested as a cause of high egg and early naupliar mortality for *C. finmarchicus* in the pre-bloom period in both the Labrador and Norwegian seas (Head et al. 2000; Ohman and Hirche 2001). By contrast, egg-laying at Stn 27 occurs during the spring bloom in both warm and cool years, so this cause of mortality is probably less important. Thus, CI abundance is no higher in warm years, when the bloom occurs early.

Concluding Remarks

We have assumed that *C. finmarchicus* population dynamics are principally the result of local processes and that advection is not important. We note, however, that these areas are known to be influenced by advection—the Nova Scotia Current at HL2 and the inshore branch of the Labrador Current at Stn 27 (see Fig.1)—and this is, to some extent, borne out in the data. For example, although the peak in abundance of young stages is substantially higher at HL2 than at Stn 27, the number of CVs accumulating in the fall is the same or lower. We contend, however, that events at these stations are representative of what is happening over larger areas, so that our analysis is valid, especially when we are considering relatively short time periods (e.g., Feb.-May or Apr.-July). We also note that our time series is as yet quite short: when we divide up the years to look at effects of environmental conditions, we have only 2–4 years to average over so that deficiencies in the sampling frequency become more of a problem and our analyses less robust. Nevertheless, we have been able to formulate hypotheses to explain inter-regional and inter-annual differences in *C. finmarchicus* dynamics between and at these stations, which

will be testable in the future both by the collection of more data by the AZMP and by the application of mathematical models leading to, we hope, predictive capacity.

References

- Campbell, R.G., Wagner, M.M., Teegarden, G.J., Boudreau, C.A., and Durbin, E.G.** 2001. Growth and development rates of the copepod *Calanus finmarchicus* reared in the laboratory. *Mar. Ecol. Prog. Ser.* 221: 161–183.
- Campbell, R.W., and Head, E.J.H.** 2000. Egg production rates of *Calanus finmarchicus* in the western North Atlantic: effect of gonad maturity, female size, chlorophyll concentration and temperature. *Can. J. Fish. Aquat. Sci.* 57: 518–529.
- Conover, R.J.** 1988. Comparative life histories in the genera *Calanus* and *Neocalanus* in high latitudes of the northern hemisphere. *Hydrobiologia* 167/168: 127–142.
- Corkett, C.J., McLaren, I.A., and Sevigny, J.-M.** 1986. The rearing of the marine calanoid copepods *Calanus finmarchicus* (Gunnerus), *C. glacialis* Jaschnov and *C. hyperboreus* Kroyer with comment on the equiproportional rule. In *Proceedings of the Second International Conference on Copepoda*, 13–17 August 1984. Edited by G. Schriver, H.K. Schminke, and C.T. Shih. National Museum of Canada, Ottawa, pp. 539–546.
- Ellertsen, B., Fossum, P., Solemdal, P., and Sundby, S.** 1989. Relation between temperature and survival of eggs and first-feeding larvae of northeast Arctic cod (*Gadus morhua* L.). *Rapp. P.-v. Réun. Cons. int. Explor. Mer* 191: 209–219.
- Head, E.J.H., and Pepin, P.** 2007. Variations in overwintering depth distribution of *Calanus finmarchicus* in the slope waters of the NW Atlantic continental shelf and the Labrador Sea. *J. Northw. Atl. Fish. Sci.* 39: 49–69.
- Head, E.J.H., Harris, L.R., and Campbell, R.W.** 2000. Investigations on the ecology of *Calanus* spp. in the Labrador Sea. I. Relationship between the phytoplankton bloom and reproduction and development of *Calanus finmarchicus* in spring. *Mar. Ecol. Prog. Ser.* 193: 53–73.
- Head, E.J.H., Brickman, D., and Harris, L.R.** 2005. An exceptional haddock year class and unusual environmental conditions on the Scotian Shelf in 1999. *J. Plankton Res.* 27: 597–602.
- Holm-Hansen, O., Lorenzen, C.J., Holmes, R.W., and Strickland, J.D.H.** 1965. Fluorometric determination of chlorophyll. *J. Cons. Cons. Int. Expl. Mer* 30: 3–15.
- McLaren, I.A., and Corkett, C.J.** 1984. Life cycles and production of two copepods on the Scotian Shelf, eastern Canada. *Syllogeus (Ntl. Mus. Can.)* 58: 362–368.
- McLaren, I.A., Head, E., and Sameoto, D.D.** 2001. Life cycles and seasonal distribution of *Calanus finmarchicus* on the central Scotian Shelf. *Can. J. Fish. Aquat. Sci.* 58: 659–670.
- Mitchell, M.R., Harrison, G., Pauley, K., Gagné, A., Maillet, G., and Strain, P.** 2002. Atlantic Zonal Monitoring Program sampling protocol. *Can. Tech. Rep. Hydrogr. Ocean Sci.* 223, 23 pp.
- Ohman, M.D., and Hirche, H.J.** 2001. Density-dependent mortality in an oceanic copepod. *Nature* 412: 638–641.
- Platt, T., Fuentes-Yaco, C., and Frank, K.T.** 2003. Spring algal bloom and larval fish survival. *Nature* 423: 398–399.
- Plourde, S., and Runge, J.A.** 1993. Reproduction of the planktonic copepod *Calanus finmarchicus* in the Lower St. Lawrence Estuary: relation to the cycle of phytoplankton production and evidence for a *Calanus* pump. *Mar. Ecol. Prog. Ser.* 102: 217–227.
- Welshmeyer, N.A.** 1994. Fluorometric analysis of chlorophyll *a* in the presence of chlorophyll *b* and pheophytins. *Limnol. Oceanogr.* 39: 1985–1992.

Understanding Copepod Life History Patterns Through Inter-Regional Comparison of AZMP Zooplankton Data[†]

**Catherine L. Johnson¹, Andrew W. Leising², Jeffrey A. Runge³, Erica J. H. Head¹,
Pierre Pepin⁴, Stéphane Plourde⁵, and Edward G. Durbin⁶**

¹Bedford Institute of Oceanography, Box 1006, Dartmouth, NS, B2Y 4A2

²National Oceanographic and Atmospheric Administration, Southwest Fisheries Science Center,
1352 Lighthouse Avenue, Pacific Grove, CA, 93950-2097, USA

³School of Marine Sciences, University of Maine, and Gulf of Maine Research Institute,
350 Commercial Street, Portland, ME, 04101, USA

⁴Northwest Atlantic Fisheries Centre, Box 5667, St. John's, NL, A1C 5X1

⁵Institut Maurice-Lamontagne, CP 1000, Mont-Joli, QC, G5H 3Z4

⁶Graduate School of Oceanography, University of Rhode Island, Narragansett, RI, 02882, USA
Catherine.Johnson@mar.dfo-mpo.gc.ca

Sommaire

Des séries temporelles de données démographiques provenant de quatre stations fixes dans l'Atlantique Nord-Ouest révèlent la variabilité dans le moment d'entrée et de sortie de la dormance, ou de la suspension du développement, chez des sous-populations du copépode *Calanus finmarchicus*. Afin de tester des hypothèses sur les signaux environnementaux contrôlant la dormance, des indicateurs basés sur les changements dans les proportions des stades de développement ont été développés. Aucun signal environnemental seul (la photopériode, la température en surface, ou la concentration de chlorophylle *a* moyenne en surface) n'a expliqué en totalité les dates d'entrée et de sortie pour toutes les stations. Parmi les hypothèses mises de l'avant pour expliquer la dormance chez les espèces de *Calanus*, nous ne pouvons éliminer l'hypothèse de la fenêtre d'accumulation de lipide pour l'initiation de la dormance ou de «l'horloge interne» modulée par les lipides contrôlant la durée de la dormance. La prémissse de base est que les individus peuvent entrer en dormance seulement si leur historique d'alimentation et de température leur permet d'accumuler suffisamment de lipides pour survivre la période hivernale, muer et initier les premiers stades de maturation et de développement des gonades. Une compréhension mécaniste de la dormance est cruciale afin de modéliser et de prédire l'effet du changement climatique sur les espèces dominantes de copépodes, ainsi que sur leurs prédateurs et leurs proies.

Introduction

In temperate and high-latitude ecosystems, several dominant oceanic copepods, including *Calanus* species, spend part of the year in a state of suspended development, or dormancy. Dormancy allows them to reduce their mortality during periods unfavourable for growth and reproduction (reviewed by Dahms 1995). Dormant copepods cease feeding and exhibit reduced metabolic rates. They also reside in deep water and are inactive, reducing mortality by both visual and non-visual predators. Emergence from dormancy and migration to the surface in winter or spring allows copepods to focus their reproductive efforts on the season when the spring diatom bloom supports high egg production rates (Dahms 1995).

Calanus finmarchicus dominates the zooplankton biomass in the North Atlantic and has a key role in the marine ecosystem as a grazer of phytoplankton and as prey for planktivorous fish, fish larvae, seabirds, and right whales. They are dormant mainly as fifth copepodid stages (CVs), the last juvenile stage of development, and dormancy begins in summer or autumn and ends in winter or early spring (reviewed by Hirche 1996). The timing of dormancy influences *C. finmarchicus* population dynamics and abundance through interactions with seasonal changes in food availability and temperature, and it also influences their availability as food for their predators. Despite extensive research on *C. finmarchicus*, the factors that control entry into and exit from dormancy remain unknown, in part because it cannot be induced under experimental conditions. Nevertheless, these control factors are critical to the population dynamics of this species (Carlotti and Radach 1996, Speirs

et al. 2006). Understanding dormancy transitions is a major challenge for modelling copepod population dynamics, particularly when evaluating the role of climate forcing in driving interannual and longer term population variability.

Seasonal cues like photoperiod and temperature, either alone or in combination, trigger the onset of dormancy in many insect species and in near-shore copepods that become dormant as “resting” eggs (Danks 1987, Dahms 1995), but photoperiod alone is not the trigger for *C. finmarchicus* (Hind et al. 2000). Warming or stratification, accompanied by declining primary production, may be a better predictor of impending unfavourable conditions. Alternatively, *C. finmarchicus* may be responding to an entirely direct cue, e.g., a decrease in food supply (Hind et al. 2000). However, *C. finmarchicus* need to achieve the CV stage and to accumulate a large quantity of wax ester, a storage lipid, before entering dormancy, so a direct cue may not result in optimal dormancy timing (Hirche 1996, Miller et al. 1998). Rey-Rassat et al. (2002) proposed that there is a threshold amount of wax ester needed to achieve moulting, gonad maturation, and the energetic requirements of dormancy. Accumulation of this threshold amount would trigger physiological responses, likely hormonally mediated (Irigoinen 2004), to descend to deep water and enter dormancy. Individuals not attaining this threshold would remain at the surface, moult to adulthood, and reproduce, although their offspring may face less favourable conditions than those experienced by individuals that entered dormancy.

For emergence from dormancy, photoperiod has been hypothesized as a control, but it probably does not provide a general cue since light does not penetrate to the depths occupied by many dormant *C. finmarchicus* populations (Miller et al. 1991). Energy consumption, particularly metabolism of

[†]This article is adapted from Johnson, CL, AW Leising, JA Runge, EJH Head, P Pepin, S Plourde, and EG Durbin (2008) Characteristics of *Calanus finmarchicus* dormancy patterns in the northwest Atlantic. ICES J. Mar. Sci. 65. Advance access: doi:10.1093/icesjms/fsm171

storage lipids, during dormancy could also influence emergence timing (Miller et al. 1991, Hirche 1996, Irigoien 2004, Saumweber and Durbin 2006) if *C. finmarchicus* must become active when they have depleted their lipid reserves to a certain level. Lipid must not be depleted below levels required for egg production or adult metabolism following emergence, especially in species that emerge before the spring bloom (Rey-Rassat et al. 2002, Irigoien 2004). A final suggestion is that the length of dormancy might be controlled by an endogenous developmental trigger, so that CVs emerge when they have developed to a given point in their prolonged moult cycle (Hind et al. 2000).

Here we investigate the control of dormancy timing and duration in populations of *C. finmarchicus* by comparing demographic data with environmental data from four coastal Atlantic Zone Monitoring Program time-series (AZMP) stations, which span approximately 5 degrees of latitude.

Methods

Data from the AZMP fixed stations on the Newfoundland Shelf (station S27, 175 m deep), the Anticosti Gyre (300 m), the Lower St. Lawrence Estuary (station LSLE, 300 m), and the Scotian Shelf (station H2, 140 m) were used (Fig. 1). Stations have been sampled approximately every two weeks since 1999, except in the Lower St. Lawrence Estuary where sampling began in 1994, with less-frequent sampling in winter

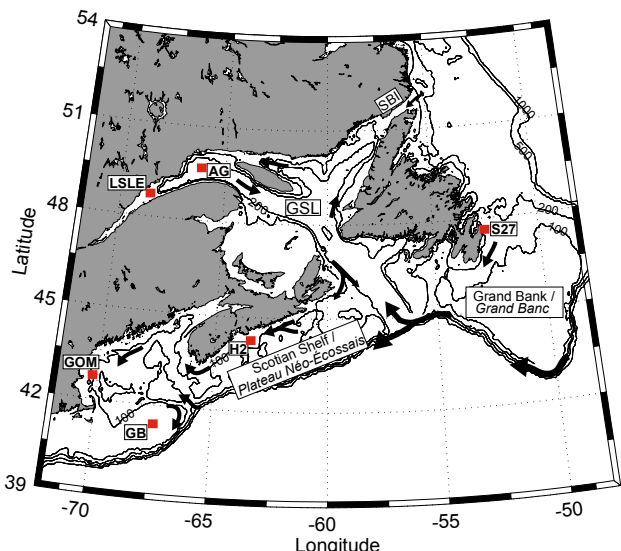


Fig. 1 Northwest Atlantic study region, including schematic surface currents and selected isobaths (in metres). Atlantic Zone Monitoring Program (AZMP) fixed stations: Anticosti Gyre (AG), Lower St. Lawrence Estuary (LSLE), Newfoundland Shelf (S27), and Scotian Shelf (H2). Other important locations include Georges Bank (GB), Gulf of Maine (GOM), Gulf of St. Lawrence (GSL), and the Strait of Belle Isle (SBI).

Région de l'étude dans l'Atlantique Nord-Ouest avec une illustration des courants de surface et quelques niveaux bathymétriques (en mètres). Les stations fixes du Programme de Monitorage de la Zone Atlantique (PMZA) : gyre Anticosti (AG), estuaire moyen du Saint-Laurent (LSLE), plateau de Terre-Neuve (S27), plateau Néo-Écossais (H2). Les autres lieux d'intérêt inclus sont le banc Georges (GB), le golfe du Maine (GOM), le golfe du Saint-Laurent (GSL) et le détroit de Belle Isle (SBI).

during periods of ice cover or bad weather. Zooplankton samples were collected using 0.75 m diameter ring nets equipped with 200 µm mesh. Nets were towed vertically from about 10 m above the bottom to the surface. Between 1994 and 2003 at the Lower St. Lawrence Estuary station, zooplankton was sampled on a weekly basis with a 1 m diameter 333 µm mesh net (for stages CIV-CVI) and a 1 m diameter 73 µm net (for CI-CIII and naupliar stages). Data collected up to and including 2005 were included in this analysis, except for the 2004 data at the Anticosti Gyre station.

Temperature and salinity data were collected using CTD profiles, and chlorophyll *a* was measured from Niskin-bottle samples and averaged over the upper 50 m at all fixed stations (http://www.meds-sdmm.dfo-mpo.gc.ca/zmp/main_zmp_e.html). The 5 m value was used as an index of surface mixed layer temperature. Deep-water temperature indices were calculated by averaging temperatures over the estimated depth range of dormant copepods at each of the four stations (Newfoundland Shelf: 100–160 m; Anticosti Gyre: 150–250 m; Lower St. Lawrence Estuary: 150–240 m; Scotian Shelf: 100–140 m). Day lengths at each station were calculated as the time between sunrise and sunset, as a function of latitude and day of year (Jarmo Lammi photoperiod calculator; <http://personal.inet.fi/cool/jjlammi/stuff.html>).

Proxies were developed to estimate dormancy entry and exit dates. The beginning of the dormancy onset period was defined as the date when the proportion of CVs in the population (i.e., CV/[CI-CVI]) rose to half its overall maximum, calculated as each year's maximum CV proportion averaged over all years. The start of the emergence period was defined as the first date when adults made up more than 10% of the population of stages from copepodid stage 1 to adult.

Emergence dates were also estimated by back-calculating the spawning dates of the first early copepodid stages to appear in spring. The development time from egg to CIII was estimated by running an individual-based model, starting eggs at each date of the year, and identifying the appropriate development time for CIIIs at the first appearance date. Spawning dates were calculated by subtracting the appropriate development time and 7 additional days—the time required for egg production to begin after moulting (Runge 1984, Plourde and Runge 1993).

One-way analysis of variance (ANOVA) was used to test whether environmental factors at onset and emergence were different among stations. A pairwise *t*-test with Bonferroni adjustment was used to test for differences in environmental factors among particular stations.

Results

The timing of onset of dormancy differed by up to three months among the four stations ($F = 22.32, p < 0.001$; Fig. 2). Onset of dormancy started earliest on the Scotian Shelf (mean date, 10 June) and latest on the Newfoundland Shelf (mean date, 24 September). There was also considerable interannual variability within regions (Figures 3–5). The appearance of adults and small peaks in early copepodid stages after the proxy onset date indicate that CVs enter dormancy over a broad range of times.

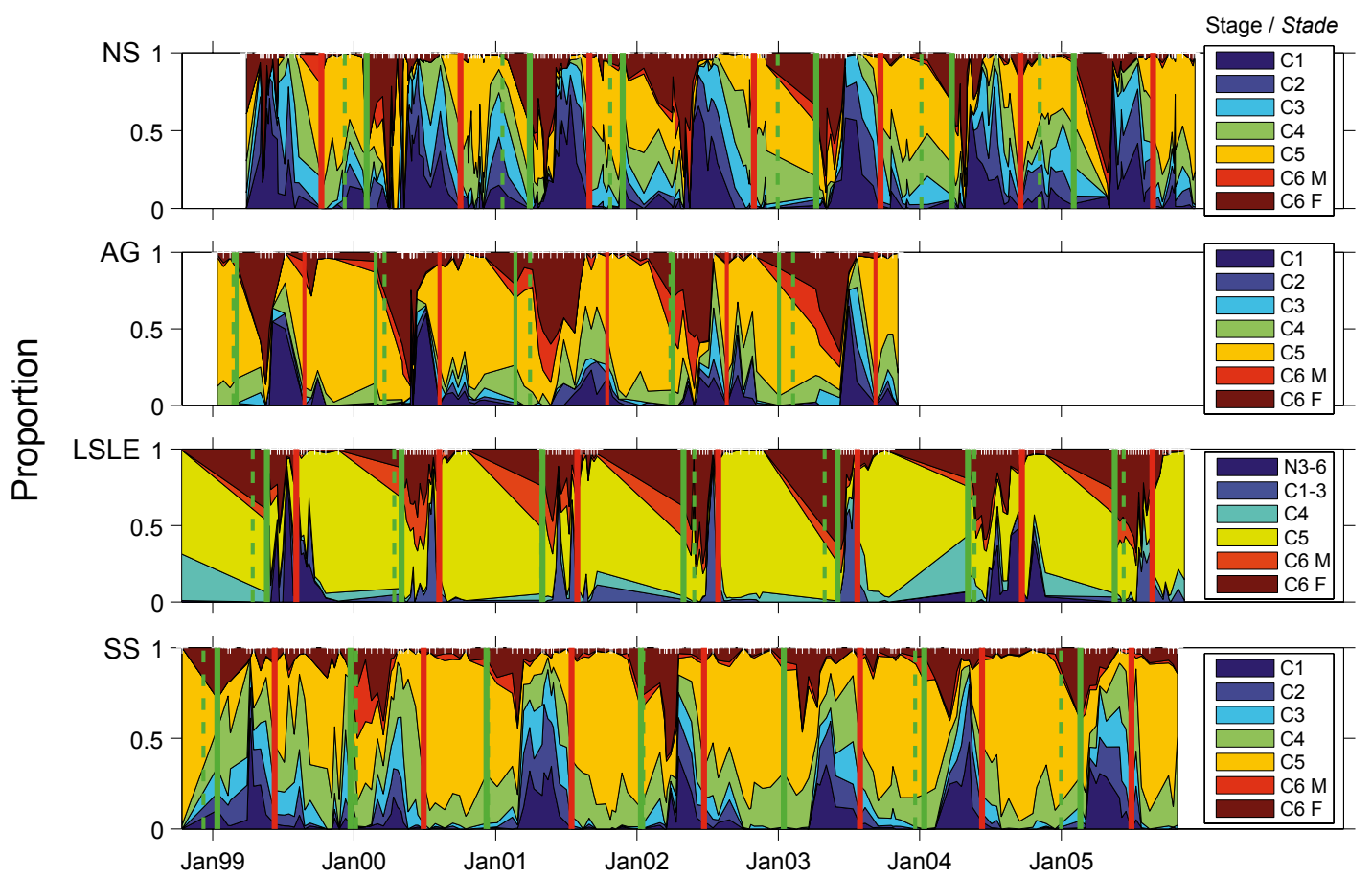


Fig. 2 Time-series demography of *C. finmarchicus* at the AZMP fixed stations. Proportion of naupliar (Lower St. Lawrence Estuary station only) and copepodid stages for each year for which data are available. Red line: estimated time of onset into dormancy; solid green line: estimated time of exit from dormancy based on the proportion of females present; dashed green line: estimated time of exit based on back-calculation from presence of early copepodid stages (saturating food conditions). See text for details of the method used for determining timing of onset and exit. NS: Newfoundland Shelf; AG: Anticosti Gyre; LSLE: Lower St. Lawrence Estuary; SS: Scotian Shelf.

Séries temporelles démographiques de *C. finmarchicus* aux stations fixes du PMZA. Proportion des stades de nauplii (station de l'estuaire moyen du Saint-Laurent seulement) et de copépodites pour chaque année où les données sont disponibles. Ligne rouge : estimation du moment d'entrée en dormance; ligne verte pleine : estimation du moment de sortie basée sur la proportion de femelles; ligne verte brisée : estimation du moment de sortie basée sur le rétrocacul à partir de la présence des premiers stades copépodites (conditions de nourriture non limitante). Se référer au texte pour les détails de la méthode de détermination du moment d'entrée ou de sortie. NS : plateau de Terre-Neuve; AG : gyre Anticosti; LSLE : estuaire moyen du Saint-Laurent; SS : plateau Néo-Écossais.

Emergence from dormancy began earliest on the Scotian Shelf (mean date, 10 January), Newfoundland Shelf (mean date, 19 February), and in the Anticosti Gyre (mean date, 23 February), and was latest in the Lower St. Lawrence Estuary (mean date, 8 May) ($F = 54.68, p < 0.001$), where emergence dates were nearly always on the first sampling date of the season. The proportion of adults in the population ramped up steadily after exceeding 10%, often to >50%. During this period, the total abundance of copepodid and adult stages was low: CVs are leaving dormancy, egg production has begun, and naupliar stages are appearing. Dormancy emergence dates estimated by back-calculation from the appearance of early copepodid stages corresponded well in most years with estimates from the stage-proportion-based proxy, except on the Newfoundland Shelf. There, the back-calculated emergence dates were considerably earlier, perhaps because early copepodid production persists sporadically through autumn and winter.

The four stations span approximately 5 degrees of latitude, with maximum and minimum day lengths differing at most

by about 45 min. The day lengths at which CVs started to enter dormancy were different among the four sites ($F = 18.38, p < 0.001$; Fig. 3). *Calanus finmarchicus* began to enter dormancy close to the summer solstice on the Scotian Shelf and during a period of declining day length elsewhere. Emergence from dormancy was generally during periods of increasing day length but sometimes began before the winter solstice. The mean day length at emergence was longer at the Lower St. Lawrence Estuary station than at the three other stations ($F = 119.2, p < 0.001$; Fig. 3).

Surface temperatures were very variable among stations, with minimum temperatures in February or March coinciding with strong vertical mixing and integrated heat loss through fall and winter, and maximum temperatures in late summer coinciding with strong stratification and shallow mixed layers (Loder et al. 1998). The amplitudes of the seasonal 5 m temperature cycles at the four sites were very different (Fig. 4). Minimum temperatures at 5 m in winter were lower at the more northerly stations, reaching about -1°C in the

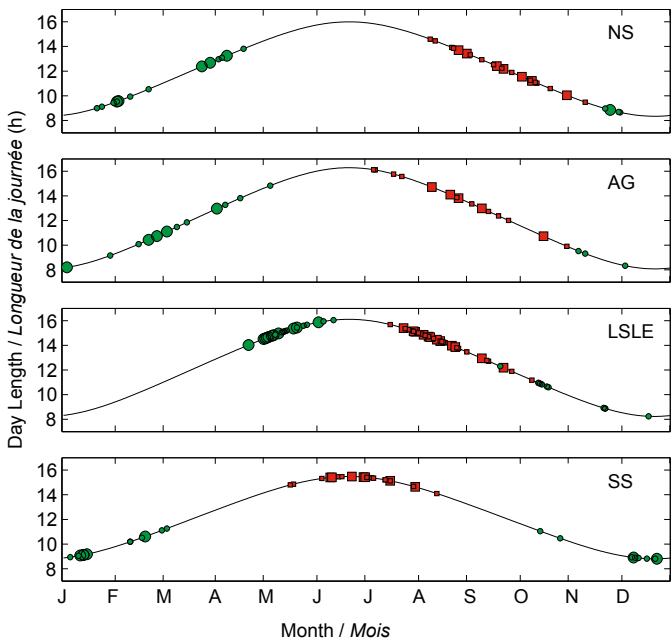


Fig. 3 Interannual variability in timing of dormancy onset and emergence superimposed on photoperiod cycles at each of the fixed stations. Large green circles: emergence date; small green circles: sampling dates before and after emergence; large red squares: onset date; small red squares: sampling dates before and after onset; solid line represents photoperiod. Abbreviations are as in Figure 2

Variabilité interannuelle du moment d'entrée et de sortie de la dormance superposée au cycle de la photopériode à chacune des stations fixes. Grands cercles verts : date de sortie; petits cercles verts : dates d'échantillonnage avant et après la sortie; grands carrés rouges : date d'entrée; petits carrés rouges : dates d'échantillonnage avant et après l'entrée. La ligne pleine représente la photopériode. Les abréviations sont les mêmes qu'à la figure 2.

St. Lawrence Estuary and on the Newfoundland Shelf. The Gulf of St. Lawrence is mostly covered with sea-ice from January to late March (Koutitonsky and Bugden 1991), while the Newfoundland Shelf is only ice-covered in some years. Minimum temperatures at 5 m generally dip to around 0.4°C on the Scotian Shelf. The highest maximum temperatures were observed on the Scotian Shelf in September and the lowest were in the lower St. Lawrence Estuary in August. The onset of dormancy began during different phases of the seasonal temperature cycle at the four stations. Onset started while the temperature was increasing on the Scotian Shelf, at around its peak in the Lower St. Lawrence Estuary, and after its peak on the Newfoundland Shelf and in the Anticosti Gyre. The temperature at onset was not significantly different on the Scotian Shelf, Newfoundland Shelf, and in the Anticosti Gyre, but was significantly lower in the Lower St. Lawrence Estuary ($F = 8.059, p < 0.001$; Fig. 4).

Chlorophyll cycles on both the Newfoundland Shelf and the Scotian Shelf were dominated by a spring peak in late March or April, with a smaller peak in late summer or autumn (Fig. 5). The onset of dormancy began about a month after the spring bloom on the Scotian Shelf and not until after the small autumn bloom on the Newfoundland Shelf. Spring chlorophyll peaks were later in the Lower St. Lawrence Estuary and the Anticosti Gyre (May–June),

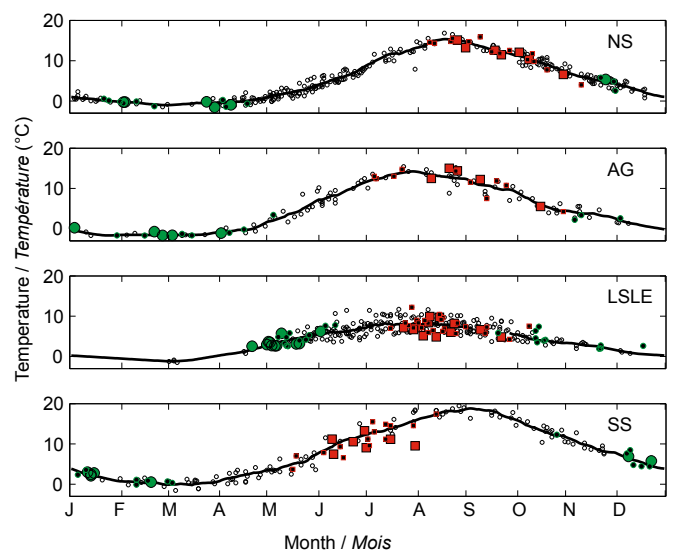


Fig. 4 Interannual variability in timing of dormancy onset and emergence superimposed on average 5 m temperature cycles at each of the fixed stations. Symbols and abbreviations are as in Figure 2. The solid line represents a 20-day running mean of temperature.

Variabilité interannuelle du moment d'entrée et de sortie de la dormance superposée au cycle moyen de la température (5 m) à chacune des stations fixes. Les symboles et les abréviations sont les mêmes qu'à la figure 2. La ligne pleine représente une moyenne mobile de 20 jours de la température.

but chlorophyll concentrations remained relatively high during summer and early autumn. At the latter stations, the onset of dormancy began during periods when climatological chlorophyll concentrations remained relatively high but were lower than the annual maxima. Chlorophyll concentrations experienced by copepods at the onset of dormancy were not significantly different among stations ($F = 2.427, p = 0.12$; Fig. 5), and the overall mean chlorophyll concentration at onset was lower than the threshold for maximum growth and development rates (Runge et al. 2006, R. G. Campbell, University of Rhode Island, pers. comm.). Emergence always began either before the spring chlorophyll peak or when chlorophyll concentrations were increasing before the peak (Fig. 5).

The duration of dormancy varied among regions (Fig. 6A). The longest duration, 8–9 months, was in the Lower St. Lawrence Estuary. Dormancy duration varied between 4 and 7 months in the Anticosti Gyre and on the Scotian Shelf. It was shortest, 3–6 months, at the Newfoundland Shelf station. There was no inverse relationship between deep-water temperature and dormancy duration (Fig. 6A), as would be expected if the initial lipid content was the same across regions and if there was a temperature-dependent endogenous timer. There was, however, a significant inverse relationship between the duration of dormancy and the surface layer temperature on the date of onset of dormancy, as would be expected if the quantity of stored lipid was temperature-dependent (Fig. 6B). Since *Calanus finmarchicus* grow larger at lower temperatures, their total lipid content is also likely to be larger at low temperatures, given adequate food concentrations (Miller et al. 2000, Saumweber and Durbin 2006).

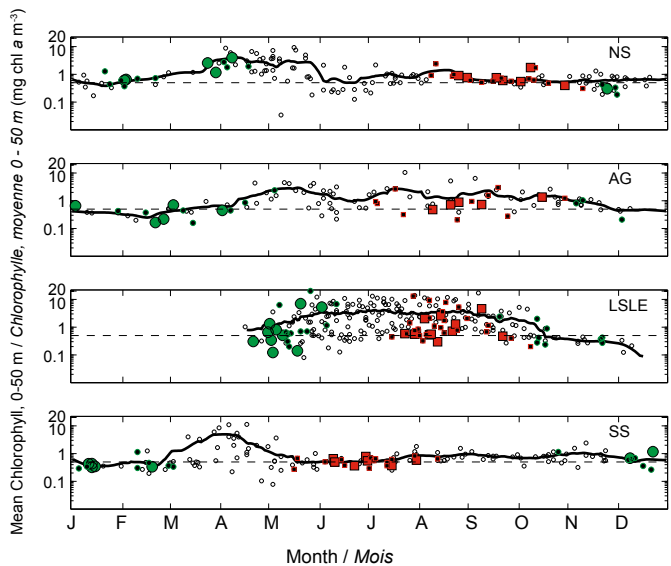


Fig. 5 Interannual variability in timing of dormancy onset and emergence superimposed on average cycles of the mean (0–50 m) chlorophyll *a* concentration at each of the fixed stations. Symbols and abbreviations are as in Figure 2. The solid line represents a 20-day running mean of chlorophyll *a* concentration. Dotted lines at 0.5 mg chl *a* m⁻³ represent approximate half-maxima for growth and egg production rates.

*Variabilité interannuelle du moment d'entrée et de sortie de la dormance superposée au cycle moyen de la concentration de chlorophylle *a* (0–50 m) à chacune des stations fixes. Les symboles et les abréviations sont les mêmes qu'à la figure 2. La ligne pleine représente une moyenne mobile de 20 jours de la concentration de chlorophylle *a*. La ligne pointillée à 0,5 mg chl *a* m⁻³ représente approximativement la moitié du maximum nécessaire pour la croissance et la production d'œufs.*

Discussion

The data collected at the AZMP fixed stations provide valuable time series of plankton and environmental conditions, but there are limitations to interpreting dormancy patterns from the observations. At all stations, advection could be a source of error if “new” individuals entering the sampling area have different environmental histories. The assumption here is that each station is representative of a broad regional area (Ouellet et al. 2003). Cross-shelf advection could bias results for the Newfoundland Shelf; however, springtime AZMP surveys in this region show little evidence of substantial differences in the relative stage composition of *C. finmarchicus* among the coastal areas, the continental slope, and the Labrador Sea (P. Pepin, unpublished data). The *C. finmarchicus* demographics at the Lower St. Lawrence Estuary station are likely a complex interaction of the dynamics of two subpopulations, one responding to the primary production cycle in the estuary and one responding to that in the northwest Gulf.

Among the potential environmental triggers, chlorophyll *a* concentration at the onset of dormancy was the only one that was relatively constant across all four stations. Variability in chlorophyll *a* concentration during summer was low at all stations, however, so chlorophyll *a* concentration alone did not offer a strong signal for induction of dormancy. Day length, sea-surface temperature, and photoperiod at onset of dormancy differed among stations, and there was also considerable interannual variability in the timing of onset and

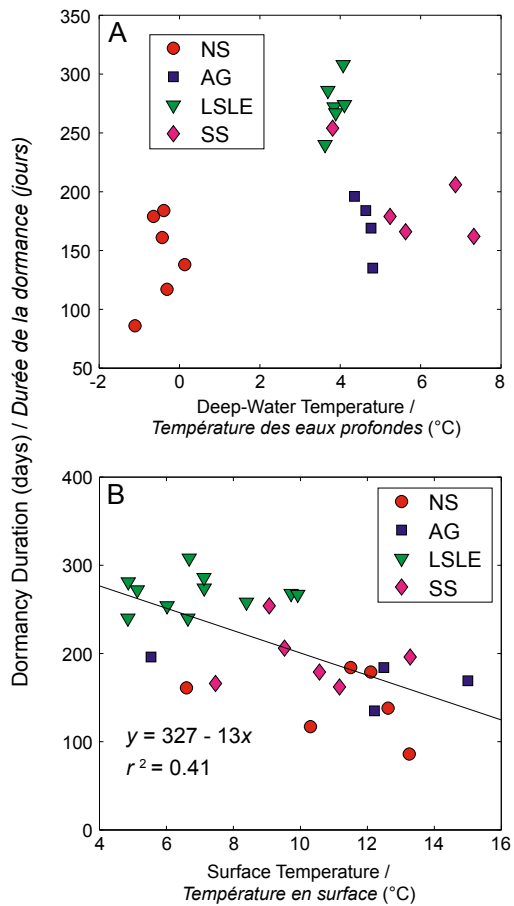


Fig. 6 Dormancy duration (difference between entry and emergence dates) as a function of (A) deep-water temperature representative of dormancy depth at each station, and (B) surface (5 m) temperature on the onset date. The regression relationship in (B) is significant ($p < 0.05$). Abbreviations are as in Figure 2.

Durée de la dormance (la différence entre les dates d'entrée et de sortie) en fonction (A) de la température des eaux profondes correspondant à la profondeur de la dormance pour chaque station, et (B) de la température en surface (5 m) à la date d'entrée. La régression en (B) est significative ($p < 0.05$). Les abréviations sont les mêmes qu'à la figure 2.

emergence within stations. Moreover, our analysis showed no consistent pattern in the gradients of environmental cues that could explain the observed dormancy entrance and exit patterns. We conclude that dormancy transitions must involve the interaction of multiple environmental factors.

The lipid accumulation window hypothesis provides a mechanistic explanation for the timing of dormancy entry involving a physiological response of the animals to their environmental history. Under this hypothesis, individuals can only enter dormancy if their food and temperature history allows them to accumulate sufficient lipid to sustain metabolism and support moulting and gonad maturation upon emergence (Rey-Rassat et al. 2002, Irigoien 2004). The capacity for lipid accumulation is probably, like body size, positively related to food availability and negatively related to temperature (Miller et al. 1977, 2000, Campbell et al. 2001). Consequently, there is a seasonal window where temperature and food conditions are propitious for an accumulation of lipids above the dormancy threshold. If the threshold is not attained by, say, midway through the CV stage, the internal process to prepare for

dormancy is not initiated and the individual continues on to moult to adulthood. Lipid data are not available for *C. finmarchicus* collected at the AZMP stations to test this hypothesis, but the interannual and among-station variability in timing of dormancy onset is consistent with variability in the timing and duration of the food and temperature conditions that form the lipid-accumulation window. The small number of females seen in autumn and winter represent the fraction of individuals that did not attain the lipid-store quota during the stage CIV/CV feeding period. Large lipid stores observed in the Lower St. Lawrence Estuary subpopulation (40–70% dry weight; S. Plourde, unpublished data) are consistent with the favourable temperature and feeding conditions for lipid accumulation during summer in the lower Estuary (Figures 4 and 5) and allow stage CVs to sustain dormancy for up to nine months (Fig. 6).

Control of dormancy duration and emergence would follow from concepts presented in Hind et al. (2000) and Saumweber and Durbin (2006). Development through stage CV continues at a reduced rate during dormancy compared with the development rate during its active phase. However, dormancy can also be terminated early if the metabolic use of wax esters during dormancy depletes lipid stores below some critical level. Under this hypothesis, the negative relationship between dormancy duration and surface temperature (Fig. 6B) would indicate that variable relative amounts of lipid stores are accumulated during the lipid-accumulation window, driven by constraints on lipid accumulation by higher temperatures (and perhaps lesser food availability). The absence of a negative relationship between dormancy duration and deep temperature (Fig. 6A) would arise because Newfoundland Shelf individuals store relatively little lipid (Fig. 6B), forcing a comparatively early exit from dormancy despite the cold temperatures.

To test the validity of the lipid accumulation window hypothesis, we intend to use a stage-based, individual-based model for *Calanus*, including processes controlling lipid accumulation and dormancy duration. The full model will show if a single parameterization of demographic and physiological processes can reproduce the observed dormancy patterns across regions. The true test of the hypothesis, however, will require field and laboratory experiments to further investigate the nature of the relationship between food availability and feeding and lipid accumulation rates. The development of a mechanistic understanding of dormancy patterns is critical for understanding the impacts of climate variability on *C. finmarchicus* population dynamics, since dormancy influences the population response to changes in ambient water temperature and the timing and duration of phytoplankton production cycles.

Acknowledgements

We thank Michael Bates for assistance with data analysis. The AZMP time series are maintained by funding from Fisheries and Oceans Canada. Support for the research was contributed by National Science Foundation and NOAA awards to JAR, AWL, and CLJ as part of the US GLOBEC program. CLJ was also supported by a National Science Foundation International Postdoctoral Research Fellowship.

References

- Campbell, R.G., Wagner, M.M., Teegarden, G.J., Boudreau, C.A., and Durbin, E.G. 2001. Growth and development rates of the copepod *Calanus finmarchicus* reared in the laboratory. Mar. Ecol. Prog. Ser. 221: 161–183.
- Carlotti, F., and Radach, G. 1996. Seasonal dynamics of phytoplankton and *Calanus finmarchicus* in the North Sea as revealed by a coupled one-dimensional model. Limnol. Oceanogr. 41: 522–539.
- Dahms, H.U. 1995. Dormancy in the copepoda – an overview. Hydrobiologia 306: 199–211.
- Danks, H.V. 1987. Insect dormancy: an ecological perspective. Biological Survey of Canada (Terrestrial Arthropods), Ottawa.
- Hind, A., Gurney, W.S.C., Heath, M., and Bryant, A.D. 2000. Overwintering strategies in *Calanus finmarchicus*. Mar. Ecol. Prog. Ser. 193: 95–107.
- Hirche, H.-J. 1996. Diapause in the marine copepod, *Calanus finmarchicus* – a review. Ophelia, 44: 129–143.
- Irigoin, X. 2004. Some ideas about the role of lipids in the life cycle of *Calanus finmarchicus*. J. Plankton Res. 26: 259–263.
- Koutitonsky, V.G., and Bugden, G.L. 1991. The physical oceanography of the Gulf of St. Lawrence: a review with emphasis on the synoptic variability of the motion. In The Gulf of St. Lawrence: Small Ocean or Big Estuary? Edited by J.-C. Therriault. Can. Spec. Pub. Fish. Aquat. Sci. 113. pp. 57–90.
- Loder, J.W., Petrie, B., and Gawarkiewicz, G. 1998. The coastal ocean off northeastern North America: a large-scale view. In The Sea, Vol. 11. Edited by A.R. Robinson and K. Brink. Harvard University Press, Cambridge, MA. pp. 105–133.
- Miller, C.B., Johnson, J.K., and Heinle, D.K. 1977. Growth rules in the marine copepod genus *Acartia*. Limnol. Oceanogr. 22: 326–335.
- Miller, C.B., Cowles, T.J., Wiebe, P.H., Copley, N.J., and Grigg, H. 1991. Phenology in *Calanus finmarchicus*: hypotheses about control mechanisms. Mar. Ecol. Prog. Ser. 72: 79–91.
- Miller, C.B., Morgan, C.A., Prahl, F.G., and Sparrow, M.A. 1998. Storage lipids of the copepod *Calanus finmarchicus* from Georges Bank and the Gulf of Maine. Limnol. Oceanogr. 43: 488–497.
- Miller, C.B., Crain, J.A., and Morgan, C.A. 2000. Oil storage variability in *Calanus finmarchicus*. ICES J. Mar. Sci. 57: 1786–1799.
- Ouellet, M., Petrie, B., and Chassé, J. 2003. Temporal and spatial scales of sea-surface temperature variability in Canadian Atlantic waters. Can. Tech. Rep. Hydrogr. Ocean Sci. 228, v+30 pp.
- Plourde, S., and Runge, J.A. 1993. Reproduction of the planktonic copepod, *Calanus finmarchicus*, in the lower St. Lawrence Estuary: relation to the cycle of phytoplankton production and evidence for a *Calanus* pump. Mar. Ecol. Prog. Ser. 102: 217–227.
- Rey-Rassat, C., Irigoien, X., Harris, R., and Carlotti, F. 2002. Energetic cost of gonad development in *Calanus finmarchicus* and *C. helgolandicus*. Mar. Ecol. Prog. Ser. 238: 301–306.
- Runge, J.A. 1984. Egg production of *Calanus pacificus* Brodsky: laboratory observations. J. Exp. Mar. Biol. Ecol. 74: 53–66.
- Runge, J.A., Plourde, S., Joly, P., Durbin, E.G., and Niehoff, B. 2006. Characteristics of egg production of the planktonic copepod, *Calanus finmarchicus*, on Georges Bank: 1994–1999. Deep-Sea Res. II 53: 2618–2631.
- Saumweber, W., and Durbin, E.G. 2006. Estimating potential diapause duration in *Calanus finmarchicus*. Deep-Sea Res. II 53: 2597–2617.
- Speirs, D.C., Gurney, W.S.C., Heath, M., Horbelt, W., Wood, S.N., and de Cuevas, B.A. 2006. Ocean-scale modeling of the distribution, abundance, and seasonal dynamics of the copepod, *Calanus finmarchicus*. Mar. Ecol. Prog. Ser. 313: 173–192.

Quality Control of Bottle Data at Maurice Lamontagne Institute

Contrôle de qualité des données bouteilles à l'Institut Maurice-Lamontagne

Laure Devine & Caroline Lafleur

Institut Maurice-Lamontagne, B.P. 1000, Mont-Joli, QC, G5H 3Z4
laure.devine@dfo-mpo.gc.ca

Abstract

This article describes the quality control tests that we at Maurice Lamontagne Institute (MLI) apply to data collected from water samples before the dataset is distributed and archived. The tests verify important metadata (sampling time and location) and examine the data from various perspectives, allowing the data manager to make judgments on the data's quality.

Introduction

Oceanographic missions nearly always include the measurement of basic physical variables like temperature and salinity. During some missions, including those made as part of the Atlantic Zone Monitoring Program, additional core variables are measured from water samples collected using bottle samplers (e.g., Niskin bottles) that are closed at discrete depths. Once the samples are taken and analyzed, the resulting data are compiled into datasets and made available to scientists. Reliable, high-quality data are the foundation for scientists to make accurate conclusions and predictions. One important role of data managers is to assure that the data they compile, distribute, and archive have been examined to assure their reliability. This activity is known as quality control (QC).

Common variables measured from water samples include dissolved oxygen, salinity, pigments, and nutrients. The quality control procedures outlined in this document are an amalgamation from many sources; we especially drew on those procedures used by NOAA's National Oceanographic Data Center during the production of the World Ocean Database (Conkright et al. 2002a, b) as well as many of the tests proposed in the GTSPP Real-Time Quality Control Manual ("Global Temperature-Salinity Pilot Project"; Unesco 1990)¹. In addition, we have sought the advice of many experts in different fields (e.g., P. Strain, Bedford Institute of Oceanography; D. Gilbert, MLI).

The dataset must first be compiled and the documentation completed before the QC procedure can begin. Essential metadata ("data about data") include time and position information, the variables measured, and the units in which they are reported. Additional metadata should be added when available; these can include information about the mission (mission number, chief scientist, start/end dates, sampling platform), about the event (sampling end times and positions, station names, comments on sampling or meteorological conditions that might affect data quality), about the data collection (instrumentation or gear used, including manufacturer and detection limits; sampling techniques, including the

Sommaire

Cet article décrit le processus de contrôle de qualité actuellement appliquée aux analyses d'échantillons d'eau de l'Institut Maurice-Lamontagne, préalablement à leur distribution et à leur archivage. Ce processus vérifie les métadonnées essentielles telles que la date d'acquisition et la localisation, et examine les données sous plusieurs angles afin de permettre au gestionnaire de données d'en juger la qualité.

Introduction

Les missions océanographiques incluent très fréquemment l'échantillonnage des variables physiques de base que sont la température et la salinité. Dans le cadre de certaines missions, incluant celles du Programme de Monitorage de la Zone Atlantique (PMZA), la prise de mesures sur des variables clés additionnelles implique également la récolte d'échantillons d'eau à des profondeurs discrètes avec des bouteilles (ex. bouteille Niskin) installées sur un appareil de prélèvement. Une fois l'analyse du contenu des échantillons effectuée, tous les résultats sont assemblés dans des jeux de données et mis à la disposition des scientifiques. La qualité de ces données est essentielle pour que les scientifiques puissent en tirer des conclusions fiables. Un rôle important joué par les gestionnaires de données est d'assurer que les données qu'ils compilent, distribuent et archivent ont été examinées pour déterminer leur fiabilité. Cette activité constitue le processus de contrôle de qualité (acronyme anglais QC).

Le contenu en oxygène dissous, en pigments et en éléments nutritifs de même que la salinité sont des variables couramment mesurées. Les procédures de contrôle de qualité présentées dans ce document proviennent de plusieurs sources; nous nous sommes particulièrement basés sur les procédures utilisées par le *National Oceanographic Data Center* de la NOAA lors de la production de la *World Ocean Database* (Conkright et al. 2002a, b) ainsi que sur plusieurs algorithmes proposés par le manuel *GTSPP Real-Time Quality Control Manual (Global Temperature-Salinity Pilot Project)*; Unesco 1990¹). Nous avons également demandé l'avis de spécialistes dans les domaines concernés (P. Strain, Institut océanographique de Bedford; D. Gilbert, IML).

Avant que ne débute le QC, il faut procéder à la compilation des données et de la documentation disponible. Les métadonnées («données sur les données») essentielles à obtenir sont la date et la position d'échantillonnage, les variables mesurées et leurs unités. Toute autre métad donnée peut être ajoutée selon la disponibilité de l'information, par exemple : sur la mission (numéro de mission, scientifique responsable, dates de la mission, plateforme d'échantillonnage), sur l'événement (nom

¹ For more detailed information, see the technical documents available at the Oceanographic Data Management System web site http://www.osl.gc.ca/sgdo/en/docs_reference/documents.html

¹ Pour de plus amples informations, consultez le document technique disponible sur le site du Système de Gestion des Données Océanographique : http://www.osl.gc.ca/sgdo/fr/docs_reference/documents.html

number of replicates), and about data analysis (a description of how the samples were stored, analysis method, precision of measurements, any comments on the analyses that might affect data quality). The quality control of historical data is somewhat different from that of recently collected data in that it could entail a suite of other tests and complications, e.g., checking for duplicates already present in data archives, incomplete metadata, and a limited ability to resolve inconsistencies and errors.

A preliminary examination of the dataset should be made before the structured QC procedure is begun in order to detect gross errors (order-of-magnitude-type problems). Here we ask ourselves the following questions: For data stored in an array, do the column headers align with the appropriate data values? Are the units correct? Were there data-handling errors noted in the field notebook, e.g., a leaking water sampler? Were there problems with sampling or sample storage? What value or symbol was used to indicate “no data”? We try to resolve any problems identified at this point and add QC flags as appropriate (see next section).

Our quality control of bottle data includes the validation of temperature, salinity, chlorophyll, dissolved oxygen, nitrate, nitrite, phosphate, and silicate measurements from a sample of seawater. The quality control procedure is composed of a set of tests that can be divided into five steps, similar to those used to QC conductivity-temperature-depth (CTD) data.

- Step 1: Tests validating the important metadata such as the time and position
- Step 2: Tests comparing data values within a profile
- Step 3: Comparison of the profile to a climatology
- Step 4: Comparison of all profiles from the same mission
- Step 5: Visual inspections of the cruise track, station data (ratios [e.g., N:P] and profiles), and of data from the entire mission (replicates, bottle versus CTD measurements, ratios and profiles, variable patterns with time).

While all metadata can be modified, in particular the time-space coordinates, without making the profile unusable, no data are modified by the quality control procedure. A quality flag is added to identify the data as good, doubtful, erroneous, or missing only for the step 2 tests. If the data must be modified for some reason, these modifications are made outside the quality control procedure. The quality flags must be manually adjusted in consequence and the modifications documented.

Description of the Quality Flags

The tests performed during step 2 add quality flags to the temperature, salinity, chlorophyll, dissolved oxygen, nitrate, nitrite, phosphate, and silicate data. The quality flag is a whole number between 0 and 9. The meanings of the quality flags are as defined in Unesco (1990) with two exceptions: while flags 6 through 8 were originally reserved for future use, we have assigned meanings to flags 7 and 8 according to our needs (Table 1).

The quality flags of higher value (except 7) take precedence over those with lower value; e.g., a QC flag of 0 has a lower

de la station, date et position de la fin de l'échantillonnage, commentaires sur les conditions météorologiques et sur l'échantillonnage), sur la manière dont les échantillons ont été récoltés (équipement d'échantillonnage ainsi que sa limitation, technique d'échantillonnage incluant le nombre de réplicats), sur la méthode d'analyse (une description des méthodes d'entreposage et d'analyse des échantillons, précision des mesures, commentaires sur l'analyse). Le contrôle de qualité de données historiques est quelque peu différent de celui des données récentes. Le QC de ces données peut imposer des tâches supplémentaires telles que la recherche de la présence de duplicitas dans les données déjà archivées, la recherche des métadonnées manquantes, et des possibilités réduites d'identifier les incohérences et les erreurs.

Un examen préliminaire du jeu de données est effectué avant de débuter les procédures de QC afin de détecter des erreurs «évidentes» (ex. des problèmes dans l'ordre de grandeur des valeurs rapportées). On procède alors en posant des questions telles que : Est-ce que les colonnes de données sont bien alignées et identifiées ? Est-ce que les unités de mesures sont correctes ? Y-a-t'il des commentaires sur la manipulation des échantillons comme une bouteille qui fuit ? Y-a-t'il eu un problème d'échantillonnage ou de conservation ? Quelle valeur a été utilisée pour les mesures manquantes ou inexistantes ? Nous essayons de régler les problèmes identifiés à ce stade et d'ajouter les sémaphores de qualité (voir section suivant) appropriés au besoin.

Le contrôle de qualité détaillé des données bouteilles permet de déterminer la validité des mesures individuelles de température, salinité, chlorophylle, oxygène dissous, nitrate, nitrite, phosphate et silice. Il se compose d'un ensemble de tests subdivisé en 5 étapes similaires aux étapes du QC des données d'un profiteur conductivité-température-profondeur (CTD)

- Étape 1 : Contrôle des métadonnées importantes telles que le temps et la position
- Étape 2 : Contrôle des enregistrements d'un profil les uns par rapport aux autres
- Étape 3 : Comparaison des données avec une climatologie
- Étape 4 : Comparaison des profils d'une même mission
- Étape 5 : Visualisation des métadonnées et des données par station (rapports [ex. N:P] et profils) et pour la mission entière (réplicats, données des bouteilles versus données CTD, rapports et profils, tendance des variables dans le temps).

Toute métadonnée erronée ou problématique peut être modifiée, en particulier la coordonnée temps-espace, sans rendre un profil inutilisable. Par contre, une donnée n'est jamais modifiée par le QC lui-même. Un sémaphore de qualité est ajouté pour qualifier les données de bonnes, douteuses, erronées ou manquantes seulement pour les tests de l'étape 2. Si les données doivent être modifiées pour une raison ou une autre, ces modifications sont apportées en dehors du contrôle de qualité. Le sémaphore de qualité doit être ajusté en conséquence et les modifications documentées.

Description des sémaphores de qualité

Les tests de l'étape 2 ajoutent des sémaphores de qualité aux données de température, salinité, chlorophylle, oxygène dis-

Table 1 Meaning of individual quality control flags.

Signification des sémaphores de qualité individuels.

Flag / Sémaphore	Meaning / Signification
0	No quality control / aucun contrôle de qualité
1	Value seems correct / la donnée semble correcte
2	Value appears inconsistent with other values / la donnée semble incrédule par rapport aux autres données
3	Value seems doubtful / la donnée semble douteuse
4	Value seems erroneous / la donnée semble erronée
5	Value was modified as a result of QC / la donnée a été modifiée
6	Reserved for future use / réservé à un usage futur
7	Possible problem with data point—further investigation required (MLI temporary flag) / la donnée semble problématique, vérification nécessaire (sémaphore temporaire, IML)
8	QC was performed by data producer / le QC a été fait par le producteur des données
9	Value missing / la donnée est manquante

priority than a flag of 9. As such, if a test judged a data value as doubtful (flag 3) and the following test judged it as erroneous (flag 4), the quality flag 4 would be retained. The QC flag 5 is assigned manually, generally as part of the QC process (as the result of investigations involving flags of 3 or 4). The QC flag of 7 is an exception since it is temporary. Data judged erroneous (flag 4) in a test are not considered in any subsequent tests.

Table 2 presents the list of tests we currently perform at our institute. The QCFF (“Quality Control Failed Flag”; modified from Unesco 1990) allows one to determine which test(s) the quality flag results from. It applies to the step 2 QC tests as well as to one step 3 test. Each test is associated with a number 2^x , where x is a whole positive number. Before running the quality control, a QCFF value of 0 is attributed to each line of data (i.e., to all the data from a given depth at a given station). When a test fails, the value of 2^x that is associated with that test is added to the QCFF. In this way one can easily identify which tests failed by analyzing the QCFF value. For example, if a data value failed test 2.9, then the QCFF would be 512. If test 2.7 had already failed, then the QCFF would be 640 (512+128). If the QC flag of a record is modified by hand, a value of 1 is added to the QCFF.

Descriptions of the Quality Control Tests

The first three tests reveal obvious errors: test 1.1 verifies that all the mission profiles were sampled from the same ship, test 1.2 verifies that the date and time of the beginning and end of the profile fall within the mission dates, and test 1.3 verifies that the profile's position is possible, that is, that the latitude falls between 90°N and 90°S and the longitude between 180°E and 180°W. Test 1.4 uses a detailed map of the coast of the Estuary and Gulf of St. Lawrence to check whether the profile's position falls on land. This test is also done for missions that take place in the Hudson Bay area or off the eastern Canadian coast, but the coordinates are adjusted and the available maps are not as detailed. Finally, test 1.5 checks the ship speed between two consecutive profiles. The ship speed is

sous, nitrate, nitrite, phosphate et silice. Le sémaphore de qualité est un nombre entier compris entre 0 et 9. La signification des sémaphores de qualité est celle de l'Unesco (1990) à l'exception de 2 sémaphores : alors que les sémaphores 6 à 8 sont réservés à un usage futur pour l'Unesco, nous avons défini les sémaphores 7 et 8 afin de répondre à nos besoins (Tableau 1).

La priorité des sémaphores est croissante, le sémaphore 0 étant le moins prioritaire et le sémaphore 9, le plus prioritaire (sauf le sémaphore 7). Par conséquent, si un test a jugé une donnée douteuse (sémaphore 3) et que le test suivant juge la même donnée erronée (sémaphore 4), c'est le sémaphore 4 qui sera conservé. Le sémaphore 5 est assigné manuellement par le gestionnaire de données suite au QC (suivant l'attribution des sémaphores 3 ou 4 résultant de l'examen des données). Le sémaphore 7 est une exception car il est temporaire. Les données jugées erronées (sémaphore 4) ne sont pas utilisées dans les tests ultérieurs.

Le tableau 2 dresse une liste des tests actuellement effectués à l'IML. Le sémaphore QCFF («*Quality Control Failed Flag*»; modifié de l'Unesco, 1990) est un sémaphore global qui permet de retracer la provenance du sémaphore de qualité. Il ne s'applique qu'aux tests de l'étape 2 et à un test de l'étape 3. À chaque test est associé un nombre 2^x où x est un nombre entier positif. Avant d'exécuter le contrôle de qualité, on attribue une valeur de QCFF de 0 à un enregistrement (soit toutes les données à une profondeur à une station donnée). Lorsqu'un test échoue, la valeur 2^x qui lui est associée est ajoutée au QCFF. On peut ainsi facilement retracer les tests échoués d'un enregistrement en décomposant le QCFF. Par exemple, si un enregistrement échoue le test 2.9, alors le QCFF sera de 512. Si en plus, le test 2.7 avait déjà échoué, alors le QCFF sera de 640 (512+128). Si un sémaphore de qualité d'un enregistrement est modifié à la main, une valeur de 1 est ajoutée au QCFF.

Description des tests du contrôle de qualité

Les trois premiers tests permettent de trouver les erreurs évidentes : le test 1.1 s'assure que toutes les données ont été échantillonnées à partir de la même plateforme, le test 1.2 vérifie que toutes les données récoltées l'ont été pendant la durée de la mission et le test 1.3 examine les positions des données qui doivent se situer entre 90°N et 90°S en latitude et entre 180°E and 180°O en longitude. Le test 1.4 permet de vérifier que les données ont bien été échantillonnées dans l'eau en comparant leur position avec une carte détaillée de la côte de l'estuaire et du golfe du St-Laurent. Ce test est aussi appliqué pour les données en provenance de la baie d'Hudson et de la côte est du Canada, mais les cartes disponibles sont moins précises pour ces régions. Le dernier test de ce groupe, le test 1.5, compare la vitesse de déplacement de la plateforme entre deux profils. La vitesse de la plateforme est calculée à partir des données temps-espace (date/heure-position) entre la fin d'un profil et le début du profil suivant. Si la position ou la date/heure finale

calculated using the time-space information at the beginning of the profile and those from the end of the preceding profile. If the end position or date/time of the preceding profile is missing, the test uses the coordinates at the beginning of the preceding profile to determine ship speed. The calculated speed is compared with the ship's cruising speed. Test 5.1 plots the cruise track on a map, allowing the identification of gross position errors.

Tests 2.1 and 2.2 check if the temperature, salinity, chlorophyll, dissolved oxygen, nitrate, nitrite, phosphate, and silicate data are globally and regionally possible. Except for nitrite, these values are from Appendix 9 of the World Ocean Database 2005 (WOD05); regionally possible values are those listed for the coastal North Atlantic (Johnson et al. 2006). Nitrite was excluded from the WOD05 since the data were not examined to ensure their quality; the nitrite ranges we use are from WOD98 (1998) and are used as a gross check. If a data value is judged impossible and thus erroneous, its QC flag is set to 4.

Test 2.4 checks whether the temperature, salinity, chlorophyll, dissolved oxygen, and nutrient data fall within the permitted limits according to depth interval. Again, these values are from the WOD05 for the coastal North Atlantic (Johnson et al. 2006; nitrite: WOD98 1998), except that salinity was modified to reflect conditions particular to the Gulf of St. Lawrence. A data value is judged doubtful if it does not fall within the permitted interval and its QC flag is set to 3.

The test for a constant profile, test 2.5, verifies whether the temperature, salinity, chlorophyll, dissolved oxygen, and nutrient data of a profile have identical values within the profile. To fail this test, the variable must have the same value at all depths. The quality flags are then set to 7 and the values must be checked individually and the flags modified to a valid QC code. The test is done for all the replicates of a variable.

Table 2 Description of quality control tests. The associated QCFF values are in parentheses.

Liste des tests de la procédure de contrôle de qualité. La valeur QCFF associée apparaît entre parenthèses.

Test	Description
Test 1.1	GTSPP platform identification / <i>GTSPP, identification de la plateforme</i>
Test 1.2	GTSPP impossible date/time / <i>GTSPP, date/heure impossible</i>
Test 1.3	GTSPP impossible location / <i>GTSPP, position impossible</i>
Test 1.4	GTSPP position on land / <i>GTSPP, position sur la terre</i>
Test 1.5	GTSPP impossible speed / <i>GTSPP, vitesse de la plateforme impossible</i>
Test 2.1	Global impossible variable value / <i>Valeur de la variable impossible à l'échelle planétaire</i> (2)
Test 2.2	Regional impossible variable value / <i>Valeur de la variable impossible à l'échelle régionale</i> (4)
Test 2.4	Profile envelope / <i>Limite de la variable par couche de profondeur</i> (16)
Test 2.5	Constant profile / <i>Profil constant</i> (32)
Test 2.6	Freezing point / <i>Point de congélation</i> (64)
Test 2.7	Replicate comparisons / <i>Comparaison des réplicats</i> (128)
Test 2.8	Bottle versus CTD measurements (temperature, salinity, dissolved oxygen) / <i>Comparaison des échantillons bouteilles avec les mesures du CTD (température, salinité, oxygène dissous)</i> (256)
Test 2.9	Excessive gradient or inversion (temperature, salinity, nitrite+nitrate, phosphate) / <i>Gradient ou inversion excessifs (température, salinité, nitrite+nitrate, phosphate)</i> (512)
Test 2.10	Surface dissolved oxygen data versus percent saturation / <i>Limite de l'oxygène dissous en surface (% saturation)</i> (1024)
Test 3.5	Petrie monthly climatology (temperature, salinity) / <i>Climatologie mensuelle de Petrie (température, salinité)</i>
Test 3.6	Brickman monthly climatology (nitrate, phosphate, silicate) / <i>Climatologie mensuelle de Brickman (nitrate, phosphate, silice)</i> (2048)
Test 5.1	Cruise track visual inspection / <i>Visualisation du trajet du navire pour la mission</i>
Test 5.2	Ratio and profile visual inspection (station data, profile by profile) / <i>Visualisation des profils et rapports (par profil)</i>
Test 5.3	Replicates visual inspection (data from entire mission) / <i>Visualisation des réplicats (par mission)</i>
Test 5.4	Bottle versus CTD measurements visual inspection (data from entire mission) / <i>Visualisation des données bouteilles par rapport aux données CTD (par mission)</i>
Test 5.5	Ratio and profile visual inspection (data from entire mission) / <i>Visualisation des profils et rapports (par mission)</i>
Test 5.6	Variable patterns with time (data from entire mission) / <i>Visualisation des tendances temporelles (par mission)</i>

d'un profil est manquante le test utilise l'information du début pour déterminer la vitesse. La vitesse calculée est comparée à la vitesse de croisière de la plateforme. Le test 5.1 est appliqué pour permettre de visualiser la route empruntée par la plateforme permettant au gestionnaire de données de détecter des incohérences évidentes de position ou de date d'échantillonnage.

Les tests 2.1 et 2.2 examinent les données de température, salinité, chlorophylle, oxygène dissous, nitrate, nitrite, phosphate et silice pour déterminer si elles sont possibles à l'échelle planétaire et régionale. Les valeurs limites de chaque variable, à l'exception du contenu en nitrite, sont tirées de l'annexe 9 de la *World Ocean Database 2005* (WOD05); les valeurs limites régionales sont celles de la zone côtière de l'Atlantique Nord (Johnson et al. 2006). Le contenu en nitrite n'a pas été examiné par WOD95. Par contre, la version 1998 de cette même base de données (WOD98) contient des valeurs qui nous ont permis de fixer les limites de cette variable. Si une donnée est jugée impossible, donc erronée selon les tests 2.1 et 2.2, son sémaphore de qualité est alors de 4.

Le test 2.4 vérifie si les données de température, salinité, chlorophylle, oxygène dissous et sels nutritifs se situent à l'intérieur des limites permises par intervalle de profondeurs. Pour ce test également, les valeurs sont tirées de WOD05 pour la zone côtière de l'Atlantique Nord (Johnson et al. 2006 ; nitrite : WOD98 1998) à l'exception des valeurs limites de salinité qui ont été modifiées pour refléter les masses d'eau du golfe du Saint-Laurent. La donnée est

jugée douteuse si sa valeur ne se situe pas à l'intérieur de l'intervalle permis et son sémaphore de qualité est fixé à 3.

Le test du profil constant, test 2.5, vérifie si les valeurs de température, salinité, chlorophylle, oxygène dissous et sels nutritifs d'un même profil sont identiques sur une partie de la pro-

Test 2.6 checks that the recorded temperature is not below the freezing point: salinity and pressure are used to calculate the freezing point and this is compared to the recorded temperature. If lower, the value is considered erroneous and its flag is set to 4.

Test 2.7 compares replicates of a sample among themselves. It applies to temperature, salinity, chlorophyll, dissolved oxygen, and nutrient data. Test 2.8 compares analyses resulting from bottle data with the same data type sampled by the CTD. Temperature, salinity, and dissolved oxygen are examined for test 2.8; chlorophyll is not considered because the CTD fluorometers are not calibrated presently. The maximum tolerated differences (Table 3) were determined empirically by examining several datasets. The quality flags of data that fail these tests are set to 7, thus the values must be subsequently verified individually and a valid QC flag assigned.

Test 2.9, for excessive gradients and inversions, calculates the vertical gradients or inversions of temperature, salinity, nitrate, and phosphate to see whether they exceed the values permitted. The gradient is obtained as the difference between one observation and the previous observation divided by the difference in depth between the two observations. The exercise is repeated for all replicates of the same variable. The limits are based on the maximum gradients and inversions given in WOD01 (Conkright et al. 2002a) for nitrate and phosphate and in Unesco (1990) for temperature and salinity (although we modified the inversion for salinity from 5 to 0.1 to better reflect local conditions). Data that fail this test are given a flag of 7.

The last step 2 test, 2.10, verifies that the percent oxygen saturation in surface waters, i.e., 0–10 m, falls between 85% and 150%. If the dissolved oxygen value fails this test, it is assigned

fondeur du profil. Pour échouer le test, il faut qu'une variable ait exactement la même valeur à toutes les profondeurs. Son sémaphore de qualité est alors de 7. Les valeurs devront être validées individuellement et un sémaphore de qualité valide devra leur être assigné une fois le QC terminé. L'exercice est répété pour tous les réplicats d'une variable.

Le test 2.6 compare la température de congélation, calculée à partir de la salinité et de la pression, à la valeur de température mesurée. Une valeur de température plus basse que la température de congélation correspondante est jugée erronée et un sémaphore de 4 lui est attribué.

Le test 2.7 compare les réplicats d'un échantillon entre eux. Il s'applique aux données de température, salinité, chlorophylle, oxygène dissous et sels nutritifs. Le test 2.8, quant à lui, compare les données des échantillons d'eau aux données équivalentes enregistrées par la sonde CTD. Il s'applique à la température, la salinité et l'oxygène dissous. La chlorophylle n'est pas considérée parce que le senseur de fluorescence n'est présentement jamais calibré dans notre laboratoire. Les écarts maximaux tolérés entre les réplicats d'une même variable (Tableau 3) ont été déterminés empiriquement en examinant plusieurs jeux de données. Toutes les données qui échouent le test 2.7 ou 2.8 ont un sémaphore de 7. Elles doivent être vérifiées ultérieurement et un sémaphore adéquat doit leur être attribué.

Dans le test 2.9, les gradients verticaux ou les inversions de température, salinité, nitrate et phosphate sont calculés afin de déterminer si elles excèdent les valeurs permises. Le gradient est obtenu par la différence entre une observation et l'observation précédente divisée par la différence de profondeur entre les deux observations. L'exercice est répété pour tous les réplicats d'une variable. Les limites permises sont tirées de WOD01 (Conkright et al. 2002a) pour le nitrate et le phosphate, et de l'Unesco (1990) pour la température et la salinité. Nous avons cependant modifié les critères d'inversion de la salinité de 5 à 0.1 pour correspondre aux masses d'eau locales. Les données qui échouent le test ont un sémaphore de 7.

Le dernier test de l'étape 2, le test 2.10, vérifie que le pourcentage de saturation en oxygène dissous en surface, c'est-à-dire entre 0 et 10 m, se situe entre 85 % et 150 %. Si la valeur d'oxygène dissous échoue ce test, un sémaphore 3 lui est attribué. Cependant, un très bas pourcentage de saturation des eaux de surface peut refléter un déficit réel qui se produit quand le broutage est intense ou à la fin d'un bloom de phytoplancton alors que l'activité bactérienne est importante (P. Strain, communication personnelle). Il se peut également qu'une masse d'eau de faible contenu en oxygène dissous soit remontée à la surface par un courant ascendant ou qu'une masse d'eau se refroidisse très rapidement créant ainsi un déséquilibre avec l'oxygène atmosphérique (D. Gilbert, communication personnelle). Réciproquement, un taux de saturation supérieur à 100 % est couramment observé dans des eaux

Table 3 Differences between values of a same variable that are allowed by the QC procedure. Replicate comparisons refer to replicate samples measured using the same analysis method; method comparisons refer to the same variable measured using different methods (e.g., CTD O₂ sensor and Winkler titration).

Écarts tolérés entre les valeurs d'une même variable par la procédure de contrôle de qualité. La comparaison des réplicats se réfère aux analyses effectuées avec une seule méthode sur un même échantillon. La comparaison des méthodes de mesure s'applique dans le cas où une variable est analysée ou mesurée de deux manières différentes (ex : le contenu en oxygène dissous mesuré avec un senseur fixé sur le CTD ou par titrage).

Variable	Tolerated difference / Écart toléré
<i>Replicate comparisons / Comparaison des réplicats</i>	
Temperature / Température	0.01°C
Salinity / Salinité	0.01
Dissolved oxygen / Oxygène dissous	0.5 mL L ⁻¹
Chlorophyll / Chlorophylle	0.5 mg m ⁻³
Nitrate	3.5 mmol m ⁻³
Nitrite	0.1 mmol m ⁻³
Phosphate	0.5 mmol m ⁻³
Silicate / Silice	4.0 mmol m ⁻³
<i>Method comparisons / Comparaison des méthodes de mesure</i>	
Temperature / Température	0.1°C
Salinity / Salinité	0.2
Dissolved oxygen / Oxygène dissous	1.0 mL L ⁻¹

a quality flag of 3. However, very low percent surface saturations may reflect O₂ deficits that occur when grazing becomes intense or when a bloom dies off and becomes food for bacteria (P. Strain, pers. comm.); they may also occur when seawater with low O₂ saturation is upwelled to the surface or when seawater cools too quickly for the dissolved oxygen to be in equilibrium with the atmosphere (D. Gilbert, pers. comm.). Conversely, surface saturations >100% are routinely seen in well-mixed or highly productive waters (values as high as 200% have been reported; P. Strain, pers. comm.). Therefore, the data manager will want to examine values flagged under this test to determine if one of these conditions were present. Consistent large deviations from 100% at the surface may indicate bad sensor calibration or a problem with titrations.

The step 3 tests involve comparisons with climatologies. Petrie et al. (1996) compiled a temperature and salinity climatology for the Gulf of St. Lawrence. The average and standard deviations of temperatures, salinities, and densities at fixed depths from 21 regions of the Gulf were calculated for each month. Test 3.5 uses this climatology to determine the validity of temperature and salinity observations from a mission. Test 3.6 is based on the nutrient climatology published by Brickman and Petrie (2003) for the Gulf of St. Lawrence, in which monthly averages and standard deviations of nitrate, phosphate, and silicate measurements were calculated for four depth intervals in 12 Gulf regions. We use this climatology to determine the validity of the nutrient observations of each profile from a mission. For both tests 3.5 and 3.6, a warning is given if the difference between the observations and the climatology exceeds three standard deviations. While no flags are added to the temperature and salinity values, the nutrient data are flagged 7 until they are more closely examined. It is then the data manager's responsibility to determine whether to add quality indicators to the temperature and salinity observations and to assign valid QC flags to the nutrient observations that were identified during these tests.

Comparisons with climatologies are problematic since a data point cannot be rejected simply because it fails the test: it might reflect an unusual event or it may be erroneous. In addition—and this is especially true for nutrient data—certain regions of the Gulf have only sparse measurements, especially at some times of the year, and coastal samples or measurements made in the upper estuary may show strong differences compared to the climatology. These factors must also be taken into consideration.

Test 5.2 allows one to examine the data from each station separately, with variables plotted against depth. The following variables are displayed:

- T-S diagram of the CTD data at the bottle sample depths
- CTD profiles of temperature, salinity, and dissolved oxygen with bottle sample measurements of the same variables plotted by depth
- Observations of chlorophyll, nitrate, nitrite, phosphate, and silicate by depth.
- N:P and N:Si ratios plotted with depth. The ratios are calculated from the averages of the replicates judged correct or possibly problematical (QC=1 or 7).

de surface bien mélangées ou très productives (des valeurs atteignant jusqu'à 200 % ont déjà été mesurées; P. Strain, communication personnelle). Le gestionnaire de données doit donc inspecter les valeurs jugées possiblement problématiques par ce test pour déterminer si l'une des situations précédentes prévalait lors de l'échantillonnage. La persistance d'un écart important de 100 % du pourcentage de saturation des eaux de surface peut indiquer un problème d'étalonnage du senseur d'oxygène dissous du CTD ou de mauvais titrages.

L'étape 3 du contrôle de qualité consiste à comparer les données avec des climatologies. Petrie et al. (1996) ont établi une climatologie des températures et salinités du golfe du Saint-Laurent. Les températures, salinités et densités moyennes à des profondeurs fixes, de 21 régions du golfe, ont été calculées pour chaque mois ainsi que leurs écarts-types respectifs. Le test 3.5 utilise cette climatologie pour déterminer la validité des observations de température et de salinité d'une mission. Le test 3.6, quant à lui, emploie la climatologie publiée par Brickman et Petrie (2003) pour le golfe du Saint-Laurent dans laquelle les valeurs moyennes par mois et les écarts-types des contenus en nitrate, phosphate et silice ont été calculés pour 4 intervalles de profondeur dans 12 régions du golfe. Nous utilisons cette climatologie pour déterminer la validité des observations de sels nutritifs de chaque profil d'une mission. Pour ces deux tests, un avertissement est émis si l'écart entre les observations et la climatologie excède trois écarts-types. Alors que seul l'avertissement est disponible pour la température et la salinité, un sémaphore de 7 est attribué aux sels nutritifs en attendant un examen plus approfondi. La responsabilité revient donc au gestionnaire de données de modifier ou d'ajouter un sémaphore de qualité aux données de température et de salinité et un sémaphore de qualité valable aux observations de sels nutritifs.

La difficulté, avec les comparaisons climatologiques, est qu'une donnée ne peut pas être rejetée simplement parce qu'elle échoue un des deux tests. Il se peut que le profil reflète un événement particulier ou bien qu'il soit réellement erroné. Pour certaines régions du Golfe, spécialement à certaines périodes de l'année, la climatologie des sels nutritifs est bâtie sur peu d'observations. Par exemple, les eaux très côtières et les eaux de l'estuaire supérieur ont des différences réelles souvent très marquées avec la climatologie. Il faut considérer ces phénomènes avant de déterminer la qualité d'une observation.

Le test 5.2 permet de visualiser les données de chaque station séparément sur la colonne d'eau. Les variables suivantes sont tracées :

- Diagramme TS des données du CTD aux profondeurs d'échantillonnage des bouteilles
- Température, salinité et oxygène dissous du CTD et données des mêmes variables des échantillons d'eau (bouteille) en fonction de la profondeur
- Observations de chlorophylle, nitrate, nitrite, phosphate et silice en fonction de la profondeur
- Rapports N:P et N:Si, en fonction de la profondeur. Les rapports sont déterminés à partir de la moyenne des réplicats jugés corrects ou possiblement problématiques (sémaphore 1 ou sémaphore 7).

These individual station plots are carefully examined for aberrant patterns.

Theoretically, replicates should have a 1:1 ratio, although this is rarely the case in practice. To identify potentially erroneous observations, test 5.3 plots replicate measures of temperature, salinity, chlorophyll, dissolved oxygen, and nutrients from the whole mission against each other. Outlier values are examined individually and quality flags assigned as necessary. Bad replicates may indicate sampling problems (verify field notebooks for indications of sample mix-ups or bottle leaks), transcription errors (check raw analysis files, verify calculations used to convert raw measurements to final units), or analysis problems (e.g., problems with standards, instrument malfunction, incorrect calibration factors). Beware of suspicious patterns (see Fig. 1).

Les graphiques par station sont examinés avec soin pour identifier tout profil aberrant.

Le rapport entre une mesure et son réplicat devrait théoriquement donner 1. En pratique, c'est rarement le cas. Afin d'identifier de potentielles observations fautives, dans le test 5.3, les réplicats de température, salinité, chlorophylle, oxygène dissous et sels nutritifs sont tracés en fonction de leurs premières mesures respectives pour l'ensemble de la mission. Les valeurs aberrantes sont examinées individuellement et un sémaphore de qualité leur est assigné si nécessaire. Les réplicats incohérents peuvent indiquer des problèmes d'échantillonnage (il faut alors rechercher dans les cahiers de terrain des commentaires concernant les mélanges d'échantillon ou les fuites de bouteille), des erreurs de transcription (vérifier les données originales, revoir les calculs de conversion des mesures brutes aux résultats finaux), ou des problèmes d'analyse (problèmes de standard, appareillages défectueux, facteurs d'étalonnage incorrects). Le gestionnaire de données doit rester vigilant aux patrons étranges (Fig. 1).

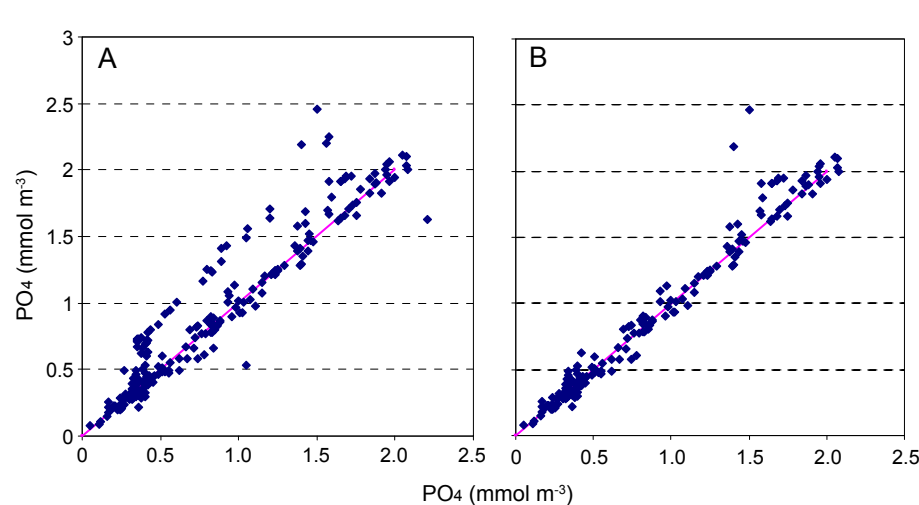


Fig 1 (A) The replicate differences in this example were not random. Examination of the raw analysis file revealed a bad standard for one series of analyses. (B) Data analyzed using the bad standard were flagged doubtful and are not plotted here (mission IML-2000-24).

(A) Les différences entre les réplicats de cet exemple ne sont pas aléatoires. Un examen du fichier brut d'analyse a révélé que le standard d'une des séries était erroné. (B) La série d'échantillons analysés avec le mauvais standard a été jugée douteuse et les données n'apparaissent plus sur le graphique (mission IML-2000-24).

Similarly, measurements made of the same variable but using different methods should agree; however, again this is rare in practice. To identify potentially bad observations, test 5.4 plots bottle data measurements of temperature, salinity, chlorophyll, and dissolved oxygen against the corresponding measurements made with the CTD for the whole mission. If the calibration of a CTD sensor is inadequate (or not done), the relationship between the bottle data values and the sensor readings will not be strong. Nevertheless, outlier values can still be identified and investigated by this method.

Test 5.5 plots the data resulting from bottle sample analyses of temperature, salinity, chlorophyll, dissolved oxygen, nutrients, and N:P and N:Si ratios for the whole mission by depth to reveal any potentially aberrant observations (Fig. 2).

For all the graphs generated during tests 5.2, 5.3, 5.4, and 5.5, bottle data already flagged during previous tests as doubtful (QC=3), erroneous (QC=4), or possibly problematical (QC=7) are plotted with different symbols indicating their

Dans le même ordre d'idée, les mesures de la même variable avec des méthodes différentes devraient normalement concorder mais la pratique démontre régulièrement des différences. Afin d'identifier de possibles valeurs aberrantes, dans le test 5.4, les données de température, salinité, chlorophylle et oxygène dissous des échantillons d'eau sont tracées en fonction des données CTD correspondantes pour l'ensemble de la mission. Si l'étalonnage d'un senseur du CTD est inadéquat, la concordance sera faible. Cependant, les valeurs s'écartant de manière importante de la relation pourront, tout de même, être identifiées.

Le test 5.5 permet de visualiser les données de température, salinité, chlorophylle, oxygène dissous, sels nutritifs, rapport N:P et rapport N:Si des échantillons d'eau pour l'ensemble de la mission. Celles-ci sont tracées en fonction de la profondeur afin d'identifier de potentielles observations fautives (Fig. 2).

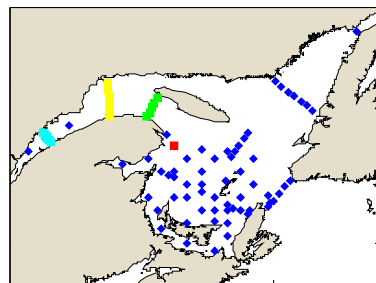
Pour tous ces graphiques, les données des échantillons d'eau jugées douteuses (sémaphore 3), erronées (sémaphore 4) ou possiblement problématiques (sémaphore 7) antérieurement aux tests 5.2 à 5.5, sont tracées avec des symboles différents de manière à mettre en évidence leur qualité. Aucun sémaphore n'est assigné par les tests de l'étape 5. Les valeurs extrêmes sont examinées et les sémaphores sont ajustés manuellement au besoin.

Le test 5.6 permet la visualisation simultanée des données de chlorophylle, oxygène dissous, nitrate, phosphate, silice, rapport N:P et rapport N:Si des échantillons d'eau, pour l'ensemble de la mission, en fonction de la profondeur et du temps (Fig. 3). Les données de profondeur sont d'abord tracées sous forme d'histogramme. Les données moyennes des variables à ces profondeurs y sont superposées. Seules

Cruise number / Numéro de mission : 06008

Cruise start / Début de la mission : 21-Jun-2006

Cruise end / Fin de la mission : 09-Jul-2006



All data / Toutes les données

TESL

TSI

TASO

Station 7.6

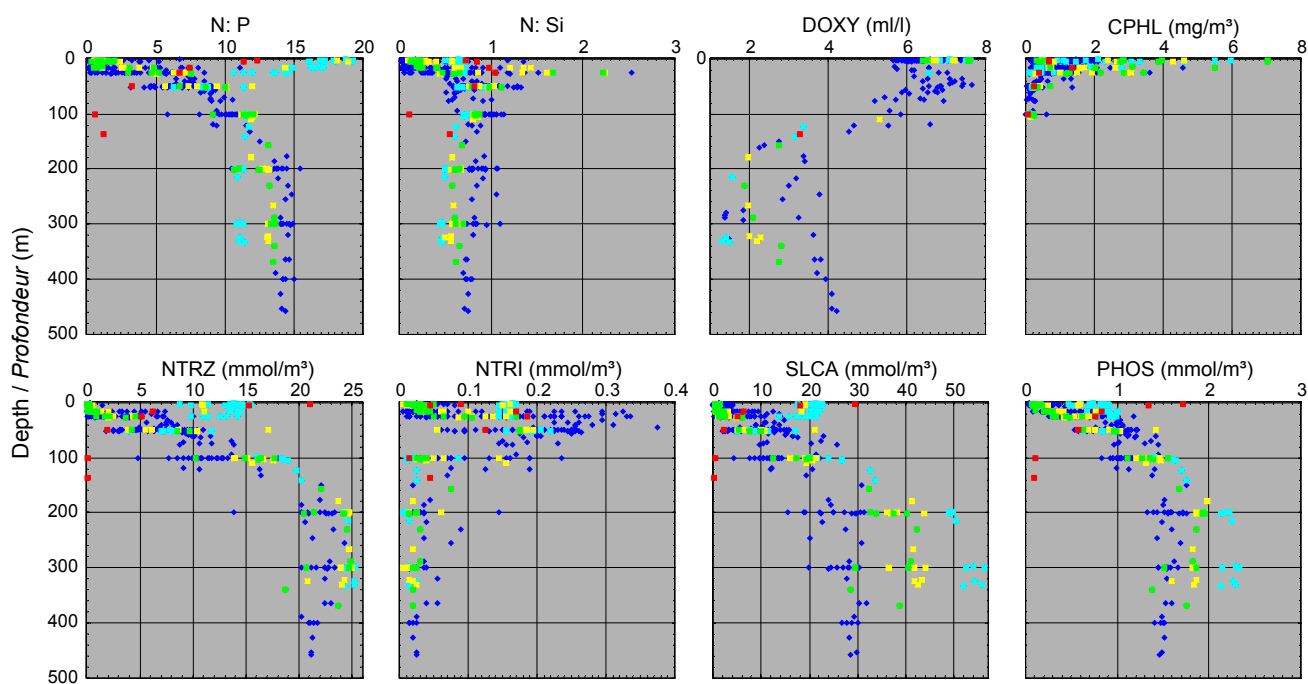


Fig. 2 Output graphic from IML's quality control procedure, test 5.5, ratio and profile visual inspection (data from entire mission). Note the outliers in several of the graphics (red symbols). Upon further examination, these points were found to be from the same station (7.6). It was determined that the sampling order had been mixed up, so the deep samples were actually surface samples and vice versa. Sample depths were corrected and all data were flagged 5 ("value changed as a result of QC"). In this figure, we can also see how the values of certain variables differ with geographic location. We see three distinct groupings of dissolved oxygen, phosphate, silicate, and the ratios with depth: the values in light blue are from the TESL transect in the upper Estuary and the intermediate values (yellow and green symbols) are from the TSI and TASO transects, respectively, farther downstream in the Estuary.

Graphiques résultants du test 5.5, visualisation des profils et rapports (par mission), de la procédure de contrôle de qualité de l'IML. Notez les valeurs anormales dans plusieurs des graphiques (symboles rouges). Nos recherches nous ont permis de découvrir que toutes ces observations ont été faites à la même station (7.6). Nous avons déduit qu'il y avait eu un mélange des échantillons et que les plus profonds étaient en fait les moins profonds et vice-versa. Les profondeurs ont été modifiées et nous avons assigné un sémaphore de 5 (la donnée a été modifiée) à ces données. Dans cette figure, nous pouvons également observer à quel point les valeurs de certaines variables varient selon la zone géographique. Nous distinguons trois ensembles distincts de valeurs d'oxygène dissous, phosphate et silice, de même que dans les rapports. Les valeurs en bleu pâle ont été obtenues le long de la section TESL dans l'estuaire supérieur; les valeurs intermédiaires (en jaune et vert) proviennent des sections TSI et TASO qui se situent vers l'aval du Golfe par rapport à l'Estuaire.

QC flag. No QC flags are automatically assigned with these visual tests. Outlier values are examined individually and quality flags determined as necessary.

Test 5.6 allows one to simultaneously view the bottle data analyses of chlorophyll, dissolved oxygen, nitrate, phosphate, silicate, and the N:P and N:Si ratios for the whole mission as a function of depth and time/space (Fig. 3). The bottle sample depths are first plotted as histograms, then the variable averages at these depths are plotted as points superimposed on the depths. Only data judged correct or possibly problematical (QC=1 or 7) are used to calculate the averages. This type of graph allows one to identify data that deviate from the overall general pattern.

les données jugées correctes (sémaphore 1) ou possiblement problématiques (sémaphore 7) sont utilisées pour calculer les moyennes. Ce type de graphique permet d'identifier les données qui s'écartent de la tendance générale.

À la fin du processus de QC, les données ayant le sémaphore temporaire 7 doivent être réexaminées. Il incombe au gestionnaire de données d'en déterminer la qualité et d'assigner un sémaphore valide. Aucun sémaphore 7 ne doit apparaître dans les archives du jeu de données traité.

Commentaires généraux

La section précédente décrit les tests faisant partie de la procédure de base du QC des données d'échantillons d'eau de l'IML.

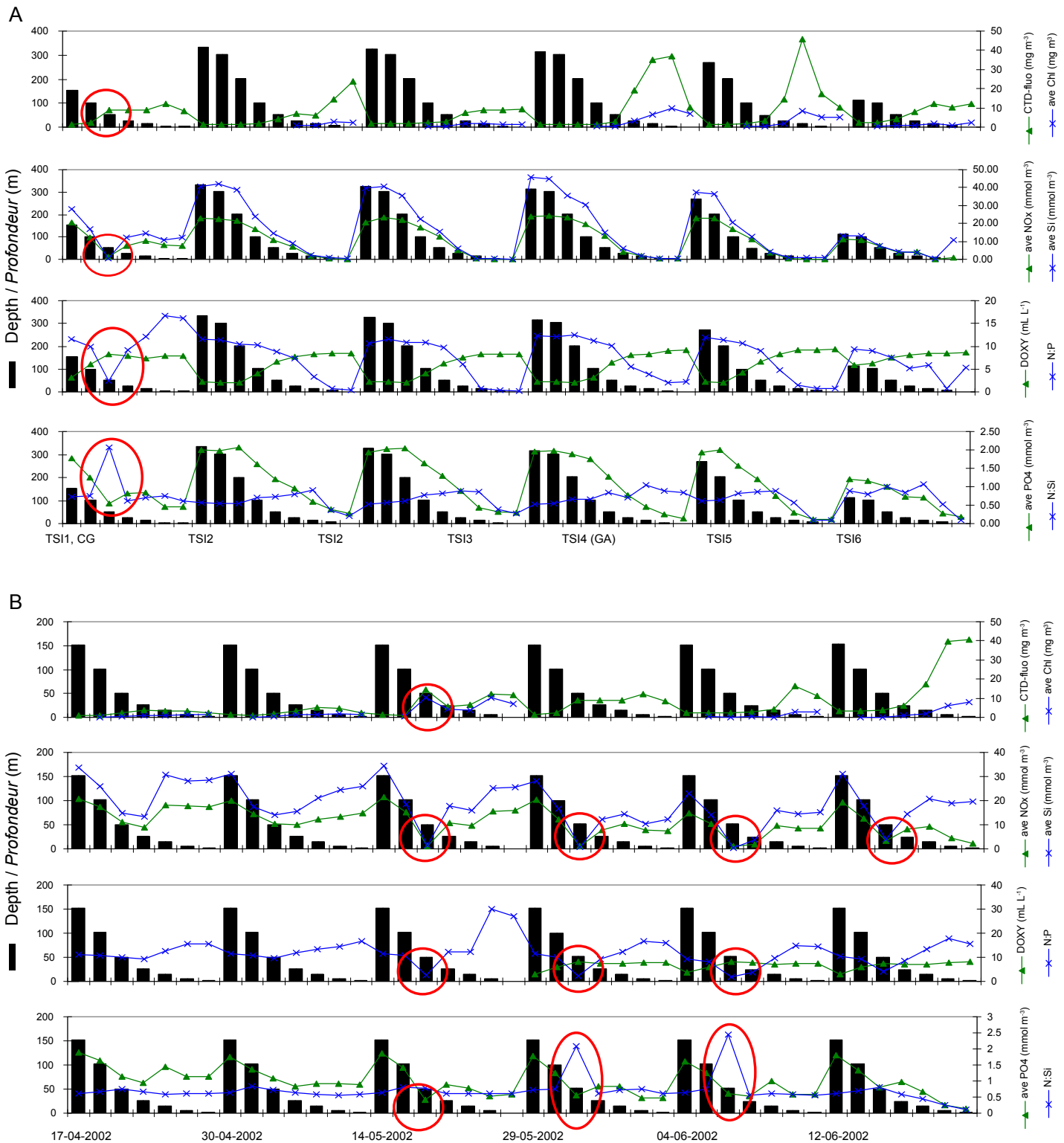


Fig. 3 (A) Mission IML-2002-23, Sept-Îles transect (TSI), 29 May 2002. The Gaspé Current fixed station (TSI1, CG; far left) showed peculiar data at 50 m: low nitrate, silicate, N:P; high N:Si, O₂, fluorescence. Data from this depth were initially flagged doubtful. (B) Mission IML-2002-01, Fixed station monitoring, Gaspé Current station, 17 April to 12 June 2002. The 50 m samples from 14 May and 4 June show nutrient and chlorophyll patterns similar to the 29 May sampling (sampled during mission IML-2002-23). Quality flags for all data were set to 1, indicating correct data.

(A) Mission IML-2002-23, section Sept-Îles (TSI), 29 mai 2002. La station fixe du courant de Gaspé (TSI1, CG; à gauche complètement) possède des valeurs particulières à 50 m : nitrate, silice et N:P faibles; N:Si, oxygène dissous et fluorescence élevés. Les données de cette profondeur ont initialement été jugées douteuses. (B) Mission IML-2002-01, station fixe du courant de Gaspé, 17 avril 2002 au 12 juin 2002. Les échantillons à 50 m du 14 mai et du 04 juin ont les mêmes propriétés que ceux du 29 mai (pendant la mission IML-2002-23). Nous avons attribué un sémaphore de 1 à ces données, ce qui indique qu'elles nous semblent correctes.

At the end of the QC procedure, the bottle data that have undergone these quality control tests must be re-examined if the quality flag assigned was 7 (temporary QC flag). The data manager must assess the validity of the value and assign a valid flag. No QC flags of 7 should remain in the archived dataset.

Final Comments

We have described the basic tests that are done within MLI's QC procedures, but a data manager may wish to perform additional tests. For example, examining the relationships between variables can reveal potential problems. We already inspect NO_3 vs. PO_4 and NO_3 vs. Si by profile and for all data from a mission combined: these nutrients have well-described relationships (Redfield 1958, Levasseur and Therriault 1987), even though it must be kept in mind that these relationships can differ in coastal or estuarine areas. Additionally, Si, PO_4 , and NO_3 vs. O_2 are also frequently examined (P. Strain, BIO, and Z.-P. Mei, UQAR, pers. comm.). The visualization of contour plots can also be useful in identifying outliers: a bull's eye or other unrealistic feature may identify an aberrant data point that has slipped through the above checks because it is difficult to identify non-representative values in sparsely sampled areas. A dataset may include variables that are not included in the routine QC tests; for these, the data manager should attempt to identify gross errors by looking for regionally impossible values.

It is interesting to note that the values for the variable ranges by basin as a function of depth (tests 2.1, 2.2, and 2.4) have been modified since the release of WOD98 (1998). In addition, the excessive gradient and inversion values (test 2.9) have been modified—and the gradient/inversion tests for O_2 , chlorophyll, and silicate eliminated—since the WOD98 document was published. This is an indication of the dynamic nature of the understanding of these variables and highlights the importance of careful consideration before doubtful or erroneous flags are assigned.

Data resulting from the Atlantic Zone Monitoring Program coming from MLI are submitted to these QC procedures before being distributed and loaded to the data archive. We can see the usefulness of the high-frequency fixed station data compared to the transect sampling twice a year. Figure 3A shows data from the Sept-Îles transect, where we see an odd pattern in the TSI1 (Gaspé Current) profile. Data related to these anomalous features were initially flagged doubtful. However, when the Gaspé Current fixed station data were examined, this feature was seen in the week preceding and the weeks following the transect mission (Fig. 3B), signifying a real pattern. The QC flags were finally set to indicate correct data.

When faced with anomalous values, a data manager must consider carefully before assigning quality flags to the data. Could some real phenomenon have caused the unusual values (e.g., upwellings, currents, increased freshwater inputs)? Are there potential anthropomorphic sources that might explain the values? Are bad instrument calibrations or unstable standards responsible? A piece of advice sent by a colleague has always helped guide the first author when she is faced with a particularly troublesome dataset: "Flagging 'bad' points in datasets is a tricky business. One should always worry about mislabeling as 'doubtful' or 'erroneous' data that are interest-

Il se peut toutefois qu'un gestionnaire de données soit intéressé par des tests additionnels. L'examen des relations existantes entre des variables peut servir à identifier des observations problématiques. Nous inspectons couramment les relations NO_3 versus PO_4 et NO_3 versus Si par profil et pour l'ensemble d'une mission. Ces éléments nutritifs ont des relations bien connues (Redfield 1958, Levasseur et Therriault 1987) même si elles peuvent démontrer des relations différentes en milieu côtier et estuaire. Les relations sels nutritifs (Si, PO_4 , NO_3) versus oxygène dissous sont fréquemment examinées dans d'autres laboratoires (P. Strain, BIO, et Z.-P. Mei, UQAR, communications personnelles). La visualisation des graphiques de contour des variables peut permettre de diagnostiquer une incohérence qui aurait échappé au contrôle de qualité parce qu'il est difficile d'identifier des valeurs non représentatives dans des régions partiellement échantillonées. Si un jeu de données comporte des variables exclues du QC, il peut alors s'avérer nécessaire de rechercher manuellement les valeurs impossibles à l'échelle régionale.

Un fait intéressant à noter est que les plages de valeurs acceptables en fonction de la profondeur (test 2.1, 2.2 et 2.4) pour les différents bassins océanographiques ont évoluées depuis la publication de WOD98 (1998). Les valeurs acceptables pour les gradients et inversions (test 2.9) ont également été modifiées voire même abolies dans le cas des contenus en oxygène dissous, en chlorophylle et en silice. C'est la démonstration de la nature dynamique de la compréhension des variations de ces variables et cet exemple nous confirme qu'il faut être très prudent dans l'assignation d'un sémaphore de qualité.

Toutes les données du PMZA produites à l'IML sont soumises à ce processus de QC avant d'être distribuées et archivées. Depuis que nous effectuons le QC à l'IML, nous nous sommes rendu compte qu'il est essentiel d'examiner les données sous tous les angles possibles. L'étude des données échantillonées fréquemment en station fixe par rapport aux données des sections échantillonées deux fois l'an en est un bon exemple. La figure 3A montre des données de la section de Sept-Îles où l'on note un profil apparemment anormal à TSI1 (courant de Gaspé). Les données associées à cette anomalie ont d'abord été jugées douteuses. Cependant, un examen des données temporelles de la station courant de Gaspé a révélé que les mêmes caractéristiques ont été observées dans les semaines précédant et suivant l'échantillonnage de la section (Fig. 3B), suggérant donc un patron normal. Par conséquent, les données sont jugées correctes.

En conclusion, quand un gestionnaire de données est confronté avec des valeurs anomalies, il doit examiner attentivement les données avant de leur assigner un sémaphore de qualité. Est-ce qu'un phénomène réel peut donner de tels résultats (remontée des eaux, courants, augmentation des apports d'eau douce) ? Est-ce qu'un apport anthropomorphique peut être la source de l'anomalie ? Est-ce l'étalonnage des appareils ou leur instabilité peut en être responsable ? Voici la traduction d'un conseil reçu d'un collègue et dont l'auteure principale de cet article s'inspire lorsqu'elle est confrontée à un jeu de données particulièrement compliqué : « Juger une valeur comme 'mauvaise' dans un jeu de données est une affaire délicate. On doit toujours faire attention aux erreurs de jugement en étiquetant 'douteuse' ou

ing or unusual but real. Good data should take precedence over expectations of what the numbers should be" (P. Strain, BIO, pers. comm.).

References / Références

- Brickman, D., and Petrie, B.** 2003. Nitrate, silicate and phosphate atlas for the Gulf of St. Lawrence. Can. Tech. Rep. Hydrogr. Ocean Sci. 231, xi+152 pp.
- Conkright, M.E., Antonov, J.I., Baranova, O., Boyer, T.P., Garcia, H.E., Gelfeld, R., Johnson, D., Locarnini, R.A., Murphy, P.P., O'Brien, T.D., Smolyar, I., and Stephens, C.** 2002a. World Ocean Database 2001, Volume 1: Introduction. Edited by S. Levitus. NOAA Atlas NESDIS 42, U.S. Government Printing Office, Washington, D.C., 167 pp. http://www.nodc.noaa.gov/OC5/WOD01/readme01.html#_1_63 (accessed 12 Sept. 2007).
- Conkright, M.E., O'Brien, T.D., Boyer, T.P., Stephens, C., Locarnini, R.A., Garcia, H.E., Murphy, P.P., Johnson, D., Baranova, O., Antonov, J.I., Tatusko, R., Gelfeld, R., and Smolyar, I.** 2002b. World Ocean Database 2001, CD-ROM Data Set documentation. National Oceanographic Data Center Internal Report 16.
- Johnson, D.R., Boyer, T.P., Garcia, H.E., Locarnini, R.A., Mishonov, A.V., Pitcher, M.T., Baranova, O.K., Antonov, J.I., and Smolyar, I.V.**
- 'erronée' une donnée remarquable ou inhabituelle mais réelle. Les bonnes données doivent l'emporter sur les valeurs auxquelles on s'attend» (P. Strain, communication personnelle).
2006. World Ocean Database 2005 documentation. Edited by S. Levitus. NODC Internal Report 18, U.S. Government Printing Office, Washington, D.C., 163 pp.
- Levasseur, M.E., and Therriault, J.-C.** 1987. Phytoplankton biomass and nutrient dynamics in a tidally induced upwelling: the role of the $\text{NO}_3:\text{SiO}_4$ ratio. Mar. Ecol. Prog. Ser. 39: 87-97.
- Petrie, B., K. Drinkwater, A. Sandström, R. Pettipas, D. Gregory, D. Gilbert, and P. Sekhon.** 1996. Temperature, salinity and sigma-t atlas for the Gulf of St. Lawrence. Can. Tech. Rep. Hydrogr. Ocean Sci. 178, v+256 pp.
- Redfield, A.C.** 1958. The biological control of chemical factors in the environment. Am. Sci. 46:205-221.
- Unesco.** 1990. GTSPP real-time quality control manual. Intergovernmental Oceanographic Commission, Manuals and Guides no. 22.
- WOD98, World Ocean Database 1998. <http://www.nodc.noaa.gov/OC5/indwod98.html> (accessed 12 Sept. 2007).

Estimation of Mixed Layer Depth at the AZMP Fixed Stations

Joe Craig¹ and Denis Gilbert²

¹Northwest Atlantic Fisheries Centre, Box 5667, St. John's, NL, A1C 5X1

²Institut Maurice-Lamontagne, CP 1000, Mont-Joli, QC, G5H 3Z4

joe.craig@dfo-mpo.gc.ca

Sommaire

Nous examinons des données récoltées aux sept stations fixes du Programme de Monitorage de la Zone Atlantique afin de comparer des méthodes d'estimation de la profondeur de la couche mélangée (*Mixed layer depth*, MLD). Ces sites sont diversifiés du point de vue océanographique, géographique et des facteurs climatiques qui les affectent et fournissent donc d'excellents contrastes pour évaluer la méthode du seuil, du gradient et une méthode mixte d'estimation du MLD. Nous avons trouvé que les estimations du MLD basées sur le maximum du gradient de densité étaient toujours plus élevées que celles obtenues par la méthode du seuil ou la méthode mixte du seuil du gradient. Malgré que ce résultat soit dû en partie au fait que la zone de mélange immédiatement au-dessus du milieu de la pycnocline soit incluse dans l'estimation par la méthode du maximum du gradient, le cycle annuel plus marqué révélé par cette méthode en fait un indice plus robuste dans la perspective de relier les processus biologiques et physiques.

Introduction

An ongoing initiative of the Atlantic Zone Monitoring Program (AZMP) is the integrated examination of biological and physical processes in the ocean to understand and model ocean productivity and the influence of environmental changes. The vertical structure of the ocean critically influences the abundance and distribution of nutrients that are available for primary production, making knowledge of this vertical structure important in developing an understanding of the lower food chain dynamics (Sverdrup 1953).

The density structure of the ocean is characterized by spatial and temporal variability over a broad range of scales. This makes it very challenging to establish metrics of the structure that can be uniformly applied to all regions and that allow intercomparison of biological or physical features or events. For instance, it is well known that the dynamics of

the spring bloom are strongly influenced by density stratification. A better understanding of this link can be obtained by comparing bloom dynamics among regions. Unfortunately, despite recent efforts, methods of characterizing the oceans' density distribution are not universally standardized and optimal methods vary from region to region. A method that works well for the tropics is frequently found to be of little use in the temperate zones, or one that works well for a highly stratified system may fail in locations or at times when stratification is weak.

At recent AZMP meetings, a zonal approach to characterize ocean density structure was deemed necessary and motivated us to try different methods to determine which works best in our region. We are primarily interested in comparing the annual cycles and interannual variability, with the latter being potentially modulated by recent climate change at the various

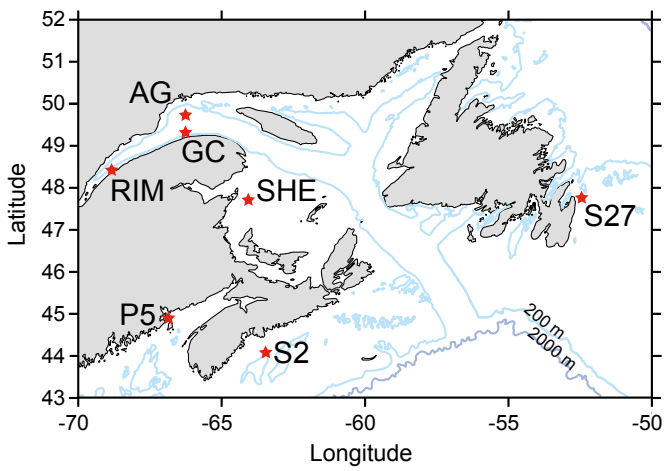


Fig. 1 Fixed stations of the AZMP used in this study: Rimouski (RIM), Station 27 (S27), Shediac (SHE), Anticosti Gyre (AG), Gaspé Current (GC), Prince 5 (P5), Halifax Station 2 (S2).

Les stations fixes du PMZA utilisées dans cette étude : Rimouski (RIM), Station 27 (S27), Shediac (SHE), gyre Anticosti (AG), courant de Gaspé (GC), Prince 5 (P5), Halifax Station 2 (S2).

fixed stations in the Atlantic zone (Fig. 1). Our criteria for evaluating the methods are: a) how well they enhance the signal-to-noise ratio, and b) how much confidence we can place in the indices once they are calculated.

Data

All data were obtained from the AZMP website (http://www.meds-sdmm.dfo-mpo.gc.ca/zmp/main_zmp_e.html), which is maintained by Integrated Science Data Management (ISDM), a branch of Canada's Federal Department of Fisheries and Oceans. For each site, the hydrographic data comprising pressure, temperature, and electrical conductivity (CTP) were downloaded for eight years (1999–2006 inclusive). Depth was calculated from the hydrostatic pressure (Morgan 1994); the salinity and thence σ_t were calculated from conductivity and temperature using the standard UNESCO algorithms (Fofonoff and Millard 1983). The in situ density (about 0.5 kg m⁻³ greater than σ_t at 100 m) was not used in this analysis. The frequency of CTP observations varied from site to site and from year to year (Fig. 2). Some sites did not have sufficient data to resolve annual cycles for certain years while others are rarely or never sampled in winter or early spring, making it impossible to determine a complete annual cycle.

The raw data were edited during post-processing and at their final posting on the AZMP web page. Typical adjustments include compensation for the motion of the ship, instrument vortex shedding and time lags, and binning or decimation of the raw data. The degree of decimation varied within and among stations with the result that the vertical sampling interval varied but was generally less than 0.3 m at most sites. A final visual inspection was carried out and any values deemed doubtful were discarded.

Methods

The station files were partitioned by individual casts and subjected either to filtering or decimation before any further calculations

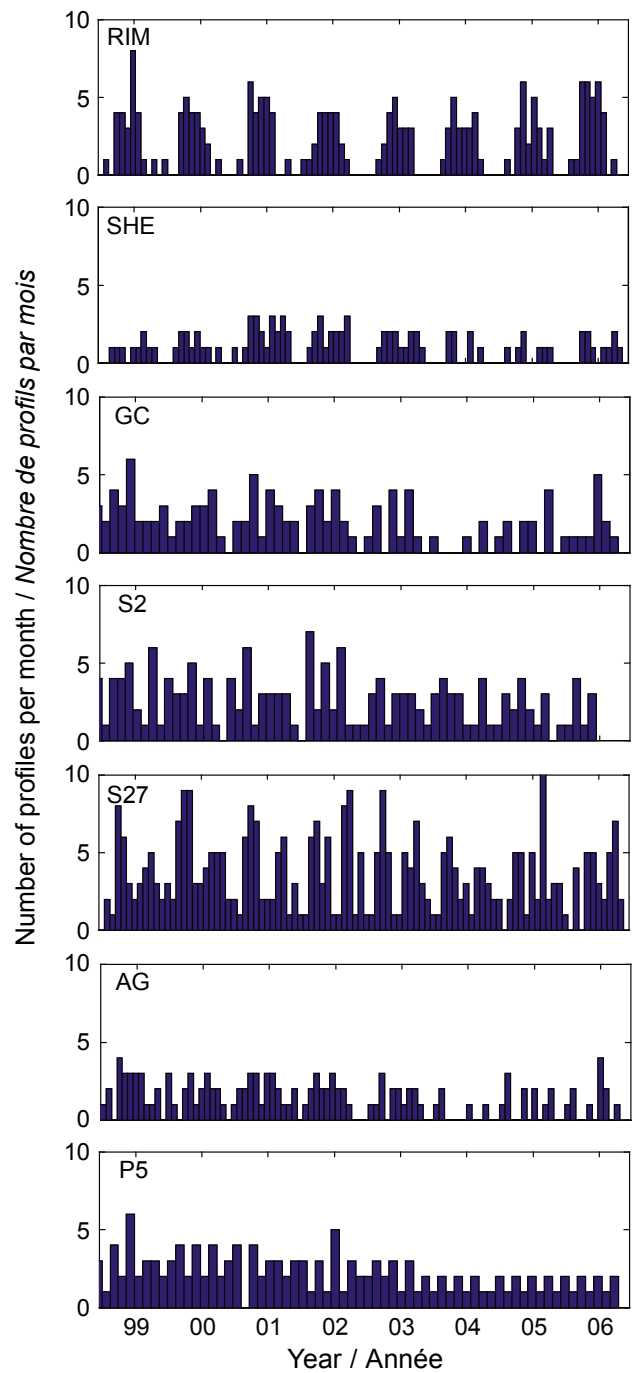


Fig. 2 Histograms showing the number of CTP profiles per month taken at the AZMP fixed stations from 1999 through 2006. (See Figure 1 for station abbreviations.)

Histogrammes montrant le nombre de profils CTP par mois aux stations fixes du PMZA de 1999 à 2006. (Se référer à la figure 1 pour l'identification des stations.)

were performed. To create a filtered profile, water density was subjected to 10 iterations of a three-point smoothing procedure:

$$\sigma_{t,j} = \frac{1}{3} (\sigma_{t,i-1} + \sigma_{t,i} + \sigma_{t,i+1})$$

where i and j are the sample numbers of the raw and smoothed data, respectively, with $\sigma_{t,j=1} = (\sigma_{t,1} + \sigma_{t,2})/2$ and $\sigma_{t,j=n} = (\sigma_{t,n-1} + \sigma_{t,n})/2$ to prevent truncating the data. However, we note that the potential to bias the calculations by masking features near the surface and bottom increases in proportion with the number of filtering iterations.

Other degrees of smoothing were attempted by varying the number of points included in the running mean and the number of iterations. The object was to minimize noise in the numerical derivative of σ_t with respect to depth (z):

$$(d\sigma_t / dz)_{zm} = (\sigma_{t,i} - \sigma_{t,i-1}) / (z_i - z_{i-1})$$

which was calculated and assigned to an intermediate mean depth $zm = (z_i + z_{i-1})/2$ for all data in each profile. The depth at which this gradient reached its maximum value was determined for each cast.

The mixed layer depths (MLD) were also estimated using the conventional threshold method and a gradient threshold method as follows. A mean value of surface density was calculated for each cast by averaging σ_t over the upper 5 m and noting the depth at which σ_t differed from the mean surface value by 0.01 kg m⁻³ (threshold). This effectively sets a lower bound of 5 m for our MLD estimates. The gradient threshold estimate used by Cassault et al. (2003) was obtained as the depth at which the gradient as calculated above was equal to or greater than 0.01 kg m⁻⁴. Figure 3 shows the MLD depths as estimated by the three methods on contrasting density profiles.

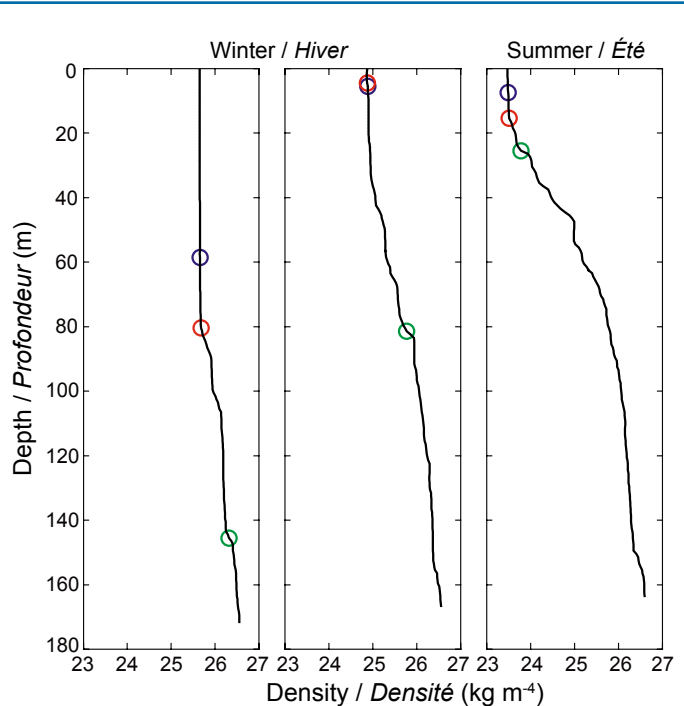


Fig. 3 The threshold MLD (blue), gradient threshold MLD (red), and depth of maximum gradient MLD (green) plotted as circles on the typical density profiles for the winter (left and centre) and summer (right) at S27.

Estimations de MLD par les méthodes du seuil (en bleu), du seuil du gradient (en rouge) et de la profondeur du maximum du gradient (en vert) représentées par des cercles sur des profils typiques de densité pour l'hiver (à gauche et au centre) et l'été (à droite) à S27.

A stratification index was also calculated for each cast as a two-point surface (5 m) to 50 m density (σ_t) gradient:

$$SI = (\sigma_{t(50m)} - \sigma_{t(5m)}) / 45.0$$

The variability of the density is frequently quite high near the surface. This is why the density at 5 m was used in this calculation.

Because of the diversity of vertical sampling intervals and the potential sensitivity of the gradient calculations to noise, some experimentation was conducted to determine an optimal sampling interval by decimating the data. A value of 1 m was thought to be an appropriate initial value, and the MLD calculations were repeated using decimated data. All data were subject to the same procedures.

Summarizing, two input density data sets were created: a filtered version from 10 applications of a three-point running mean filter with a one-sided, two-point filter applied to the end points to avoid series truncation; and a 1 m subsampled version without any filtering aside from averaging over the 1 m intervals.

Results

For each fixed station, the density threshold and gradient threshold MLDs were compared with the depth of the maximum density gradient. Annual cycles, based on 1 m subsampled data, are shown together with the standard deviations based on monthly means for all years (1999–2006) for the depth of the maximum density gradient (Fig. 4). Finally, the monthly mean stratification indices were plotted along with markers one standard deviation above and below the mean values (Fig. 5).

The results of the three methods differed from station to station and in two instances depended strongly on whether the data were filtered or decimated. For example, at the Rimouski station, the depth of the maximum gradient was considerably deeper than the MLD as calculated by the threshold and gradient threshold methods when filtered data were used. At Prince 5, there was little evidence of any annual cycle (Fig. 4); this is probably because of the strong tidal flows that are always present and give rise to vigorous mixing throughout the year.

The maximum gradient depth exhibited very strong annual cycles at both Station 2 and Station 27, with amplitudes approaching 100 m at both sites for the filtered and 1 m subsampled data. In contrast, the annual cycles yielded by the threshold methods were much weaker, with amplitudes less than 50 m. The gradient threshold and threshold MLDs had comparable annual cycles for Station 2, but their amplitudes were about half those of the maximum gradient MLD. On the other hand, the standard deviation of the depth of maximum gradient was very high in the winter and fall at both stations. The annual variability of the mixed layer depth was relatively weak for the Gaspé Current, Shedia, and Anticosti Gyre stations, although the maximum density gradient was consistently deeper.

Repeating the calculations using data uniformly decimated to 1 m without filtering resulted in subtle changes to all mixed layer and gradient calculations. The magnitudes of these changes were generally smaller than the standard deviations of the respective monthly means except at the Rimouski and Prince 5 stations. At Rimouski, the depths, their standard deviations, and the degree of scatter of the maximum gradient

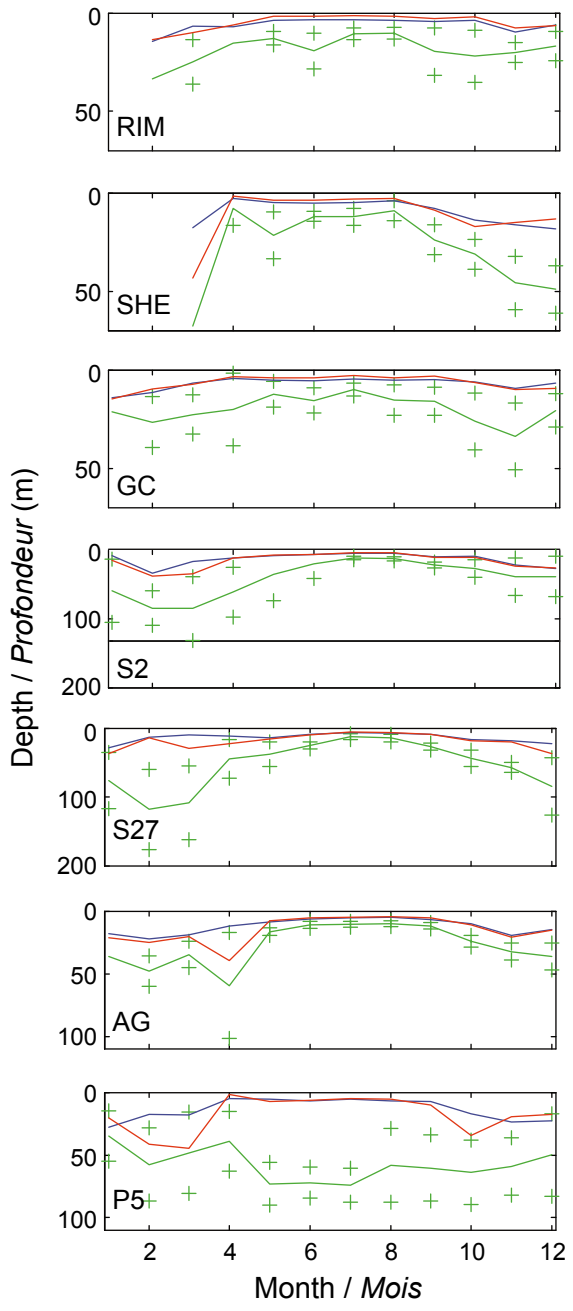


Fig. 4 Monthly mixed layer depths (in metres) estimated from decimated data by the threshold (blue) and gradient threshold (red) methods and the depth of the maximum density gradient (green). The green crosses indicate one standard deviation about the mean depth of maximum gradient for months for which there were three or more observations. (See Figure 1 for station abbreviations.)

Profondeur (en mètres) de la couche mélangée, par mois, estimée après décimation des données par la méthode du seuil (en bleu), du seuil du gradient (en rouge) et de la profondeur du maximum du gradient de densité (en vert). Les croix vertes indiquent un écart-type de la profondeur moyenne du maximum du gradient pour les mois où il y a au moins trois observations. (Se référer à la figure 1 pour l'identification des stations.)

decreased dramatically from those obtained with filtered data when decimated data were used. A similar effect was seen in the threshold gradient depth at Prince 5, where the annual cycle fluctuated less erratically with decimated data. The depth of maximum gradient at this site did not appear to be especially sensitive to the change from filtering with running means or decimation. For the results shown in Figure 4, we

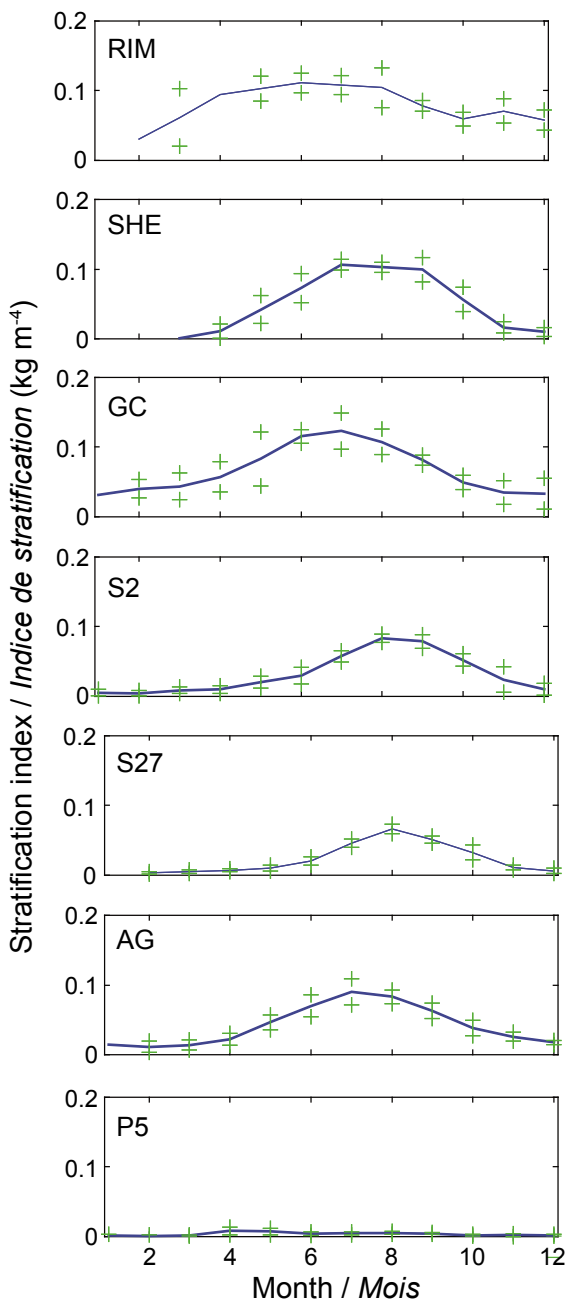


Fig. 5 Monthly mean stratification indices and standard deviations in units of kg m^{-4} for each station. (See Figure 1 for station abbreviations.)

Moyennes et écart-types mensuels des indices de stratification en unité de kg m^{-4} à chacune des stations. (Se référer à la figure 1 pour l'identification des stations.)

used data decimated to 1 m intervals because this appeared to give more plausible results for Rimouski. The effects of filtering and the methods are shown in Tables 1-3, where the differences are expressed in terms of the root mean square (RMS).

The annual cycles of stratification (Fig. 5) clearly illustrate the contrasting regimes that influence the density structures at each site, with features in the annual cycles of stratification being reflected in the cycles for the mixed layer depths. For example, at Station 2 and Station 27, the annual cycles are strong for both stratification and MLD. Tidal energy maintains a well-mixed water column throughout the year at Prince 5;

Table 1 RMS differences for MLD calculated using filtered and 1 m data.

Moyennes quadratiques des différences du MLD calculées en utilisant des données filtrées et sous-échantillonées à 1 m d'intervalle.

	RIM	S27	SHE	AG	GC	P5	S2
Maxgrad	127	23	17	23	15	25	30
Threshold	6	2	5	3	3	9	6
Gradthreshold	29	14	10	8	7	32	14

Table 2 RMS differences among methods for MLD calculated using filtered data.

Moyenne quadratiques des différences du MLD entre les méthodes d'estimation employant les données filtrées.

	RIM	S27	SHE	AG	GC	P5	S2
Maxgrad/Threshold	132	49	23	15	27	55	46
Maxgrad/Gradthreshold	125	50	22	22	25	47	39
Threshold/Gradthreshold	4	7	6	2	2	34	16

Table 3 RMS differences among methods for MLD calculated using 1 m data.

Moyenne quadratiques des différences du MLD entre les méthodes d'estimation pour les données sous-échantillonées à 1 m d'intervalle.

	RIM	S27	SHE	AG	GC	P5	S2
Maxgrad/Threshold	17	48	23	14	20	56	46
Maxgrad/Gradthreshold	18	43	22	14	21	54	43
Threshold/Gradthreshold	2	13	7	4	3	18	9

this is seen in the consistently weak stratification and deep maximum gradient depth. Phase relations are evident when comparing Station 2 with the Gaspé Current station, where the shoaling of the mixed layer and the stratification maxima occur a month or two earlier in the year.

Discussion and Conclusions

Considering the potentially higher signal-to-noise ratio of the relatively strong annual cycle of the maximum density gradient depth when compared with threshold and gradient threshold MLD estimates, its utility in climatological studies and in exploring the links between physical and biological processes may warrant further investigation in the Atlantic zone. It is presently unclear if this stronger cycle can yield additional information over that which can be had from increasing its MLD amplitude by adjusting the criteria for defining the mixed layer. Although other methods are arguably just as easy to apply and conceptually as simple, this method does not require recourse to arbitrary references or thresholds whose optimal values may vary seasonally or between and within regions. It is not without its limitations, however. Recent work has unveiled what appear to be intrusions of slope water causing very deep maximum gradients. These may contribute to the high standard deviations in the winter for Station 2 and Station 27. The maximum gradient method also has the potential of generating an MLD when the upper layer is strongly stratified and there is no true “mixed” layer. However, the true test of its utility will come when it is linked to biological variables.

The depth of the maximum gradient was estimated for profiles collected at sites influenced by contrasting oceanographic conditions, including estuarine (Rimouski, Shédiac, Anticosti Gyre), advective (Gaspé Current, Station 2, Station 27), and tidally energetic (Prince 5). The results were consistent with what might be expected from the oceanography at these sites and the respective annual cycles in stratification.

The standard deviation of the maximum density gradient was sensitive to the season. We have also observed that it depends somewhat on the apparent vertical resolution of the density data. Seasonal dependence of the variability of mixed layer depth has been reported by other investigators, notably Kara et al. (2000), who attributed it to the weaker pycnocline arising from wintertime wind forcing and strong cooling. Calculating maxima from weak gradients is inherently high in uncertainty. As to the possible role of vertical resolution on MLD estimation, we note that the instruments and data acquisition protocols typically used for the AZMP yield a vertical resolution of 0.10 m, based on an acquisition rate of 8 Hz¹ and deployment speed of 50 m min⁻¹. This was limited to 0.2 m by the resolution of the pressure sensor. Considering the variability in accuracy and precision arising from, among other things, the frequently hostile environments in which these measurements are made, it is difficult to imagine that a resolution of less than 1 m is always physically meaningful and without artefacts. Instrumental anomalies may have caused the spurious gradients that resisted removal by running mean filtering. Fortunately, greater precision and accuracy for the annual cycle of the maximum gradient depth resulted from decimation of the data to 1 m intervals, and it might thus be worthwhile to consider 1 m as a starting point in determining what can be expected as a limit of resolution in further mixed layer depth studies.

In closing, some discussion of the physical significance of the depth of the maximum gradient is in order. Between the mixed layer and the bottom is a transition zone spanning the pycnocline. Because the depth of maximum gradient does not necessarily occur at the base of the mixed layer, its depth is generally deeper than the mixed layer depth. Additionally, this difference in depth can depend on the thickness of the pycnocline. The thickness usually will be small during summer and large during winter. For this reason, the amplitude of the annual cycle for the depth of maximum gradient will also be greater than that for the mixed layer depth. In terms of climatology, this may be advantageous because a higher amplitude annual cycle may improve signal-to-noise ratios and thereby better facilitate interannual comparisons.

Future work could include calculating harmonic regressions of the annual cycles, experimenting with uniform decimation followed by filtering as a means of reducing the effects of instrumental artefacts in the data, and investigating the effects of increasing the threshold values for density and its gradient.

¹ At some sites, the CTP instrumentation may sample at 2 Hz or 24 Hz.

Preliminary results appear to indicate that the three methods yield depths that are similar in their correlations ($r \sim -0.5$) with the stratification indices; a more detailed study may assist in evaluating which, if any, method captures the more useful information from the density structure.

Acknowledgements

We are most grateful to those involved in the acquisition and archiving of the data, to Brian Petrie for his meticulous review, Eugene Colbourne and Jim Helbig for their suggestions and time in reviewing this and earlier versions of this document, and the insightful comments from delegates to the 2006 National Science workshop in Mont-Joli.

References

- Cassault, B., Vézina, A.F., and Petrie, B. 2003. Atlas of surface mixed layer characteristics for the Scotian Shelf and the Gulf of Maine. *Can. Data Rep. Hydrogr. Ocean Sci.* 164: v + 306 pp.
- Fofonoff, N.P., and Millard, R.C. Jr. 1983. Algorithms for computation of fundamental properties of seawater. *Unesco Tech. Papers in Mar. Sci.* No. 44, 53 pp.
- Kara, A.B., Rochford, P.A., and Hurlburt, H.E. 2000. An optimal definition for ocean mixed layer depth. *J. Geophys. Res.* 105(C7):16803-16821.
- Morgan, P.P. 1994. SEAWATER: A library of MATLAB computational routines for the properties of sea water. *CSIRO Marine Laboratories Report* 222, 29 pp.
- Sverdrup, H.U. 1953. On conditions for the vernal blooming of phytoplankton. *J. Cons. Int. Explor. Mer* 18: 287-295.

A Preliminary Assessment of the Performance of an Automated System for the Analysis of Zooplankton Samples from the Gulf of St. Lawrence, Northwest Atlantic

Stéphane Plourde¹, Pierre Joly¹ and Xabier Irigoien²

¹Institut Maurice-Lamontagne, B.P. 1000, Mont-Joli, QC, G5H 3Z4

²AZTI - Tecnalia / Unidad de Investigación Marina, Herrera Kaia Portualde z/g, 20110 Pasaia (Gipuzkoa)
stephane.plourde@dfo-mpo.gc.ca

Sommaire

Une analyse préliminaire de la performance d'un système d'analyse automatisée avec le logiciel ZooImage d'échantillons de zooplancton provenant du golfe du Saint-Laurent est présentée. La méthode est basée sur l'acquisition d'images digitalisées d'une fraction de chaque échantillon (station) de zooplancton, l'extraction automatisée des organismes (vignettes), de la construction d'un sous-ensemble de référence représentatif de la communauté en différentes catégories, et de l'optimisation d'un «classeur» suite à l'analyse de ce sous-ensemble avec différents algorithmes. L'utilisation d'un «classeur simplifié» comportant 8 catégories a permis de bien estimer la biomasse de zooplancton dans des échantillons récoltés avec un filet 333 µm de vide de maille. Bien que prometteuse avec un succès de classification global de 70 %, l'estimation de l'abondance de catégories représentant différents groupes de stades de développement et/ou d'espèces de copépode dans des échantillons récoltés avec un filet 158 µm de vide de maille s'est avérée beaucoup plus variable. Une analyse détaillée de matrices de confusion comparant la performance des classifications automatisées et manuelles a démontré des échanges complexes d'images mal classifiées (perte et contamination) entre différentes catégories. Ce travail est la première étape d'une étude en cours visant à déterminer l'applicabilité de cette approche automatisée pour l'analyse d'échantillons de zooplancton de l'Atlantique Nord-Ouest.

Introduction

Zooplankton biomass and composition have routinely been monitored in the Lower St. Lawrence Estuary (LSLE) since 1992 (Plourde et al. 2001) and in the Gulf of St. Lawrence (GSL) as part of the Atlantic Zone Monitoring Program (AZMP) conducted by the Department of Fisheries and Oceans, Canada (DFO) since 1999. The AZMP was established to follow the long-term evolution of oceanographic conditions in the northeast Canadian waters (northwest Atlantic) by monitoring physical-chemical water properties such as temperature, salinity, and nutrients, and lower trophic level variables such as the biomass and species composition of the phyto- and zooplankton communities. While physical-chemical data dating from the late 1960s are available for the GSL, long-term past information about the zooplankton community is more fragmented or almost nonexistent. However, DFO has conducted numerous surveys in the past 20–30 years that have included sampling of the zooplankton community, and numerous zooplankton samples are routinely collected as part of several current surveys for fish larvae and fish stock assessments in the GSL, some annually. Most of these zooplankton samples are

not analyzed due to limited financial resources; consequently hundreds of samples are stored in our facility. These samples represent a great potential for filling gaps in the description of the spatial and temporal evolution of the zooplankton community, especially during periods (e.g., the 1980s) or regions (e.g., the northeast GSL) that are seriously undersampled.

The automated analysis of zooplankton samples offers a cost effective way to analyze historical zooplankton samples. This technique has been recently developed based on advances in image analysis and recognition capabilities with the aim of effectively obtaining biologically significant data such as biomass and some level of taxonomic composition from preserved zooplankton samples. The automated analysis of preserved zooplankton samples has been used to estimate biomass (Alcaraz et al. 2003), obtain size spectra (San Martin et al. 2006), and describe the high-resolution synoptic spatial distribution of biomass of general zooplankton groups (Zarauz et al. 2007). However, to our knowledge, very few comparisons have been either done or published to assess the performance of automated analysis in reliable estimates of zooplankton abundance at an interesting taxonomic resolution.

Our objective is to conduct a preliminary comparison between the automated analysis of zooplankton samples with the ZooImage software and the traditional taxonomic laboratory procedure and assess the potential of this automated approach. Despite the preliminary status of this work (small number of samples analyzed), the results appear promising and were presented at the 4th International Zooplankton Symposium held in Hiroshima, Japan, in June 2007.

Methodology

Field Sampling

Zooplankton samples were collected from early July to late September 1999 in the LSLE off Rimouski, QC ($48^{\circ}40.000' N$; $68^{\circ}35.000' W$; 340 m depth), using a 1 m diameter ring net (mesh size of 333 μm or 158 μm) that was towed vertically from the bottom to the surface at 0.5 m s⁻¹. Catches were immediately transferred to 4 L plastic jars containing filtered sea water and were maintained at 4–6°C in coolers during their transport to the laboratory at the Maurice Lamontagne Institute, Mont-Joli, QC. After 1–2 h of sorting for live specimens in the laboratory, samples were preserved in 4% formalin neutralized with sodium borate.

Traditional Sample Analysis

Biomass comparisons were made using the 333 μm samples while abundance and composition comparisons used the 158 μm samples. For all samples, the macrozooplankton larger than 3 mm were removed for further analysis (Harvey et al. 2005), leaving the mesozooplankton, which were highly dominated by copepods. A fraction of the 333 μm sample was used to estimate the copepod wet biomass. The fraction was collected on a 333 μm sieve, transferred to a pre-weighed aluminum dish, and weighed on a Mettler PE 160 electronic balance (± 0.001 g) after excess water had been carefully removed. For the mesozooplankton abundance and composition determinations, the 158 μm samples were first fractionated with a Folsom splitter and aliquots were taken with a 10 mL Stemple pipette. A minimum (maximum) of 400 (600) organisms were identified in each sample. Aliquots analyzed for the biomass (333 μm) and abundance (158 μm) were stored in 20 mL vials in 4% formalin for subsequent automated analysis. Thus the same aliquots were used for both analysis methods.

Automated Sample Analysis

Image acquisition and vignette extraction. Because of time constraints, the current work comprises six stations (samples). Images from the aliquots were acquired with an EPSON 4990

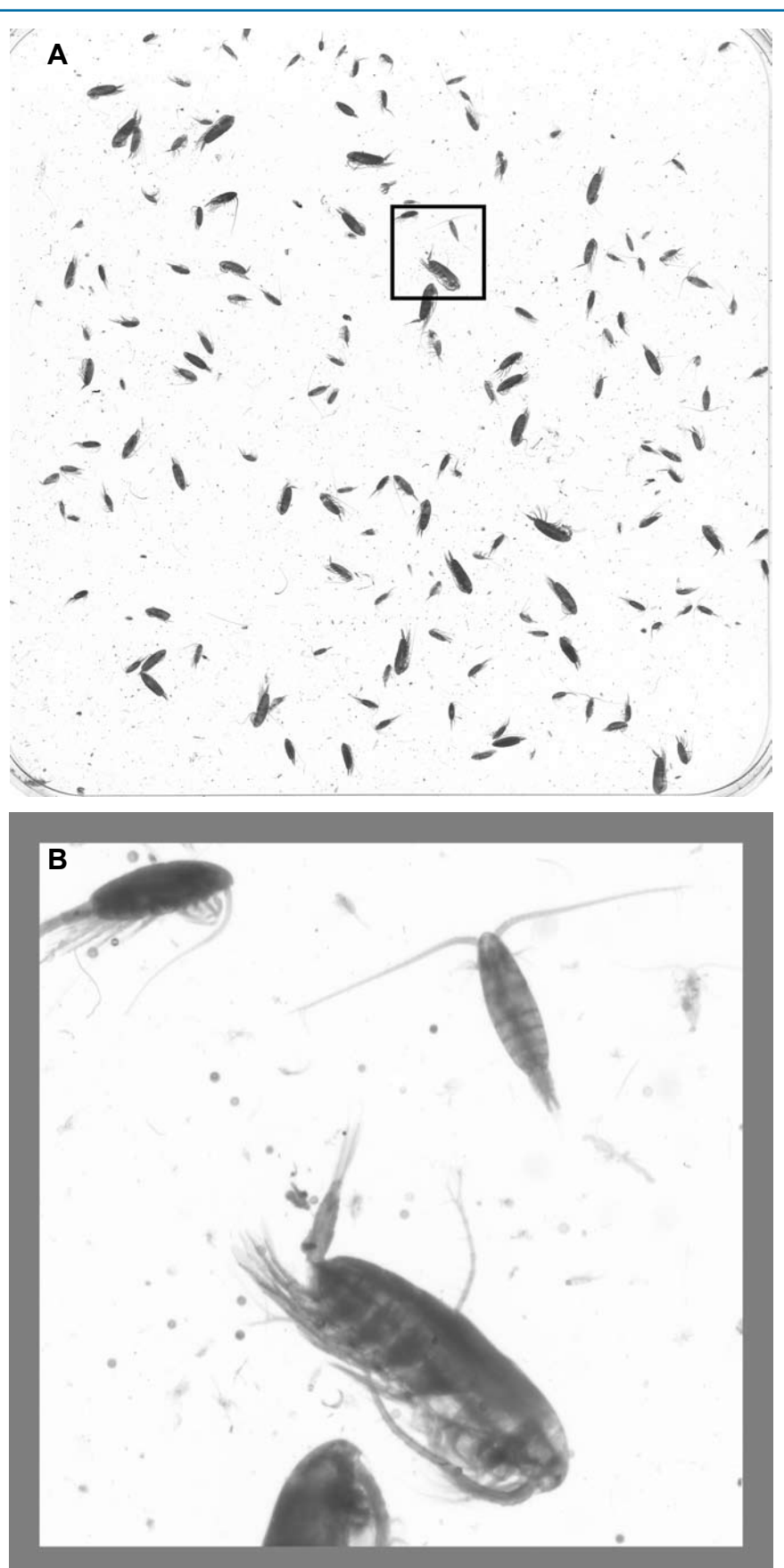


Fig. 1 Example of a 158 μm sample aliquot scanned at 2400 dpi (10680 x 10755 pixels, 11.3 x 11.38 cm) with (A) actual physical size and (B) inset of image (300 dpi in both instances).

Exemple d'un aliquot provenant d'un échantillon de 158 μm numérisé à 2400 dpi (10680 x 10755 pixels, 11,3 x 11,38 cm); (A) la totalité de l'image numérisée et (B) un encart de l'image. Les deux images sont présentées à 300 dpi.

scanner (See Fig. 1 for an example). Aliquots were transferred to 96 cm² polystyrene plates with a little water added to ensure that most individuals were lying on the bottom of the plate and were in focus. The total number of organisms in each aliquot was obtained by summing the results from the two 96 cm² plates. Aliquots from the 333 µm samples for biomass estimates were first stained with a fluorescent red dye (eosin) to increase contrast and then scanned based on a red-white scale at 600 dpi. The 158 µm aliquots for the detailed taxonomic classification were not stained and were scanned using a grey scale pattern at 2400 dpi. These two resolutions are the ones currently supported by the ZooImage software.

Vignettes (i.e., each organism isolated by the software during image processing) were extracted with the ZooImage 1.1.0 software (<http://www.sciviews.org/zooimage>). This software is an interface using both a statistical (R software) and an image analysis (ImageJ software) package. Vignettes were extracted from the scanned images of the aliquots, and 26 characteristics (length, area, texture, and so on) were measured and stored in a data file generated for each aliquot (sample). This data file represents the information used by the software for subsequent analyses and taxonomic classification. More details about the extraction procedure can be found at <http://www.sciviews.org/zooimage>.

Information about the collection (e.g., cruise, station, location, date, sample volume) and analysis (e.g., fraction, aliquot) of each sample are stored in a metadata file. This file is used by the software to automatically calculate estimates of biovolume and number of individuals (density or abundance) of the different categories estimated by the software.

Training the ZooImage software for automated identification: building the classifier. The creation of the training set and classifier is critical and is entirely dependent upon the user's knowledge and objectives. The training set is a bank of images of organisms classified in different categories by the user. The classifier is the statistical representation of the training set. For each category, ZooImage measures the same set of parameters that are measured on vignettes extracted from aliquots (samples), creating a multivariate reference on which each vignette's characteristics are compared and eventually classified in the most similar category. By default, ZooImage classifies all vignettes, including those composed of more than one organism as well as artefacts (e.g., scratches on the bottom of the plates, air bubbles, detritus). Therefore, the training set and the classifier should include all types of extracted vignettes in order to minimize bias during analysis. The performance of a classifier is evaluated by a confusion matrix analysis (<http://www.sciviews.org/zooimage>). This analysis compares the manual and automated classification of the organisms of the training set, identifying in which categories images of a given category have been misclassified and conversely, from which categories vignettes wrongly classified in a single category are originating. Confusion matrix analysis is the tool used to optimize both the number of categories and the type of recognition methods (algorithm) applied to create the classifier (see <http://www.sciviews.org/zooimage> and Grosjean et al. 2004 for details).

Two different approaches were used to build our training sets: (1) vignettes extracted from images of aliquots or (2) images from pre-identified organisms sorted by developmental stage and species. The first approach was chosen for the training set used to estimate biomass in the 333 µm samples because the low resolution (600 dpi, 1 pixel= 42 µm) of the images resulted in a rather low capacity of discrimination among the different categories. This simplified low-resolution classifier resulted in eight categories (653 vignettes used) and a classification success of 77.5% with a linear discriminant function (LDA) analysis. The second approach was chosen to build a detailed classifier using 2400 dpi images because of their greater potential for taxonomic discrimination (1 pixel=10.5 µm). We built the detailed training set by scanning a number of pre-identified organisms stored by individual (e.g., adult female) or grouped (e.g., late naupliar stages, early copepodid C1-3) development stages and species (e.g., *C. finmarchicus*, *C. glacialis*) in a collection used as a reference for taxonomists in our laboratory. However, vignettes extracted from aliquots were used for some rarer organisms not yet included in the taxonomist's reference bank as well as artefacts. Our initial training set included a total of 1985 organisms belonging to 54 categories, which was reduced to 39 categories following optimization. Although still preliminary, this detailed classifier showed a 70.5% classification success using the Neural Network Analysis (NNA).

Estimates of biomass, abundance, and composition. Biomass for each of the 333 µm samples was estimated from the area of each vignette classified in the different categories by ZooImage based on the eight-category, 600 dpi classifier. For each sample (station), the mean area of each category was transformed to biovolume assuming that the volume would correspond to that of an ellipsoid, which is a reasonable assumption given that copepods heavily dominate the community (Alcaraz et al. 2003). Biovolume was converted to dry mass according to Alcaraz et al. (2003). Wet weight measured with the classical method was converted to dry weight assuming that dry weight represents 13% of wet weight for samples from the GSL (Plourde et al. unpublished).

Abundances of the 39 categories in the 158 µm samples were calculated by ZooImage from the results of the automated analysis in combination with the metadata related to sample collection and analysis. The accuracy of the software to estimate mesozooplankton abundance was first tested by comparing overall abundance for general groups such as total copepods, *Calanus-Metridia* spp., small copepods (mainly *Pseudocalanus* spp., *Oithona* spp., *Acartia* spp., *Oncea* spp.), and calanoid nauplii. We also compared abundance in each sample (n=6) for the 16 copepod-related categories, but a more detailed assessment of the performance of the classifier was also performed for the 39 categories.

Results

Mesozooplankton Biomass in 333 µm Samples With the Simplified 600 dpi Classifier

There was good agreement between the biomass of mesozooplankton in the 333 µm samples estimated with the automated and traditional approaches (Fig. 2). Despite the rather

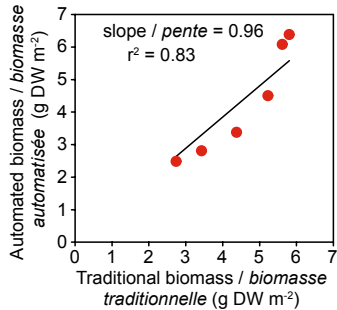


Fig. 2 Comparison between the biomass (dry weight) in 333 µm samples estimated with the automated 600 dpi classifier and measured with the traditional method.

Comparaison de la biomasse (poids sec) dans les échantillons 333 µm estimée à l'aide de la méthode automatisée à 600 dpi et mesurée selon la méthode traditionnelle.

small number of observations, the high regression coefficient ($r^2=0.83$) and slope (=0.96) close to 1 suggest that the use of biovolume measured with ZooImage and transformed to biomass units assuming a common shape for copepods could be a reliable way to estimate zooplankton biomass in communities/samples dominated by copepods.

Mesozooplankton Abundance and Composition in 158 µm Samples With the Detailed 2400 dpi Classifier

In general, the automated analysis with the detailed 2400 dpi classifier resulted in abundance estimates of the four general copepod groups that compared reasonably well with traditional taxonomic analysis (Fig. 3). The slope between the automated and traditional estimates of total copepod abundance was close to 1 and had a high regression coefficient (0.87), indicating that the software was capable of accurately counting the number copepods in an aliquot. Similarly, the comparison between methods for *Calanus-Metridia* spp., small copepods, and calanoid nauplii gave good results (r^2 between 0.70 and 0.97), but with some indications of an overestimation in the abundance of calanoid nauplii and

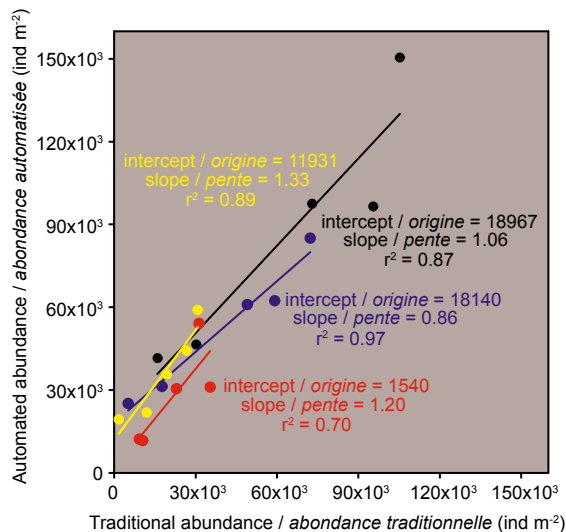


Fig. 3 Comparison between the abundance of total copepods (black), *Calanus-Metridia* spp. (red), copepods < 1 mm (blue), and Calanoid nauplii (yellow) in 158 µm samples estimated with the automated 2400 dpi classifier and with the traditional analysis.

Comparaison de l'abondance totale des copépodes (noir), de Calanus-Metridia spp. (rouge), copépodes < 1 mm (bleu) et des nauplii de calanoïdes (jaune) dans les échantillons 158 µm estimée à l'aide de la méthode automatisée à 2400 dpi et mesurée selon la méthode traditionnelle.

Calanus-Metridia spp. (slope > 1) and an underestimation in the abundance of small copepods (slope < 1) (Fig. 3).

A more detailed comparison of the results for the 16 copepod categories is shown in Figure 4. The automated analysis performed quite differently when estimating abundance according to categories. Considering all samples (averaged abundance), the software appeared to provide reasonable estimates of the abundance of dominant categories, as demonstrated by C1-3 and C4-6 *C. finmarchicus/glacialis*, different groups of stages of *C. hyperboreus*, C1-5 of *Microcalanus/Scolecitricella/Pseudocalanus*, and *Oncaea* spp. (Fig. 4). On the other hand, the software poorly estimated the rarer *Paraeucheata norvegica* adults, *Acartia* spp., and the abundant *Oithona* C1-6 spp. and calanoid nauplii. However, regression coefficients (filled circles in Fig. 4, $n=6$) between the automated and traditional abundance estimates greatly varied among categories and did not appear related to the accuracy of the averaged abundance estimates (bars in Fig. 4). Although quite preliminary, this suggests that the quality of the automated analysis could be dependent on the composition of the zooplankton community,

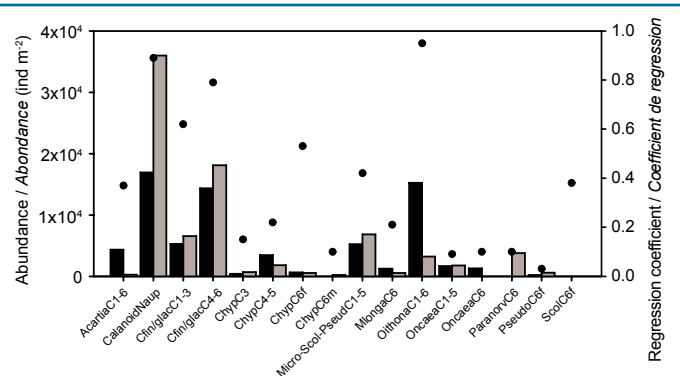


Fig. 4 Comparison between the averaged abundance of 16 copepod categories in 158 µm samples estimated with the automated 2400 dpi classifier (grey) and with traditional analysis (black). Regression coefficients between individual abundance estimates from the automated and traditional analyses are denoted by the filled circles.

Comparaison de l'abondance moyenne de 16 catégories de copépodes dans les échantillons 158 µm estimée à l'aide de la méthode automatisée à 2400 dpi (gris) et mesurée selon la méthode traditionnelle (noir). Le coefficient de régression entre les mesures individuelles d'abondance effectuées pour chaque catégorie est représenté par les cercles noirs.

but correction factors could be derived for categories showing good regression coefficients that were either underestimated (e.g., *Oithona* C1-6) or overestimated (e.g., calanoid nauplii).

A detailed analysis of the accuracy of the classification provided by the confusion matrix revealed useful information on how the detailed 39-category classifier behaved (Fig. 5). For each of the 39 categories, the number of vignettes accurately classified (black bars), misclassified (grey bars), originating from other categories (white bars), and manually classified (training set; filled circles) in each category are shown on the left y-axis. The classification success (%) (open circles, right y-axis) for each category was calculated from the proportion of images correctly classified (black bars) relative to the initial number of vignettes manually classified (filled circles). The total number of vignettes classified in a given category by the detailed classifier is given by the total of the black and white bars. This

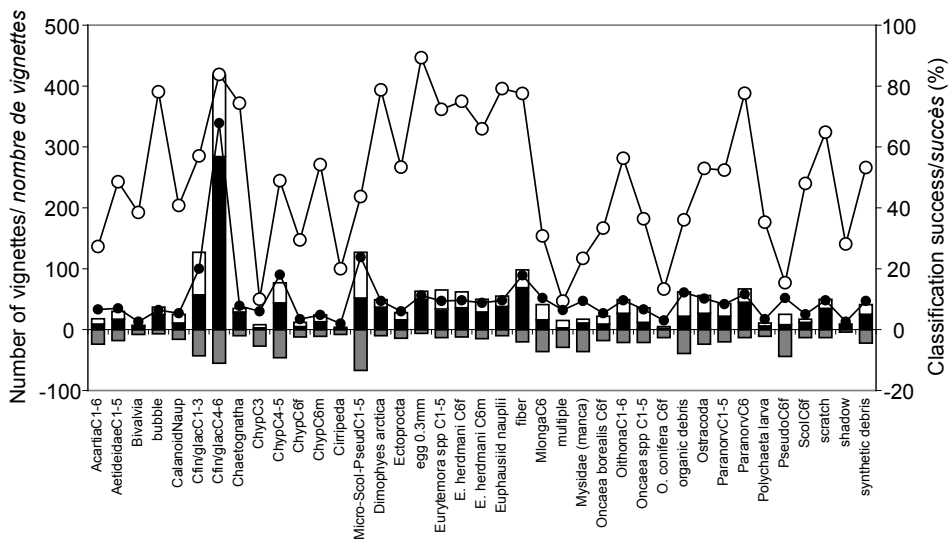


Fig. 5 Confusion matrix analysis. Comparison of the performance of the automated 2400 dpi classifier and the manual classification (training set) for the 39 categories. Black circles: number of vignettes manually classified in each category of the training set; black bars: number of vignettes successfully classified; grey bars: number of vignettes misclassified into other categories (lost); white bars: number of vignettes originating from other categories (contamination); white circles: classification success (%).

Analyse de matrice de confusion. Comparaison de la performance entre le «classeur» 2400 dpi automatisé et la classification manuelle pour les 39 catégories du sous-ensemble de référence. Cercles noirs: nombre de vignettes classifiées manuellement dans chaque catégorie du sous-ensemble de référence; barres noires: nombre de vignettes classifiées avec succès; barres grises, nombre de vignettes mal classifiées dans d'autres catégories (perdues); barres blanches: nombre de vignettes provenants des autres catégories (contamination); cercles blancs: succès de classification (%).

representation clearly indicates that a good agreement in the number of vignettes between the manual (filled circles) and the automated (black + white bars) analyses could arise from either a good performance of the classifier (e.g., invertebrate eggs > 0.3 mm and *Dymophyses arctica*, with classification success > 80%) or by the combination of a poor classification success and a “contamination” from other categories (e.g., *Micro-Scol-Pseudo* C1-5, 45% classification success compensated by an equivalent contribution from other categories). This relative flux (combination of the “loss” from a category and “contamination” from other categories) of organisms also explains how reasonably good abundances of C1-3 and C4-6 *C. finmarchicus/glacialis* (Fig. 4) were estimated despite different classification success (> 25%). It is worth pointing out that the classifier accuracy was low (< 50%) for several categories of smaller organisms (< 1 mm) such as *Acartia*, *Pseudocalanus*, and *Oithona* (Fig. 5). Overall, there were relatively high negative and positive fluxes of vignettes among categories, indicating that further refinements of the classifier are needed.

Discussion

The overall accuracy (70%) of our detailed 2400 dpi classifier was somewhat lower than what was reported in the only two studies published using similar approaches targeting either zooplankton or phytoplankton. With a similar analytical approach, Grosjean et al. (2004) obtained an overall accuracy of 80–85% using a 29-category 2400 dpi classifier covering the entire zooplankton community without any copepod stage details, which likely optimized the contrast among categories in comparison to our copepod-dominated classifier because of the very different shapes and morphologies. Sosik and Olson (2007) developed an automated procedure to analyze phytoplankton composition and obtained an overall accuracy

of 88% with a 22-category classifier; individual category accuracies ranged from 69% to 99%. In both studies, training sets included a smaller number of categories than in ours, suggesting that the greater the number of categories, the harder the optimization of the classifier will be. In fact, classification accuracies ranging between 75% and 80% are generally obtained with 20–30 categories with the present version of ZooImage (P. Grosjean, Science faculty–Campus de la Plaine, Avenue du Champ de Mars, 6, Pentagone (3D08), 7000-MONS, Belgium, pers. comm.).

In addition to the number of categories, a few other shortcomings may have limited the accuracy of our detailed classifier. Firstly, the number of vignettes in the different categories was unequal (Fig. 5), which could have introduced bias in the assessments of classifier performance and sample analysis (Grosjean et al. 2004). While a preliminary analysis revealed a weak but significant ($r^2 = 0.25$, $p < 0.001$) positive non-linear relationship between the success (%) of classification and the number of vignettes in each category with a threshold around 70 vignettes, several categories included fewer than 40 organisms, indicating that they were under-represented in the training set (see Fig. 5). Secondly, our classifier was incomplete, meaning that some organisms not yet represented in the training set were classified in one or more of the existing categories. Thirdly, a low misclassification percentage of a highly abundant taxon could have resulted in a significant overestimation of the abundance of a rarer taxon. This effect is illustrated by the three-orders-of-magnitude overestimation of *P. norvegica* C6 abundance (3000 vs 5 ind m⁻²) by the automated approach relative to the traditional analysis (see Fig. 4), most likely due to “contamination” from a more abundant large copepod category. The abundant *Oithona* spp., with an accuracy of 55%, could also have represented a significant source of bias for other small copepod categories. Combined with variations in the relative abundance of categories among samples, such effects could explain the weak correspondence (low r^2) observed between the automated and traditional abundance estimates at each station in several categories (Fig. 4). These elements highlight the importance of optimizing the classifier’s performance for the most numerous taxa in order to correctly estimate their contribution but also to avoid unrealistic estimates of abundance of rarer components of the community.

The low accuracy of the detailed 2400 dpi classifier in identifying several categories of small copepod stages and species (<1 mm) suggests a limitation due to the image resolution. One would expect a positive relationship between the performance of the automated analysis and image resolution. The

size of each pixel at 2400 dpi was approximately 10–12 µm, implying that vignettes of small organisms such as *Acartia*, *Temora*, *Oithona*, and calanoid nauplii in the size range of 250–1000 µm would include a limited number of pixels, which could preclude their successful classification.

The grouping of different developmental stages and/or species into single categories should be based on the analysis of the confusion matrix to optimize the performance of the classifier, but taxonomic or functional criteria should also be considered. We started to build the training set at 2400 dpi with detailed pre-identified development stages of different copepod species but had to group them into a lower number of categories based on the results of the confusion matrix analysis (e.g., stages C4 to C6 of *C. finmarchicus* and *C. glacialis* represented by a single category). However, the discrimination among different groups of development stages in order to distinguish different phases of the life cycle could prove useful for meaningful ecological use of the data. Users might have to consider a trade-off between the accuracy of their automated analysis and the taxonomic or ecological information of their data. This appears manageable since ZooImage provides the tools to appreciate the potential error associated with their classifier and sample analysis. Finally, a rigorous quantitative assessment of the performance of the automated analysis could lead to the determination of correction factors based on accurate regression coefficients between automated and classical estimates in some of the categories.

We are presently conducting a more complete assessment of the performance of the automated analysis based on 40 samples collected using the AZMP protocol (202 µm mesh nets) that are more representative of the entire GSL zooplankton community. The main objectives of this on-going work are to:

- Complete the pre-identified training set at 2400 dpi with missing taxa and equilibrate the training set (similar number of organism in each category)

- Optimize the performance of this new detailed classifier at 2400 dpi for the analysis of standard zooplankton samples collected following the AZMP protocol
- Compare estimates of biomass and abundance of each category between the automated and traditional analyses
- Determine the lower size limit under which the detailed 2400 dpi classifier performs poorly, thus identifying the categories not well estimated at this image resolution
- Establish a relationship between the number of particles in the aliquots and the performance of the automated analysis (density effect) in order to develop a standard analysis procedure.

References

- Alcaraz, M., Saiz, E., Calbet, A., Trepaut, I., and Broglio, E. 2003. Estimating zooplankton biomass through image analysis. Mar. Biol. 143: 307–315.
- Grosjean, P., Picheral, M., Warembourg, C., and Gorsky, G. 2004. Enumeration, measurements, and identification of net zooplankton samples using the ZOOSCAN digital imaging system. ICES J. Mar. Sci. 61: 518–525.
- Harvey, M., St-Pierre, J.-F., Devine, L., Gagné, A., Gagnon, Y., and Beaulieu, M.-F. 2005. Oceanographic conditions in the Estuary and the Gulf of St. Lawrence during 2004: zooplankton. DFO CSAS Res. Doc. 2005/043, 22 pp.
- Plourde S., Joly, P., Runge, J.A., Zakardjian, B., and Dodson, J.J. 2001. Life cycle of *Calanus finmarchicus* in the lower St. Lawrence estuary: The imprint of circulation and late timing of the spring phytoplankton bloom. Can. J. Fish. Aquat. Sci. 58: 647–658.
- San Martin, E., Harris, R.P., and Irigoien, X. 2006. Latitudinal variation in plankton size spectra in the Atlantic Ocean. Deep-Sea Res. II 53: 1560–1572.
- Sosik, H., and Olson, R.J. 2007. Automated taxonomic classification of phytoplankton samples with imaging in-flow cytometry. Limnol. Oceanogr.: Methods 5: 204–216.
- Zarauz, L., Irigoien, X., Urtizberea, A., and Gonzalez, M. 2007. Mapping plankton distribution in the Bay of Biscay during three consecutive spring surveys. Mar. Ecol. Prog. Ser. 345: 27–39.

Temperature, Salinity and Oxygen Measurements from Argo Profiling Floats in the Slope Water Region

Denis Gilbert and Émilie Nault

Institut Maurice-Lamontagne, CP 1000, Mont-Joli, QC, G5H 3Z4
denis.gilbert@dfo-mpo.gc.ca

Sommaire

Le programme Argo de suivi du climat océanique mondial permet l'acquisition en temps réel de profils verticaux de température et de salinité entre 2000 m de profondeur et la surface. Parmi les quelques 3000 flotteurs-profileurs Argo déployés dans l'océan mondial, près d'une centaine sont équipés de senseurs d'oxygène et cinq de ceux-ci ont été déployés dans les eaux de la pente continentale au sud de Terre-Neuve et de la Nouvelle-Écosse. Dans cet article, nous présentons des statistiques de température, salinité et oxygène, dans la région comprise entre les latitudes 35°N et 48°N et entre les longitudes 45°O et 75°O, calculées à partir de l'ensemble des données recueillies par les flotteurs-profileurs Argo de 1998 à 2007.

Introduction

The Argo program, a major component of the Global Ocean Observing System (GOOS), is an international venture that

coordinates the deployment of profiling floats for real-time monitoring of salinity and temperature in the upper 2000 m of the world ocean (<http://www.argo.ucsd.edu/>). On 31 October

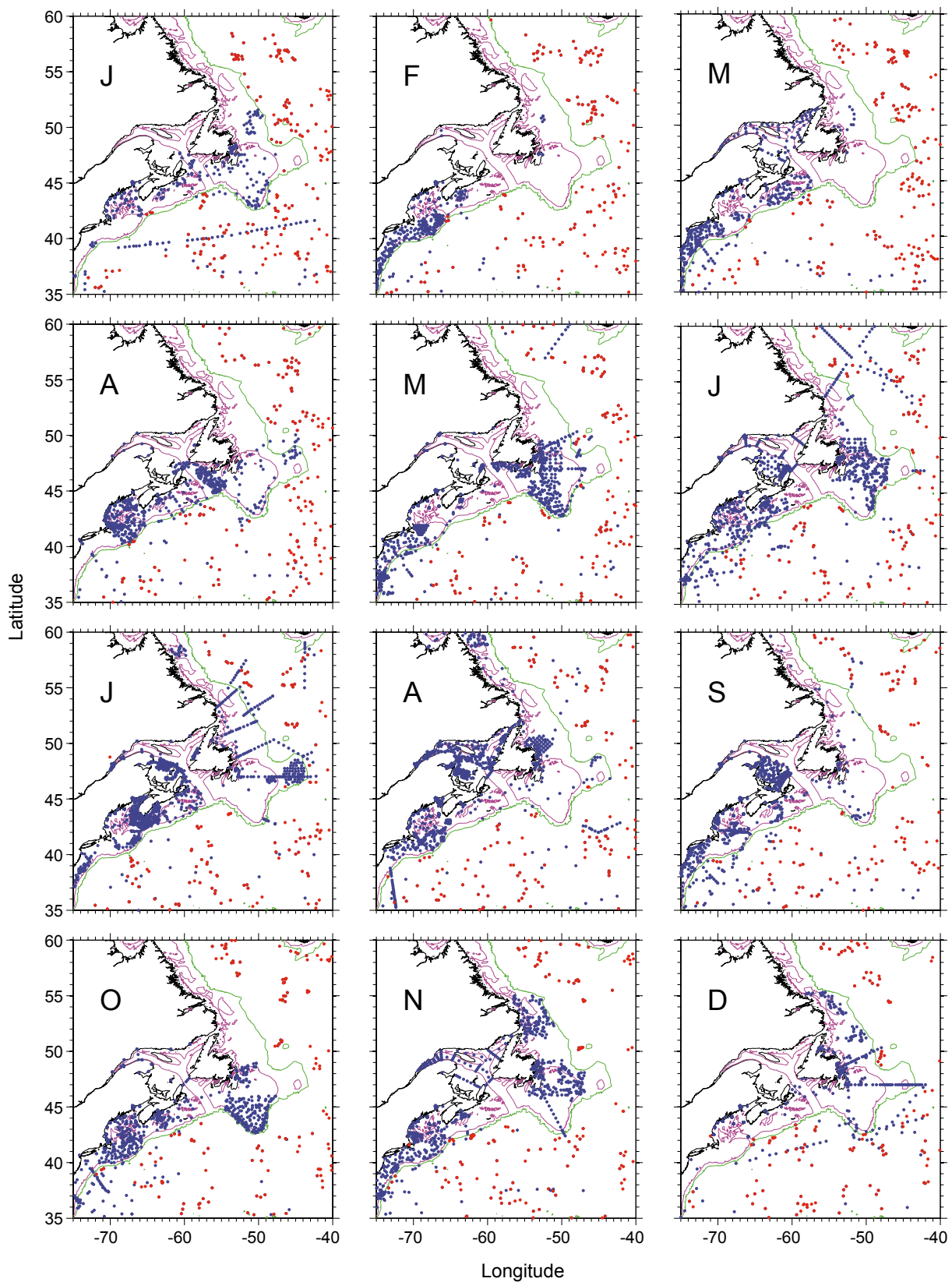


Fig. 1 Monthly distributions of temperature and salinity profiles from ship-based surveys (blue dots) and from drifting Argo floats (red dots) in 2005. CTD data collection from the ship-based surveys (mostly AZMP and groundfish assessment) and the Argo profilers nicely complement each other with minimal spatial overlap. Bathymetry contours are 200 m (magenta) and 2000 m (green).

Pour 2005, distribution par mois de l'année des profils de température et de salinité récoltés à partir de navires (points bleus) et des flotteurs-profileurs Argo (points rouges). On peut voir que les données récoltées grâce aux relevés de navires (surtout PMZA et évaluations de poissons de fond) et par les flotteurs-profileurs Argo se complètent bien avec très peu de chevauchement entre eux. Les contours bathymétriques illustrés sont ceux de 200 m (magenta) et de 2000 m (vert).

2007, Argo completed its initial building phase when the original global target of 3000 floats was reached. We are now entering a 10-year consolidation phase during which we hope to show the full potential of this array for ocean climate monitoring, seasonal weather prediction, and operational oceanography and meteorology. At an average cost of about \$200 per CTD (Conductivity-Temperature-Depth) profile, which is 10 to 15 times less expensive than equivalent data collected on ships, Argo floats represent the most affordable way of monitoring climate variability and change in the deep ocean into the foreseeable future.

The Argo program differs in many ways from traditional ship-based ocean observing systems (e.g., AZMP). Firstly, Argo profiling floats can operate in calm or rough seas throughout the year, avoiding seasonal biases in data coverage except in the rare cases of sea-ice cover in open ocean areas. Indeed, whereas ship-based observations on the eastern Canadian continental shelf and adjacent deep ocean are very sparse in December, January, and February, Argo floats provide as much wintertime data from the deep ocean as they do in other seasons (Fig. 1). A second major difference between Argo data and ship-based data is that Argo data are available in real-time to anyone. This contrasts with ship-based data for which time lags between the date of collection and the date when the data become available for public usage can range from a few days to several years or never. For example, most ship-based CTD data collected by DFO (Department of Fisheries and Oceans) are available within 1 year, but some may only become publicly available after 2 years or more. This situation motivated our choice of the year 2005 for the visual comparison of Argo and ship data coverage, as we wanted to maximize the latter.

In this article, we take a first look at Argo temperature, salinity, and oxygen data from the Slope Water region (Gatien 1976), also known as the Gulf Stream northern recirculation gyre (Hogg et al. 1986). This is the shaded region in Figure 2 between Cape Hatteras and the Tail of the Grand Bank, with the meandering Gulf Stream to the south and the continental shelf break to the north. A series of deep channels allow water mass exchanges between the Slope Water and the Gulf of Maine, the deep basins of the Scotian Shelf, and the Gulf of St. Lawrence. Hence, temperature, salinity, and oxygen observations from the Slope Water provide much-needed information on deep-ocean conditions and also on the role of open ocean forcing as a driver of climate variability on the continental shelf (Petrie and Drinkwater 1993, Gilbert et al. 2005).

The Slope Water region bounded to the north by the 200 m (2000 m) isobath has an area of 740 000 km² (650 000 km²). As Argo floats are launched in waters deeper than 2000 m, dividing the area of 650 000 km² by the target average Argo float spacing of 300 km, i.e., one float per 90 000 km², gives an average float number of 7.2 in the Slope Water region. With random float excursions into and out of the Slope Water across the Gulf Stream, we can thus typically expect to have 5 to 10 Argo floats reporting data in real-time every 10 days from the Slope Water region, giving us about 15 to 30 profiles per month (Fig. 1).

Methods

All Argo data collected between 1 November 1998 and 7 December 2007 and within the polygon defined by latitudes

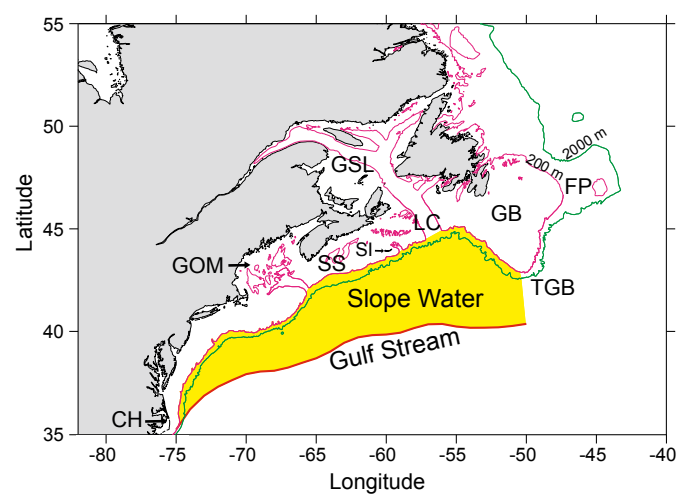


Fig. 2 Map of the northwest Atlantic Ocean showing the positions of geographical areas mentioned in the text: CH = Cape Hatteras, FP = Flemish Pass, GB = Grand Bank, GOM = Gulf of Maine, GSL = Gulf of St. Lawrence, SI = Sable Island, SS = Scotian Shelf, TGB = Tail of the Grand Bank, LC = Laurentian Channel. Bathymetry contours are 200 m (magenta) and 2000 m (green).

Carte de l'océan Atlantique Nord-Ouest montrant les positions de lieux géographiques mentionnées dans le texte : CH = Cape Hatteras, FP = passe Flamande, GB = Grand Banc, GOM = golfe du Maine, GSL = golfe du Saint-Laurent, SI = île de Sable, SS = plateau Néo-écossais, TGB = queue du Grand Banc, LC = chenal Laurentien. Les contours bathymétriques illustrés sont ceux de 200 m (magenta) et de 2000 m (vert).

35°N and 48°N and longitudes 75°W and 45°W were used in our analyses. The Argo program did not officially start until 2001, so we also included data from PALACE (Profiling Autonomous LAgrangian Circulation Explorers) floats deployed in the late 1990s during WOCE (World Ocean Circulation Experiment). We shall refer to both types as Argo floats.

For temperature and salinity, we only used real-time or delayed-mode data with quality control flag 1 (good data) in our analyses. We rejected all data with quality control flag 2 (potentially good data), as visual examination revealed some clearly erroneous observations. Data with quality control flags 3 and higher were also rejected. For oxygen, all data had quality control flag 0 (no quality control performed), as there does not yet exist an agreed-upon quality control method for this parameter. More details about quality control flags implemented by the Argo data management team can be found in Carval et al. (2006).

We shall focus on two reference surfaces for our analysis: the 27.25 kg m⁻³ potential density surface, which allows us to compare our results to those of Gilbert et al. (2005), and the 250 m depth, which enables us to compute temperature, salinity, and oxygen anomalies based on the 2005 World Ocean Atlases (WOA05) of Locarnini et al. (2006), Antonov et al. (2006), and Garcia et al. (2006) respectively. The two surfaces (250 m and 27.25 kg m⁻³ isopycnal) nearly coincide close to the continental shelf break, but the vertical distance between them increases to a few hundred metres south of the Gulf Stream. For each profile within a given 1/3° latitude x 1/2° longitude polygon, the depth of the 27.25 kg m⁻³ potential density surface was estimated and temperature, salinity, oxy-

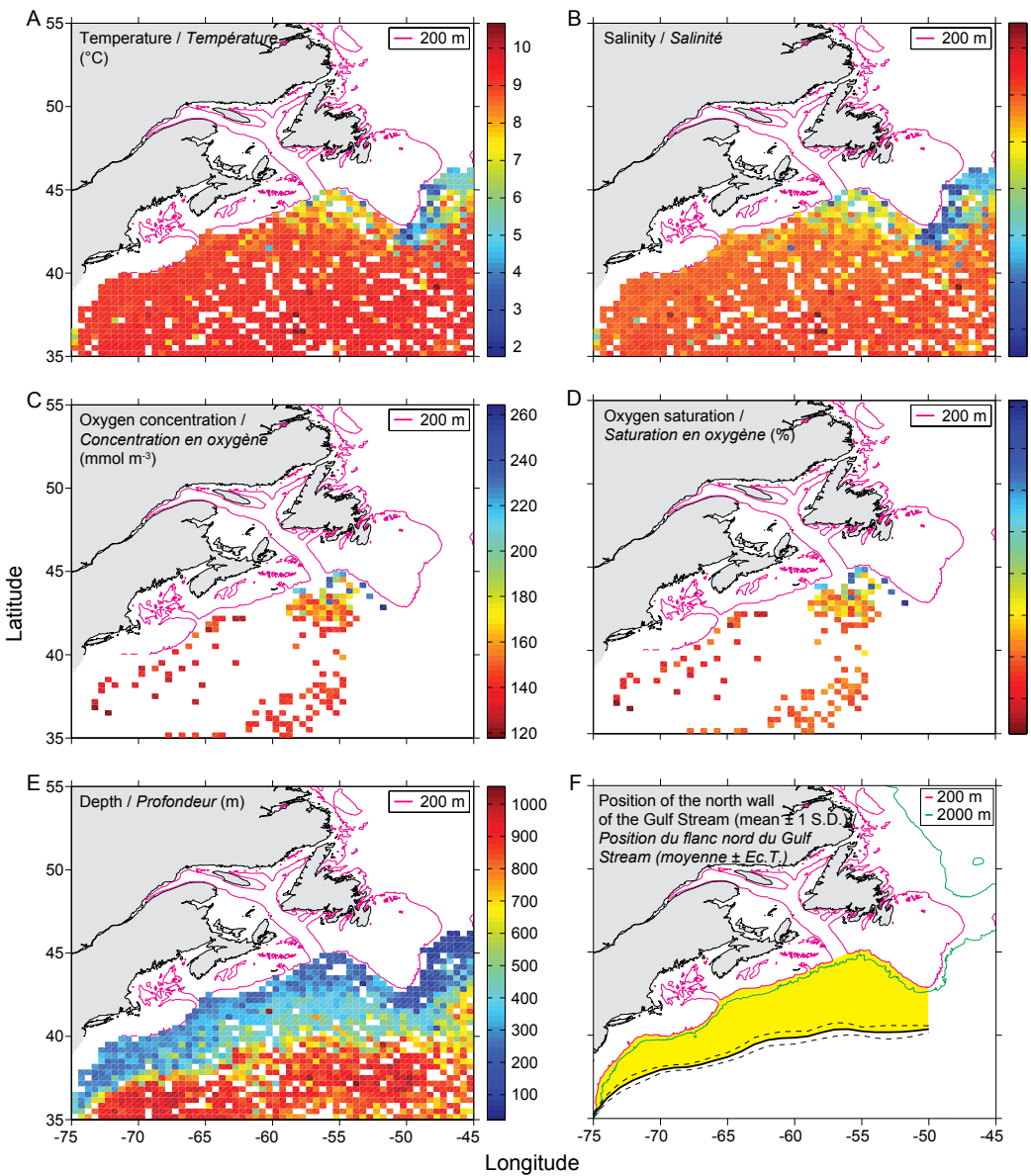


Fig. 3 Median values of (A) temperature, (B) salinity, (C) oxygen concentration, and (D) oxygen saturation interpolated onto the 27.25 kg m⁻³ potential density surface, whose depth is shown on panel E for 1/3° latitude by 1/2° longitude polygons. Panel F highlights the Slope Water region (yellow) and shows the mean latitudinal position of the north wall of the Gulf Stream plus or minus one standard deviation.

Valeurs médianes de (A) la température, (B) la salinité, (C) la concentration en oxygène et (D) la saturation en oxygène interpolées à la surface de densité potentielle de 27,25 kg m⁻³, dont la profondeur est montrée au panneau E pour des polygones de 1/3° de latitude par 1/2° de longitude. Le panneau F met en évidence la région des eaux de la pente continentale (en jaune) et montre la position latitudinale moyenne, plus ou moins un écart-type, du flanc nord du Gulf Stream.

gen concentration, and oxygen saturation were interpolated to this depth. The median of each field was then calculated for each polygon. For the computation of anomalies with respect to the depth-based 2005 World Ocean Atlas, we interpolated temperature, salinity, oxygen concentration, and oxygen saturation to 250 m depth for each profile within a given 1° latitude x 1° longitude square. The mean of each field was then calculated, from which the corresponding WOA05 annual mean climatology was subtracted, giving us the anomaly for that field. To obtain a measure of statistical significance, we compared the Argo mean \pm one standard error with the WOA05 mean \pm one standard error intervals. When these intervals overlapped, the anomalies were considered not to

be significant in comparison to the typical variability.

Results

On the 27.25 kg m⁻³ potential density surface, the cold and fresh Labrador Current Water (LCW) is evident from Flemish Pass to the Tail of the Grand Bank (Fig. 3). The influence of the oxygen-rich, cold and fresh Labrador Current Water is seen to the west of the Tail of the Grand Bank, within about 150 km of the 200 m isobath south of the Grand Banks and near the mouth of the Laurentian Channel, but is less evident west of Sable Island. In the remainder of the Slope Water region, North Atlantic Central Water (NACW) dominates on the 27.25 kg m⁻³ isopycnal surface, as in Gilbert et al. (2005). The position of the Gulf Stream is indicated by a region of rapid change in the depth of the 27.25 kg m⁻³ isopycnal, from about 300 m in the Slope Water region to about 900 m in the Sargasso Sea subtropical gyre (Fig. 3E). The width of this frontal region with steep isopycnals is very narrow (40 to 80 km) west of about 70°W, widens considerably from 70°W to about 63°W, and then remains fairly constant until just before the Tail of the Grand Bank. There is a relatively close correspondence between the latitudinal position of the 650 m depth level of the 27.25 kg m⁻³ isopycnal (Fig. 3E) and the location of the north wall of

the Gulf Stream (Fig. 3F) as determined from satellite infrared imagery of sea-surface temperature. We also note that on the 27.25 kg m⁻³ isopycnal surface, there are no strong gradients in temperature or salinity across the Gulf Stream.

At 250 m depth, the statistically significant temperature anomalies were generally positive, especially along the continental shelf edge (Fig. 4A,B). This indicates that warm NACW water dominated this region more than usual in this 10-year period. These warmer-than-normal waters along the continental shelf edge were also saltier (Fig. 4C,D) and less oxygenated (Fig. 4E,F) than normal, as one would expect from the T-S-O₂ relationships (Gilbert et al. 2005) arising from the mixing LCW

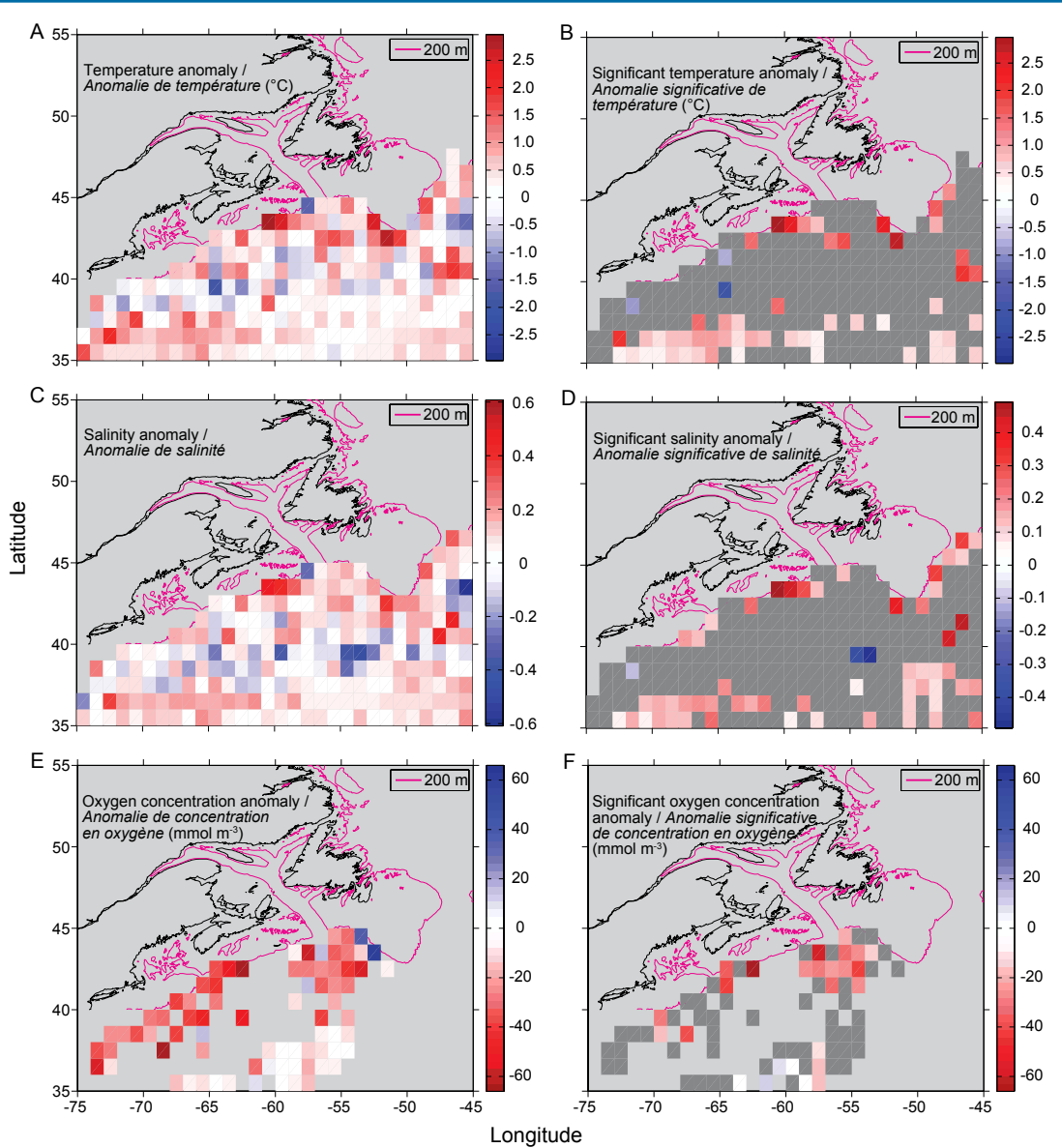


Fig. 4 Differences between 1998–2007 mean Argo observations at 250 m depth of (A) temperature, (C) salinity, (E) oxygen concentration, and the climatological fields (1° latitude $\times 1^{\circ}$ longitude) from the 2005 World Ocean Atlas. We refer to these differences as “anomalies.” In the dark grey polygons of panels B, D, and F, the anomalies are not significant.

Differences entre les observations moyennes Argo de 1998 à 2007 à la profondeur de 250 m pour (A) la température, (C) la salinité, (E) la concentration en oxygène et la climatologie (1° de latitude par 1° de longitude) tirée du World Ocean Atlas 2005. Nous présentons ces différences comme des «anomalies». Dans les polygones gris foncés des panneaux B, D et F, les anomalies ne sont pas significatives.

and NACW. We do not know whether these results were caused by changes in the spatial distribution of the water masses or by changes to the water types themselves (LCW and NACW).

Discussion

Overall, the picture emerging from the 1998–2007 Argo float measurements along the 27.25 kg m^{-3} potential density surface is very similar to the 1914–2003 climatological medians of temperature, salinity, oxygen concentration, oxygen saturation, and isopycnal depth of Gilbert et al. (2005). During these 10 years, the random motions of drifting Argo floats provided a complete spatial coverage of our study region in terms of temperature and salinity measurements. Based on annual plots of the spatial distribution of Argo profiles, we estimate that fair-

ly complete coverage of the Slope Water region has been accomplished once every 2 to 3 years since 2002, with a float density close to the global average target of one float per $90\,000 \text{ km}^2$. The spatial coverage of oxygen measurements is much less complete (Fig. 3C) because there have been very few floats deployed with oxygen sensors (one in 2004, one in 2005, and three in 2006). The relatively small number of floats with oxygen sensors is due to several factors: 1) the primary mission of Argo is to provide global measurements of temperature and salinity; 2) the addition of oxygen sensors increases the purchase cost of floats, increases data telemetry costs, and decreases total float lifetime because of increased energy demand on the float batteries; 3) oxygen sensors are still in a state of development and will require additional pilot studies for proper validation (Gruber et al. 2007). Nevertheless, our results clearly demonstrate the potential value of oxygen observations from Argo floats.

The relative homogeneity of temperature, salinity, and oxygen on either side of the Gulf Stream along the 27.25 kg m^{-3} isopycnal is consistent with the results of Bower et al. (1985), who showed that scalar properties tended to be homogeneous across the Gulf Stream at potential densities greater than 27.1 kg m^{-3} . In the words of Bower et al. (1985),

while the Gulf Stream acts as a barrier above the 27.1 kg m^{-3} isopycnal surface, its meanders and mesoscale eddies act more like a blender below the 27.1 kg m^{-3} isopycnal surface.

We note that Flemish Pass appears to hinder the passage of Argo floats. Only one float (WMO ID 62749 in March 2001) has managed to go through Flemish Pass (maximum depth $\sim 1200 \text{ m}$), crossing it at an average speed of 12 cm s^{-1} . It was a PALACE float initially launched 750 km southwest of Reykjavik (at $59.11^{\circ}\text{N}, 31.54^{\circ}\text{W}$) in November 1998, and presumably drifted through Flemish Pass at its profiling depth of 1123 m.

While it would be possible to produce seasonal and annual T-S-O₂ anomaly maps from Argo float profiles, greater

benefits of the Argo data will be realized when they are assimilated into regional ocean circulation models together with other sources of real-time observations of sea-surface height and sea-surface temperature from satellites in hindcast, nowcast and forecast modes (Davidson et al. 2006). Argo data are available to anyone, and we hope to see more and more people use them for their own needs in the future, as the value of a dataset increases in proportion to its number of users.

References

- Antonov, J.I., Locarnini, R.A., Boyer, T.P., Mishonov, A.V., and Garcia, H.E.** 2006. World Ocean Atlas 2005, Volume 2: Salinity. *Edited by S. Levitus.* NOAA Atlas NESDIS 62, U.S. Government Printing Office, Washington, D.C. 182 pp.
- Bower, A.S., Rossby, H.T., and Lillibridge, J.L.** 1985. The Gulf Stream - barrier or blender? *J. Phys. Oceanogr.* 15: 24-32.
- Carval, T., Keeley, R., Takatsuki, Y., Yoshida, Y., Loch, S., Schmid, C., Goldsmith, R., Wong, A., McCreadie, R., Thresher, A., and Tran, A.** 2006. Argo data management – User’s manual, version 2.1, 60 pp. (<http://www.usgoda.org/argo/argo-dm-user-manual.pdf>) Accessed on 9 Feb. 2008.
- Davidson, F.J.M., Wright, D.G., Lefavre, D., and Chassé, J.** 2006. The need for ongoing monitoring programs in the development of ocean forecasting capabilities in Canada. *AZMP Bulletin PMZA* 5: 43-47.
- Garcia, H.E., Locarnini, R.A., Boyer, T.P., and Antonov, J.I.** 2006. World Ocean Atlas 2005, Volume 3: Dissolved oxygen, apparent oxygen utilization, and oxygen saturation. *Edited by S. Levitus.* NOAA Atlas NESDIS 63, U.S. Government Printing Office, Washington, D.C. 342 pp.
- Gatien, M.G.** 1976. A study in the slope water region south of Halifax. *J. Fish. Res. Board Can.* 33: 2213-2217.
- Gilbert, D., Sundby, B., Gobeil, C., Mucci, A., and Tremblay, G.-H.** 2005. A seventy-two-year record of diminishing deep-water oxygen in the St. Lawrence estuary: The northwest Atlantic connection. *Limnol. Oceanogr.* 50: 1654-1666.
- Gruber, N., Doney, S.C., Emerson, S.R., Gilbert, D., Kobayashi, T., Körtzinger, A., Johnson, G.C., Johnson, K.S., Riser, S.C., and Ulloa, O.** 2007. The Argo-Oxygen program: A white paper to promote the addition of oxygen sensors to the international Argo float program. 60 pp. (http://www-argo.ucsd.edu/o2_white_paper_web.pdf)
- Hogg, N.G., Pickart, R.S., Hendry, R.M., and Smethie, W.J. Jr.** 1986. The northern recirculation gyre of the Gulf Stream. *Deep-Sea Res. A* 33: 1139-1165.
- Locarnini, R. A., Mishonov, A.V., Antonov, J.I., Boyer, T.P., and Garcia, H.E.** 2006. World Ocean Atlas 2005, Volume 1: Temperature. *Edited by S. Levitus.* NOAA Atlas NESDIS 61, U.S. Government Printing Office, Washington, D.C. 182 pp.
- Petrie, B., and Drinkwater, K.** 1993. Temperature and salinity variability on the Scotian Shelf and in the Gulf of Maine 1945-1990. *J. Geophys. Res.* 98: 20079-20089.

Monitoring Seabirds at Sea in Eastern Canada

Carina Gjerdrum¹, Erica J. H. Head² and David A. Fifield³

¹Environment Canada, Canadian Wildlife Service, 45 Alderney Drive, Dartmouth, NS, B2Y 2N6

²Bedford Institute of Oceanography, Box 1006, Dartmouth, NS, B2Y 4A2

³Environment Canada, Canadian Wildlife Service, 6 Bruce Street, Mount Pearl, NL, A1N 4T3

carina.gjerdrum@ec.gc.ca

Sommaire

Les données récoltées lors de six missions du PMZA sur le plateau Néo-Écossais, les Grands Bancs de Terre-Neuve, dans la mer du Labrador et dans le golfe du Saint-Laurent sont utilisées afin de décrire la communauté aviaire au large des côtes dans l'est du Canada en 2006. Pendant que le navire faisait route, des observateurs ont identifié et dénombré les oiseaux en regardant à 90° du côté bâbord ou tribord par séquence de 10 min jusqu'à une distance de 300 m pour l'estimation de la densité d'oiseaux marins. Nous avons observé des densités totales plus élevées au printemps par rapport à l'automne et au large des côtes de Terre-Neuve par rapport aux autres régions. Cependant, nos données ont révélé l'importance de toutes les régions pour les oiseaux migrateurs. Le mergule nain a été l'espèce rencontrée en plus grand nombre pendant les relevés et nous avons utilisé ces données afin d'explorer la relation entre cette espèce planctivore et la biomasse de trois espèces de copépodes dominants la biomasse de zooplancton.

Introduction

The east coast of Canada supports large numbers of breeding marine birds as well as millions of migrants from the southern hemisphere and northeastern Atlantic. Although tied to land during the breeding season when they raise their young, seabirds exist mostly in the marine environment. Since many spend much of their lives out of sight of land, knowledge of their pelagic distribution and ecology has been difficult to obtain. In 1969, R.G.B. Brown and P. Germain initiated what was then considered the first “modern” pelagic seabird survey—PIROP (*Programme Intégré de Recherches sur les Oiseaux Pélagiques*)—based on a systematic technique and computer database. The program was operated by the

Canadian Wildlife Service (CWS) of Environment Canada and supported by the large DFO (Department of Fisheries and Oceans) oceanographic fleet based in eastern Canada. The results of the surveys were first published in 1975, in the form of an atlas for seabirds off Eastern and Arctic Canada (Brown et al. 1975) that was subsequently updated (Brown 1986). Much of our current knowledge of the marine birds of these areas is based on the PIROP surveys. However, data are limited beyond the mid-1980s.

In 2005, CWS reinvigorated the monitoring program for seabirds at sea with the goal of identifying and minimizing the impacts of human activities. Our sampling strategy relies

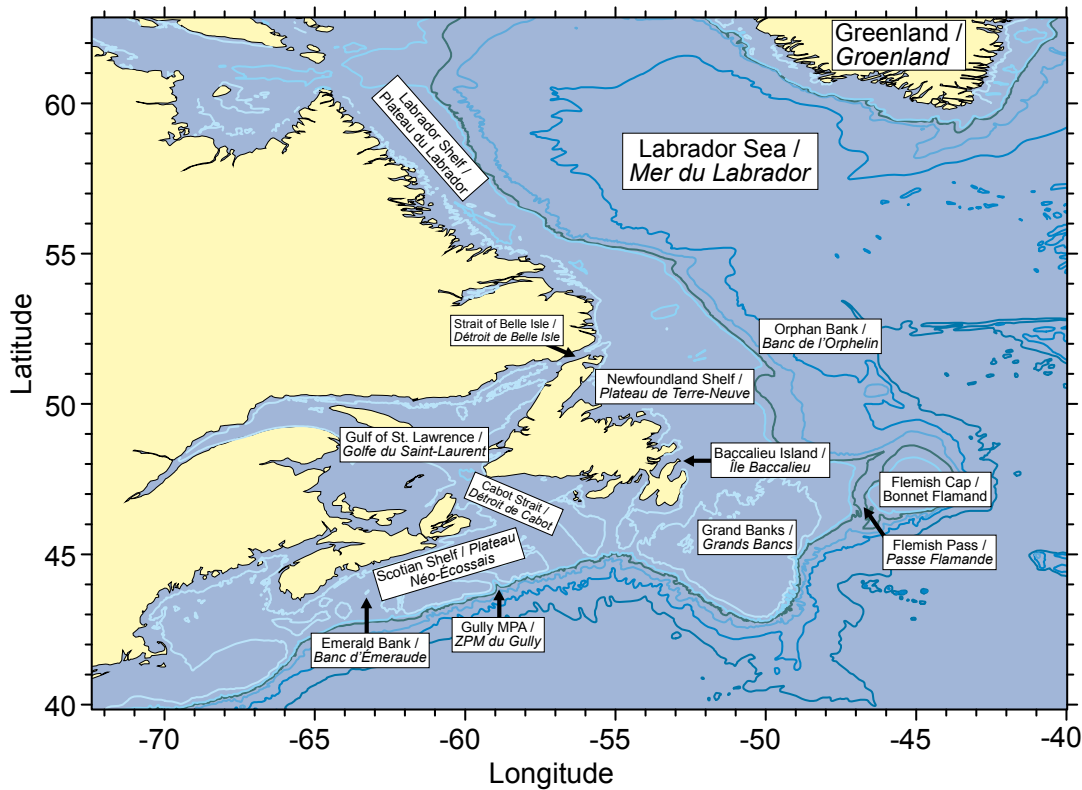


Fig. 1 Region surveyed in 2006.

Région couverte en 2006.

on ships-of-opportunity that travel throughout the region at all times of the year. The Atlantic Zone Monitoring Program (AZMP) provides observation platforms that sample transects over a broad geographic area and across multiple seasons, allowing us to monitor both intra- and interannual variability in seabird occurrence and to compare marine communities among regions. The data also provide critical, and currently unavailable, information for environmental assessments of offshore developments; identify areas where birds are at high risk for oil pollution and other human activities; and enable us to monitor trends in the marine environment. In addition, the biological, chemical, and physical data collected concurrently by DFO oceanographers provide the means to examine the linkages between seabirds and their marine habitats and to investigate seabird responses to oceanographic variability.

CWS seabird observers participated in six AZMP missions in 2006—two on the Grand Banks and northeast Newfoundland Shelf, two on the Scotian Shelf, one across the Labrador Sea, and one in the Gulf of St. Lawrence (Fig. 1). This article gives a summary of the birds observed during these surveys and highlights differences among regions and seasons. Because seabirds are not uniformly distributed across their marine habitat, but instead are influenced by the physical processes that concentrate prey and make them available to the birds, we also explore the relationship between the surface density of zooplankton and the presence of dovekie (*Alle alle*), the only Atlantic seabird to prey mostly on copepods (Montevecchi and Stenhouse 2002).

The dovekie is considered the most abundant seabird in the North Atlantic. It is a small (ca. 160 g), stout, black and

white bird that typically flies with very rapid, insect-like wing beats (Montevecchi and Stenhouse 2002) (Fig. 2). Dovekie breed between May and August in colonies on steep talus slopes in the high Arctic, with particularly large concentrations in northwest Greenland. During the non-breeding season, they live in the open ocean and are common on the Scotian Shelf, Grand Banks, and Newfoundland and Labrador shelves (Brown et al. 1975, Brown 1986). At this time of year, Brown (1988) found that the largest concentrations occurred over the shelf-breaks where apparently large numbers of zooplankton aggregate. Dovekie dive to depths of between 20 and 30 m (Falk et al. 2000), feeding almost exclusively on planktonic crustaceans. They eat primarily copepods, selecting the largest stages

of *Calanus glacialis*, *C. hyperboreus*, and *C. finmarchicus* (Bradstreet 1982, Karnovsky et al. 2003, Jakubas et al. 2007, Steen et al. 2007), but amphipods (*Themisto* and *Apherusa*) are also consumed, especially in the late summer (Bradstreet 1982, Hobson 1993). Dovekie catch one crustacean at a time (Keats 1981) and thus must feed in locally dense patches of prey to meet their daily energy requirements. The extent of the spatial overlap between dovekie and their zooplankton prey is not well known, especially outside of the breeding season. We use data collected during AZMP missions in 2006 to examine this association and predict that the spatial distribution of foraging dovekie can be determined by near-surface prey concentrations.



Fig. 2 Dovekie (*Alle alle*). Mergule nain (*Alle alle*).

Seabird Sampling Methods

Surveys were conducted while looking forward from the bridge when the vessel was moving, scanning ahead to a 90° angle from either the port or starboard side, limiting observations to a transect band 300 m wide from the beam of the ship. Each survey lasted 10 min; we conducted as many consecutive surveys as possible during the daylight hours, regardless of whether birds were present. At the beginning of each 10-min survey, we recorded the ship's position, time of day, ship speed and direction, and a number of environmental variables (i.e., visibility, sea state, swell height, wind speed and direction). All birds observed in the transect were counted and identified as present in air or on water. Binoculars were used to confirm the species identification and other details, such as age, moult, and feeding behaviours. We continuously recorded all birds observed on the sea surface throughout the 10-min surveys and estimated their perpendicular distance from the ship (0–50 m, 51–100 m, 101–200 m, 201–300 m). A count of all flying birds passing through the transect would be a measure of bird flux and would overestimate bird density (Tasker et al. 1984). Therefore, we recorded flying birds using instantaneous counts at regular intervals throughout each 10-min survey (Tasker et al. 1984). Seabird surveys were conducted along AZMP sections and while transiting between sections. Overall densities were calculated for each 10-min survey as the number of birds observed in transect (all species combined) divided by the area surveyed.

Because they are small and can be difficult to detect during certain sea conditions, we modelled dovekie detectability and estimated densities using distance sampling methods (Buckland et al. 2001, Thompson 2002). When surveying birds along a transect line, the likelihood of detecting a bird decreases the further it is from the ship, since more distant birds are harder to see and are more likely to be missed. Distance sampling is a conceptually simple technique used in many types of wildlife surveys to account for animals that go undetected. To do this, Program Distance (Thomas et al. 2006) plots a histogram of detection distances and models a detection function to determine the estimated proportion of birds detected as a function of observation distance (detection probability). Since birds are likely distributed randomly across the 300 m transect, the histogram bars would all be roughly the same height (corresponding to equal probability of detection in each distance class) if all birds present were detected. For example, the histogram in Figure 3 shows sharply declining detection probability with increasing distance, which is typical for small seabirds. We used Program Distance to estimate the detection probability of dovekie, also taking into account a number of covariates, including region (Newfoundland Grand Banks and Shelf, Scotian Shelf, Labrador Sea, and Gulf of St. Lawrence), platform speed, visibility, sea state, and wind speed. Model fit and ranking were assessed using Akaike's Information Criterion (AIC) (Burnham and Anderson 2002). Adjusted dovekie densities were then compared to patterns of *Calanus* distribution and abundance.

Zooplankton Sampling Methods

Zooplankton samples were collected at transect stations using 0.75 m diameter ring nets fitted with 200 µm mesh that are towed vertically between the bottom and the surface (if

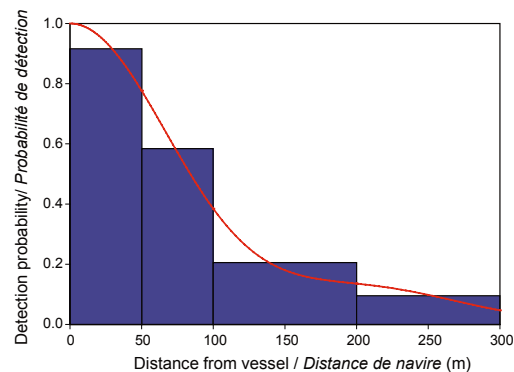


Fig. 3 Histogram and modelled detection function (red line) depicting detection distance of dovekie sightings on the water during 2006 seabird surveys.

Histogramme et la fonction de détection modélisée (ligne rouge) illustrant la distance de détection sur l'eau des mergules nains lors du relevé d'oiseaux marins de 2006.

the bottom was shallower than 1000 m) or between 1000 m and the surface (if the bottom was deeper than 1000 m). The samples were preserved in 4% formalin and enumerated using the standard AZMP protocol (Mitchell et al. 2002). In this protocol, subsamples containing at least 100 *Calanus* are analyzed, with each individual being identified to the level of species and stage.

Three species of *Calanus* (*C. finmarchicus*, *C. glacialis*, *C. hyperboreus*) have been shown to dominate the zooplankton biomass in the Labrador Sea (Head et al. 2003) and on the Scotian and Newfoundland shelves (Head and Harris 2004). Therefore, *Calanus* biomass was used as the index of zooplankton biomass in this study. In spring, *Calanus* are active, feeding, and growing, and it was assumed that all stages of all three species were in the near-surface layers. Thus, for spring samples, near-surface *Calanus* biomass was calculated using water column abundance estimates, as measured above, and the dry weights-at-stage reported by Head and Harris (2004). In fall, most *Calanus* descend to deeper layers as late-stage copepodites to spend the winter in a resting state. In order to calculate the proportion of individuals in the water column that would have been at depths of <100 m (i.e., in the near-sur-

Table 1 Fall percentages of *C. finmarchicus* copepodite stages present in the surface layer versus those in the 0–1000 m or 0–470 m (Cabot Strait) depth range averaged over stations in the slope waters of the Newfoundland Shelf, the eastern and western portions of the Scotian Shelf, and in Cabot Strait.

Pourcentages des stades copépodites de C. finmarchicus présents à l'automne dans la couche de surface contre ceux présents dans la couche 0 – 1000 m ou 0 – 470 m (déroit de Cabot) de profondeur (moyenne sur toutes les stations de la pente) sur le plateau de Terre-Neuve, les secteurs est et ouest du plateau Néo-Écossais et au déroit de Cabot.

Stage / Stade	CVI	CV	CIV	CIII	CII	CI
Newfoundland Shelf / plateau de Terre-Neuve	13	6	23	90	100	80
Cabot Strait / déroit de Cabot	48	28	66	100	100	100
Eastern Scotian Shelf / est du plateau Néo-Écossais	12	6	17	96	100	100
Western Scotian Shelf / ouest du plateau Néo-Écossais	9	3	21	97	100	100

face layers) for stations where depths were >100 m, we used results from a series of Hydro-bios Multinet tows that were taken in the slope waters of the Newfoundland and Scotian shelves and Cabot Strait in November 2001 (Newfoundland Shelf) and October 2003 (Scotian Shelf and Cabot Strait). The Multinet has five nets that can be opened and closed sequentially as the net is towed vertically. The surface layer for these tows was generally 0–200 m, except in Cabot Strait, where it was 0–100 m. Vertical distributions of copepodite stage CV *C. finmarchicus* have been reported elsewhere (Head and Pepin 2007), but here we show the percentages of the different stages that were present in the surface versus the total water column abundance (Table 1). These percentages were applied to the total water column abundance data collected using ring nets in fall 2006, together with the dry weights-at-stage reported by Head and Harris (2004), to give the biomass in the 0–200 or 0–100 m layer. For stations having depths <100 m, we used the total water column abundances and dry weights-at-stage from Head and Harris (2004). *C. glacialis* and *C. hyperboreus* were very rare in the surface layers in the Multinet tows and at stations of <100 m depth, so we have discounted their contribution to the total *Calanus* biomass in fall.

Seabird Distribution and Abundance

During the six AZMP missions conducted in 2006, we surveyed over 6883 km of ocean track (Fig. 4A, B) and counted a total of 17,477 birds from 9 families (Table 2). The majority (61%) of the birds observed were from the Alcidae, a primarily marine family of birds confined to the northern hemisphere. Dovekie accounted for most of these observations, although murre (*Uria* spp.) and Atlantic puffin (*Fratercula arctica*) were also common. Members of the family Procellariidae were relatively abundant (22%), specifically the northern fulmar (*Fulmarus glacialis*) and greater shearwater (*Puffinus gravis*). Gulls (*Larus* spp.) and terns (*Sterna* spp.) accounted for over 6% of the observations. Although overall patterns of seabird occurrence were similar among the six

missions, differences between the spring and fall and among the regions were evident.

Spring

During the spring (April–June), we surveyed the Scotian Shelf, Grand Banks and northeast Newfoundland Shelf, and the Labrador Sea (Fig. 4A). Although numbers were highly variable, average densities during this time were higher off the coast of Newfoundland (median, range; 9.0 birds km⁻², 0–1270, n = 400) than in the Labrador Sea (2.5 birds km⁻², 0–103, n = 181) and on the Scotian Shelf (0.8 birds km⁻², 0–49, n = 400). Murre, dovekie, and Atlantic puffin together accounted for 62% of the spring observations. Common murre and Atlantic puffin were common in Newfoundland Shelf waters and through the Strait of Belle Isle, while thick-billed murre (*Uria lomvia*)

Table 2 Species composition of marine birds observed within a 300 m transect during six research missions in 2006.

Composition en espèces des oiseaux marins observés sur une distance de 300 m lors des six missions de recherche de 2006.

Family / Famille	Species / Espèces	Number observed / nombre observé
Gavidae	Loon species / plongeons non identifiés	<i>Gavia</i> spp. 3
Procellariidae	Northern Fulmar / fulmar boréal	<i>Fulmarus glacialis</i> 2688
	Cory's Shearwater / puffin cendré	<i>Calonectris diomedea</i> 28
	Greater Shearwater / puffin majeur	<i>Puffinus gravis</i> 963
	Manx Shearwater / puffin des anglais	<i>P. puffinus</i> 1
	Sooty Shearwater / puffin fuligineux	<i>P. griseus</i> 180
	Unknown Shearwater / puffins non identifiés	<i>Puffinus</i> or <i>Calonectris</i> 27
Hydrobatidae	Wilson's Storm-petrel / océanite de Wilson	<i>Oceanites oceanicus</i> 17
	Leach's Storm-petrel / océanite cul-blanc	<i>Oceanodroma leucorhoa</i> 331
	Unknown Storm-petrel / océanites non identifiés	<i>Oceanodroma</i> or <i>Oceanites</i> 306
Phalacrocoracidae	Great Cormorant / grand cormoran	<i>Phalacrocorax carbo</i> 1
	Double-crested Cormorant / cormoran à aigrettes	<i>P. auritus</i> 1
Sulidae	Northern Gannet / fou de Bassan	<i>Morus bassanus</i> 281
Anatidae	Common Eider / eider à duvet	<i>Somateria mollissima</i> 22
	Black Scoter / macreuse noire	<i>Melanitta nigra</i> 5
	White-winged Scoter / macreuse brune	<i>M. fusca</i> 5
	Unknown Scoter / macreuses non identifiés	<i>Melanitta</i> spp. 1
	Common Merganser / grand harle	<i>Mergus merganser</i> 9
Scolopacidae	Red Phalarope / phalarope à bec large	<i>Phalaropus fulicaria</i> 465
	Unknown Phalarope / phalaropes non identifiés	<i>Phalaropus</i> spp. 12
Laridae	Long-tailed Jaeger / labbe à longue queue	<i>Stercorarius longicaudus</i> 74
	Parasitic Jaeger / labbe parasite	<i>S. parasiticus</i> 1
	Pomarine Jaeger / labbe pomarin	<i>S. pomarinus</i> 58
	South Polar Skua / labbe de McCormick	<i>S. maccormicki</i> 2
	Great Skua / grand labbe	<i>S. skua</i> 15
	Unknown Jaeger or Skua / labbes non identifiés	<i>Stercorarius</i> spp. 114
	Ring-billed Gull / goéland à bec cerclé	<i>Larus delawarensis</i> 6
	Herring Gull / goéland argenté	<i>L. argentatus</i> 219
	Glaucous Gull / goéland bourgmestre	<i>L. hyperboreus</i> 39
	Great Black-backed Gull / goéland marin	<i>L. marinus</i> 98
	Sabine's Gull / mouette de Sabine	<i>Xema sabini</i> 2
	Black-legged Kittiwake / mouette tridactyle	<i>Rissa tridactyla</i> 671
	Unknown Gull / goélands non identifiés	<i>Larus</i> spp. 29
	Tern / sternes	<i>Sterna</i> spp. 71
Alcidae	Common Murre / guillemot marmette	<i>Uria aalge</i> 2491
	Thick-billed Murre / guillemot de Brünnich	<i>U. lomvia</i> 1475
	Unknown Murres / guillemots non identifiés	<i>Uria</i> spp. 1246
	Razorbill / petit pingouin	<i>Alca torda</i> 45
	Dovekie / mergule nain	<i>Alle alle</i> 4519
	Black Guillemot / guillemot à miroir	<i>Cephus grylle</i> 8
	Atlantic Puffin / macareux moine	<i>Fratercula arctica</i> 859
	Unknown Alcidae / alcidés non identifiés	Alcidae 83
	Unidentified bird / oiseaux non identifiés	6
Total number observed / nombre total observé		17477

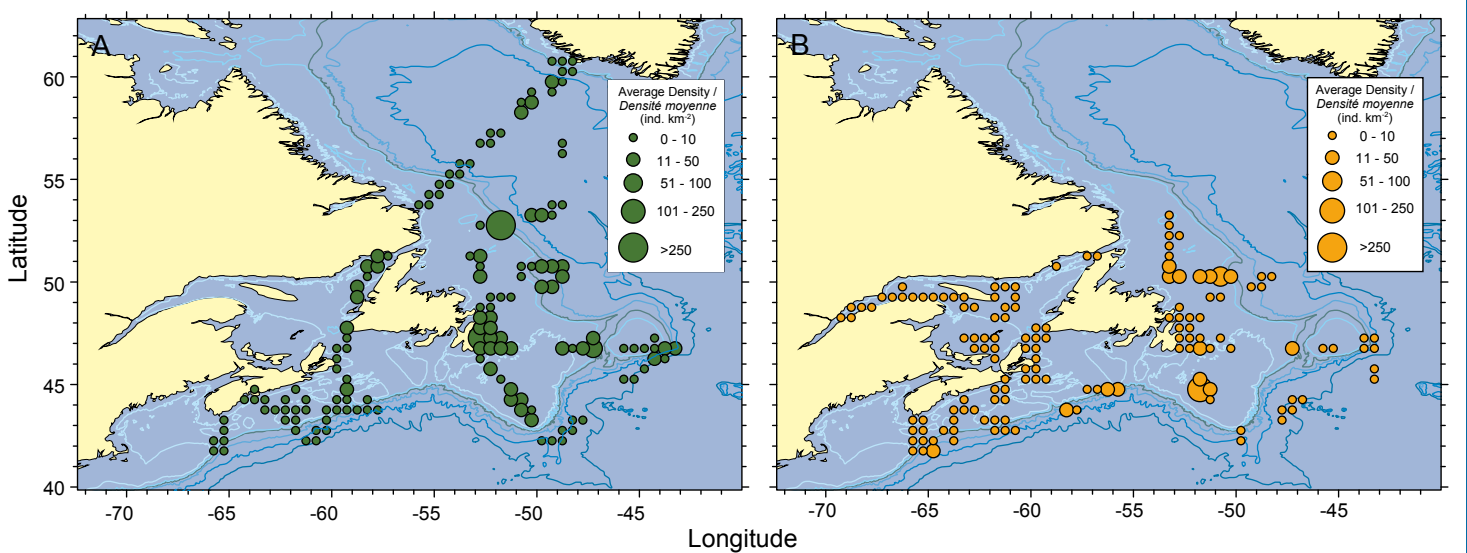


Fig. 4 Bird density (all species, total number of birds km^{-2}) averaged over half-degree quadrats during 2006 AZMP surveys in A) spring and B) fall.

Densité d'oiseaux (toutes les espèces, nombre total d'oiseaux au km^{-2}) moyennée sur des quadrats d'un demi-degré lors de relevés PMZA en 2006 au printemps (A) et à l'automne (B).

and dovekie were observed farther offshore and across the Labrador Sea. Dovekie were especially abundant along the Newfoundland Shelf edge and slope waters (Fig. 5A). At this time of year, murres and puffins are moving from offshore wintering areas and beginning to colonize breeding areas in eastern Newfoundland, Labrador, and the Arctic. Dovekie are migrating towards colonies in the eastern Arctic and Greenland.

Northern fulmar were common (15% of spring observations) throughout the survey area, although less abundant on the Scotian Shelf compared to areas off Newfoundland and Labrador. Storm-petrels (Hydrobatidae) accounted for 4% of the birds observed and were seen throughout the region. They were especially abundant off Baccalieu Island (northeastern tip of the Avalon Peninsula; Fig. 1), which is the largest Leach's storm-petrel (*Oceanodroma leucorhoa*) colony in the world and is estimated to have more than 3 million pairs. Adult and immature black-legged kittiwake (*Rissa tridactyla*) were relatively common in Cabot Strait and off the Avalon Peninsula near breeding colonies. Red phalarope (*Phalaropus fulicaria*) were only observed in large numbers as we approached Greenland, in deep Labrador Sea waters. The phalaropes were all in breeding plumage and were presumably migrating to breeding grounds in the high Arctic.

Fall

The Newfoundland and Scotian shelves and the Gulf of St. Lawrence were surveyed in the fall (October–November; Fig. 4B). Again, we observed the highest bird densities off the coast of Newfoundland (median, range; 2.0 birds km^{-2} , 0–185, $n = 326$), intermediate densities on the Scotian Shelf (0.8 birds km^{-2} , 0–101, $n = 363$), and the lowest densities in the Gulf of St. Lawrence (0.01 birds km^{-2} , 0–72, $n = 205$). For all areas combined, densities in the fall (0.8 birds km^{-2}) were significantly less than those estimated in the spring (3.2 birds km^{-2} ; Wilcoxon Test $Z = -11.9$, $P < 0.0001$). Murre, the most common species observed (26%), were concentrated almost exclusively on the Grand Banks and north-

eastern Newfoundland Shelf. Murre are known to winter in these areas but may also be migrating to areas farther south. Dovekie were observed in all regions but were common on the Newfoundland Shelf and through Cabot Strait (Fig. 5B). Although they are known to occur in large numbers on the Scotian Shelf during the non-breeding season, it is likely that not all had arrived from their northern breeding areas during the time of our fall surveys.

Greater shearwater accounted for 20% of the fall observations and were particularly abundant on the western Scotian Shelf and southeastern Grand Banks. This contrasts with the spring surveys, when greater shearwater observations were uncommon and occurred only on the eastern Scotian Shelf. Greater shearwater breed in the southern hemisphere, and it is thought that most of the non-breeding population can be found in our local waters during the austral winter. Similar to our observations in spring, northern fulmar were common (18%) and ubiquitous in fall, although less so in the Gulf of St. Lawrence. Black-legged kittiwake were distributed farther offshore during fall surveys compared to the spring but were also common in the Gulf. Although relatively rare during the spring missions (0.7% of observations), northern gannet (*Morus bassanus*) made up over 4% of the observations during the fall, all of which were on the Scotian Shelf and in the Gulf of St. Lawrence. During this time of year, immature gannets are moving to wintering areas off the coast of New England, to be followed a short time later by the adults. Leach's storm-petrels were only observed on the Scotian Shelf.

Associations Between Dovekie and Their Zooplankton Prey

Dovekie made up 26% of all the bird observations in 2006, by far the dominant species in the surveys (the next most common bird was northern fulmar, at 15%). To estimate their density more accurately, we first modelled the detection function (the probability of detecting a dovekie on the water at a given distance from the vessel) in relation to the region and several environmental factors and ranked the models

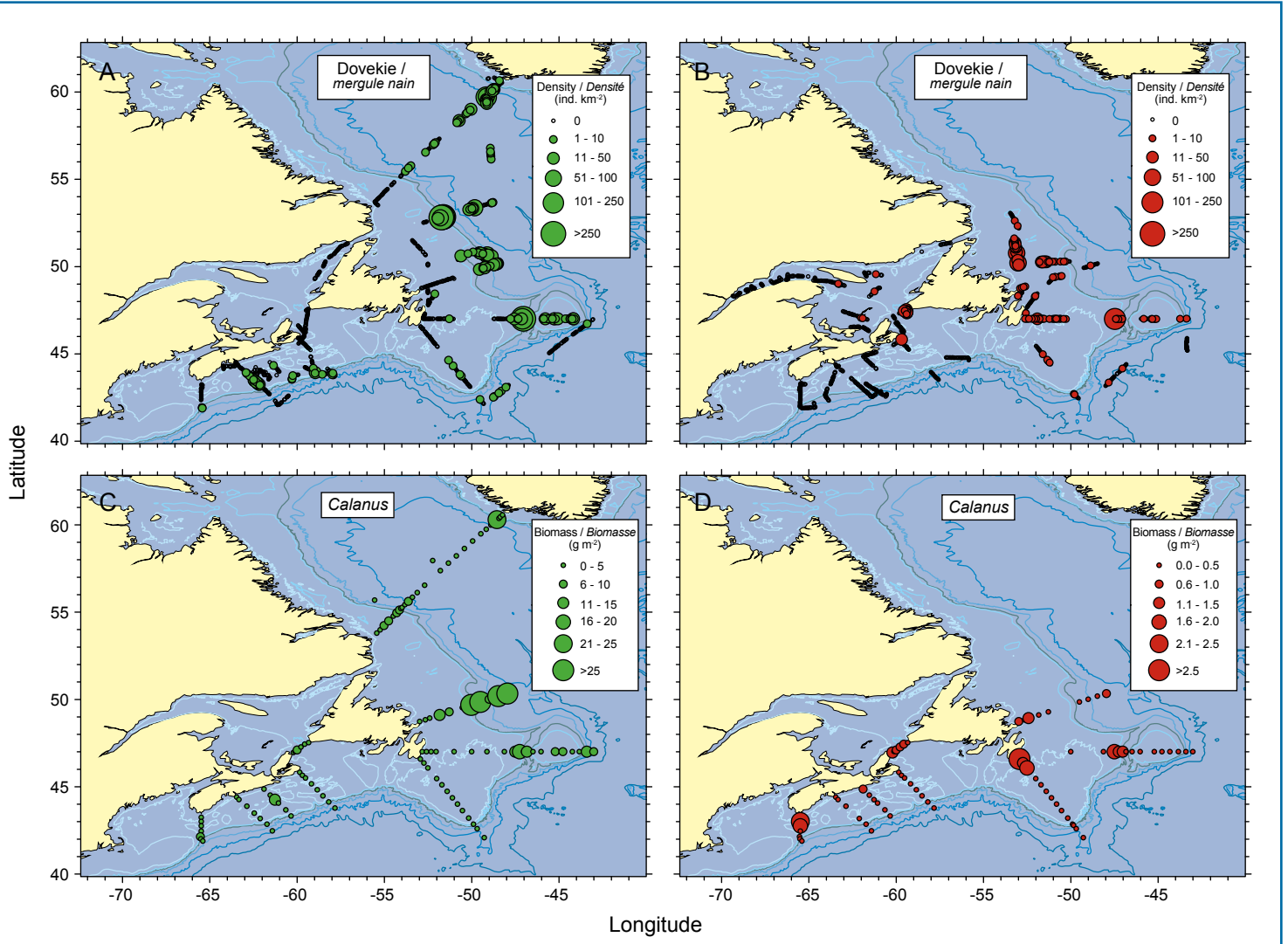


Fig. 5 Dovekie densities calculated for each 10-min survey (A and B) compared to total *Calanus* biomass (C and D) during spring (left) and fall (right) surveys in 2006.

*Densités de mergule nain calculées pour chaque relevé de 10 min (A et B) comparées à la biomasse totale de *Calanus* (C et D) lors des missions du printemps (à gauche) et de l'automne (à droite) en 2006.*

according to their AIC. Overall, we found that most birds were detected within 100 m of the vessel, but detectability dropped considerably beyond that distance (Fig. 3). Our best fit model was stratified by region and included wind speed as a covariate. Because wind speed disrupts the water's surface, it can significantly reduce the visibility of birds sitting on the water. The model that included relative sea-state estimates did not rank as high ($\Delta\text{AIC} = 117.5$), nor did models that included visibility ($\Delta\text{AIC} = 172.9$) or ship speed ($\Delta\text{AIC} = 177.7$). Using detection probabilities calculated for each region, and taking into account wind speed values of the observations in those regions, we calculated dovekie densities for each of our 10-min surveys.

Overall, dovekie were more numerous during spring surveys compared to the fall. During the spring, dovekie concentrations were highest on the northeastern Newfoundland slope (Fig. 5A), where estimates were as high as 1316 birds km^{-2} . They were also numerous through the Flemish Pass (330 birds km^{-2}), near the southwest coast of Greenland (115 birds km^{-2}), and in Orphan Basin (61 birds km^{-2}). We estimated dovekie densities to be between 11 and 50 birds km^{-2} on the Flemish Cap,

the Emerald Bank, and in the Gully Marine Protected Area. During the fall, large numbers of dovekie were again observed through the Flemish Pass (141 birds km^{-2}). Compared to spring surveys, more dovekie were observed closer to shore on the Newfoundland Shelf (up to 60 birds km^{-2}) and through Cabot Strait (Fig. 5B).

Our estimates of *Calanus* biomass in the surface layers were much higher in spring than in fall (Fig. 5C, D). This is partly due to the assumption that we made regarding the depth distributions of *Calanus*: we assumed that all individuals were near the surface in spring and only some in fall. We also note, however, that our depth resolution within the surface layers is poor, so we do not know the proportion of the *Calanus* that would have been available to the dovekie. Thus, our estimates of *Calanus* biomass are at best an index of the availability of this food. Nevertheless, we note certain features that are consistent with expectations. For example, the near-surface biomass of *Calanus* in Cabot Strait was higher, relatively speaking, in fall than in spring, which is the result of their having an extended reproductive and growth season in the region (Head and Pepin 2007). Dovekie could presumably take

advantage of this locally abundant food source, which was reflected in the high densities observed in this area during the fall surveys. In addition, *Calanus* biomass offshore from the Greenland Shelf was high in spring, which is a regular feature from year to year and results from high reproductive and survival rates for *C. finmarchicus* in this region (Head et al. 2003). This productivity is likely an important feature for the millions of dovekie that breed along the western coast of Greenland and may explain the large numbers encountered during our survey in 2006. Finally, we note the high concentrations of both *Calanus* biomass and dovekie densities in the Newfoundland slope waters, especially at the northeastern edge of the Grand Banks, which are consistent with the previous observations of Brown (1986, 1988). Future work will include statistical analyses to estimate the degree of overlap between dovekie and their prey.

Conclusions

By utilizing the AZMP sections for seabird surveys, we are able to quantify distribution and abundance over a broad geographic area. Several of the sections are surveyed at least twice a year, allowing us to examine how seabird communities in specific areas may vary by season. Future work will compare these results with historic surveys to determine what changes may have occurred in seabird communities over the past three decades. The data collected in 2006 demonstrate the importance of specific areas in eastern Canada for birds during spring and fall migration. Over time, these data will help identify critical foraging, moulting, and roosting areas; migration routes; and the timing of major migrations. In addition, the physical, chemical, and biological data collected along the same sections allow us to examine linkages between seabirds and their marine habitat. In 2006, we found spatial overlap between high dovekie densities and *Calanus* biomass. High *Calanus* concentrations in Newfoundland slope waters and near the Greenland coast appeared to be important dovekie foraging areas, as did the northeastern Grand Banks and Cabot Strait during the fall. In the future, we can examine the persistence of these patterns between seasons and across years to determine whether marine birds have the potential to be indicators of underlying ecological processes over multiple scales. Because seabird surveys are also conducted between sections where oceanographic data are not collected, a strong association between dovekie occurrence and zooplankton biomass may highlight productive areas that would otherwise go undetected. Similarly, biological surveys conducted at night when seabird surveys cannot be done may reveal important habitat for foraging birds.

Acknowledgements

The seabird surveys could not occur without the generous support of DFO scientists and staff as well as the Coast Guard officers and personnel. We would also like to thank François Bolduc for surveys conducted in the Gulf of St. Lawrence and Pierre Ryan for Newfoundland surveys.

References

- Bradstreet, M.S.W. 1982. Pelagic feeding ecology of Dovekies, *Alle alle*, in Lancaster Sound and Western Baffin Bay. Arctic 35: 126–140.
- Brown, R.G.B. 1986. Revised atlas of eastern Canadian seabirds. Canadian Wildlife Service, Ottawa.
- Brown, R.G.B. 1988. Oceanographic factors as determinants of the winter range of the Dovekie (*Alle alle*) off Atlantic Canada. Colonial Waterbirds 11: 176–180.
- Brown, R.G.B., Nettleship, D.N., Germain, P., Tull, C.E. and Davis, T. 1975. Atlas of eastern Canadian seabirds. Canadian Wildlife Service, Ottawa.
- Buckland, S.T., Anderson, D.R., Burnham, K.P., Laake, J.L., Borchers, D.L., and Thomas, L. 2001. Introduction to distance sampling: estimating abundance of biological populations. Oxford University Press, Oxford.
- Burnham, K.P., and Anderson, D.R. 2002. Model selection and multimodel inference: a practical information-theoretic approach, 2nd edition. Springer, New York.
- Falk, K., Pedersen, C.E., and Kampp, K. 2000. Measurements of diving depth in Dovekies (*Alle alle*). Auk 117: 522–525.
- Head, E.J.H., and Harris, L.R. 2004. Estimating zooplankton biomass from dry weights of groups of individual organisms. CSAS Res. Doc. 2004/045, 22 pp.
- Head, E.J.H., and Pepin, P. 2007. Variations in overwintering depth distribution of *Calanus finmarchicus* in the slope waters of the NW Atlantic continental shelf and the Labrador Sea. J. Northwest Atl. Fish. Sci. 39: 49–69.
- Head, E.J.H., Harris, L.R., and Yashayaev, I. 2003. Distributions of *Calanus* spp. and other mesozooplankton in the Labrador Sea in relation to hydrography in spring and early summer (1995–2000). Prog. Oceanogr. 59: 1–30.
- Hobson, K.A. 1993. Trophic relationships among high Arctic seabirds: insights from tissue-dependent stable-isotope models. Mar. Ecol. Prog. Ser. 95: 7–18.
- Jakubas, D., Wojczulanis-Jakubas, K., and Walkusz, W. 2007. Response of Dovekie to changes in food availability. Waterbirds 30: 421–428.
- Karnovsky, N., Kwasniewski, S., Weslawski, J.M., Walkusz, W., Beszczynska-Möller, A. 2003. Foraging behavior of little auks in a heterogeneous environment. Mar. Ecol. Prog. Ser. 253: 289–303.
- Keats, D. 1981. Dovekies. Osprey 12: 10.
- Mitchell, M.R., Harrison, G., Pauley, K., Gagné, A., Maillet, G., and Strain, P. 2002. Atlantic Zonal Monitoring Program sampling protocol. Can. Tech. Rep. Hydrogr. Ocean Sci. 223, 23 pp.
- Montevecchi, W.A., and Stenhouse, I.J. 2002. Dovekie (*Alle alle*). In The birds of North America. Edited by A. Poole and F. Gill, Academy of Natural Sciences, Philadelphia, and American Ornithologists' Union, Washington, D.C.
- Steen, H., Vogedes, D., Broms, F., Falk-Petersen, S., and Berge, J. 2007. Little auks (*Alle alle*) breeding in a high arctic fjord system: bimodal foraging strategies as a response to poor food quality? Polar Res. 26: 118–125.
- Tasker, M.L., Hope Jones, P., Dixon, T., and Blake, B.F. 1984. Counting seabirds at sea from ships: a review of methods and a suggestion for a standardized approach. Auk 101: 567–577.
- Thomas, L., Laake, J.L., Rexstad, E., Strindberg, S., Marques, F.F.C., Buckland, S.T., Borchers, D.L., Anderson, D.R., Burnham, K.P., Burt, M.L., Hedley, S.L., Pollard, J.H., Bishop, J.R.B., and Marques, T.A. 2006. Distance 6.0. Beta 3. Research Unit for Wildlife Population Assessment, University of St. Andrews, UK. <http://www.ruwpa.st-and.ac.uk/distance/> (accessed 6 March 2008).
- Thompson, W. L. 2002. Towards reliable bird surveys: accounting for individuals present but not detected. Auk 119: 18–25.

A large number of scientists and technicians participate in the AZMP, either collecting, editing, processing, analyzing, or presenting the data. The following people have each played a significant role in the activities of the program; however, the list does not include all of the personnel who have contributed. For those not mentioned in the list, but who have helped during the past years, the AZMP is truly appreciative.

Maritimes Region / Région des Maritimes

Kumiko Azetsu-Scott², Doug Gregory³, Glen Harrison², Erica Head², Ross Hendry¹, Catherine Johnson², Mary Kennedy³, Bill Li², Heidi Maass⁴, Michel Mitchell¹, Kevin Pauley^{5,6}, Tim Perry^{5,6}, Brian Petrie¹, Liam Petrie⁸, Roger Pettigrew⁸, Cathy Porter⁴, Doug Sameoto², Victor Soukhovtsev⁸, Jeff Spry^{5,6}, Igor Yashayaev¹, Phil Yeats²

Newfoundland and Labrador Region / Région de Terre-Neuve et du Labrador

Wade Bailey¹, Robert Chafe^{5,6}, Eugene Colbourne¹, Joe Craig¹, Frank Dawson^{5,6}, Charles Fitzpatrick¹, Sandy Fraser², Daniel Lane¹, Trevor Maddigan^{5,6}, Gary Maillet², Pierre Pepin², Scott Quilty^{5,6}, Greg Redmond², Maitland Samson^{5,6}, Dave Sears^{5,6}, Dave Senciali³, Tim Shears², Marty Snooks^{5,6}, Paul Stead¹, Keith Tipple^{5,6}

¹Physical Oceanography / Océanographie physique; ²Biological/Chemical Oceanography / Océanographie biologique/chimique; ³Data Management / Gestion des données; ⁴Remote Sensing / Télédétection; ⁵Sampling & Laboratory Analyses / Échantillonnage & analyses en laboratoire; ⁶Fish Surveys / Missions d'évaluation de poissons; ⁷Webmaster / Webmestre; ⁸Graphic & Data Analyst / Graphiste et analyste de données.

Un grand nombre de scientifiques et de techniciens participent au PMZA, soit à la collecte, l'édition, la réalisation, l'analyse ou la présentation des données. Les personnes suivantes ont joué un rôle significatif dans les activités du programme, mais la liste n'inclue pas tout le personnel qui a contribué. Pour ceux qui ne sont pas mentionnés dans la liste, nous aimerions leur exprimer notre gratitude pour l'aide précieuse qu'ils ont fournie au PMZA au cours des dernières années.

Québec Region / Région du Québec

Marie-France Beaulieu⁵, Laure Devine³, Marie-Lyne Dubé⁵, Alain Gagné⁵, Yves Gagnon⁵, Peter Galbraith¹, Denis Gilbert¹, Michel Harvey², Pierre Joly⁵, Caroline Lafleur^{1,3}, Pierre Larouche⁴, Caroline Lebel⁵, Sylvie Lessard^{2,5}, Patrick Ouellet², Bernard Pelchat³, Bernard Pettigrew⁵, Stéphane Plourde², Pierre Rivard⁵, Liliane St-Amand^{2,5}, Isabelle St-Pierre³, Jean-François St-Pierre^{2,5}, Michel Starr²

Integrated Science Data Management / Gestion des données scientifiques intégrée

Bob Keeley³, Mathieu Ouellet^{3,7,8}, Anh Tran³

Gulf Region / Région du Golfe

Joël Chasse¹, Doug Swain⁶

Publications

Primary Publications / Publications primaires

- Doniol-Valcroze, T., D. Berteaux, P. Larouche and R. Sears.** 2007. Influence of thermal fronts on the habitat selection of four rorqual whale species in the Gulf of St. Lawrence. *Mar. Ecol. Prog. Ser.* **335**: 207-213.
- Greenan, B. J. W., B. D. Petrie, W. G. Harrison and P. M. Strain.** 2008. The onset and evolution of a spring bloom on the Scotian Shelf. *Limnol. Oceanogr.* **53** (in press).
- Head, E. J. H., and P. Pepin.** 2007. Variations in overwintering depth distribution of *Calanus finmarchicus* in the slope waters of the NW Atlantic continental shelf and the Labrador Sea. *J. Northw. Atl. Fish. Sci.* **39**: 49-69.
- Head, E.J.H., and D.D. Sameoto.** 2007. Interdecadal variability in zooplankton and phytoplankton abundance on the Newfoundland and Scotian shelves. *Deep-Sea Res. II* **54**: 2686-2701.
- Johnson, C. L., A. W. Leising, J. A. Runge, E. J. H. Head, P. Pepin, S. Plourde and E. G. Durbin.** 2008. Characteristics of *Calanus finmarchicus* dormancy patterns in the Northwest Atlantic. *ICES J. Mar. Sci.* **65** (in press).
- Lu, Y., D. G. Wright and I. Yashayaev.** 2007. Modelling hydrographic changes in the Labrador Sea over the past five decades. In *Observing and modelling ocean heat and freshwater budgets and transports*. Edited by I. Yashayaev. *Prog. Oceanogr.* **73**(3-4): 406-426. doi:10.1016/j.pocean.2007.02.007.

Ouellet, P., L. Savard and P. Larouche. 2007. Spring oceanographic conditions and northern shrimp *Pandalus borealis* recruitment success in the north-western Gulf of St. Lawrence. *Mar. Ecol. Prog. Ser.* **339**: 229-241.

Petrie, B. 2007. Does the North Atlantic Oscillation affect hydrographic properties on the Canadian Atlantic continental shelf? *Atmos.-Ocean* **45** (3): 141-151. doi:10.3137/ao.450302.

Yashayaev, I., M. Bersch and H. M. van Aken. 2007. Spreading of the Labrador Sea water to the Irminger and Iceland basins. *Geophys. Res. Lett.* **34**, L10602. doi:10.1029/2006GL028999.

Yashayaev, I., H. M. van Aken, N. P. Holliday and M. Bersch. 2007. Transformation of the Labrador Sea Water in the subpolar North Atlantic. *Geophys. Res. Lett.* **34**, L22605. doi:10.1029/2007GL031812.

Yashayaev, I., and A. Clarke. 2008. Evolution of North Atlantic water masses inferred from Labrador Sea salinity series. *Oceanography* **21**(1) (in press).

Yashayaev, I., N. P. Holliday, M. Bersch and H. M. van Aken. 2008. The history of the Labrador Sea Water: production, spreading, transformation and loss. In *Arctic-subarctic ocean fluxes: defining the role of the Northern Seas in climate*. Edited by R. R. Dickson, J. Meincke and P. Rhines. Springer (in press).

NAFO Research Document Series / Séries de Documents de recherche OPANO

- Colbourne, E. B., J. Craig, C. Fitzpatrick, D. Senciall, P. Stead and W. Bailey.** 2007. An assessment of the physical oceanographic environment on the Newfoundland and Labrador Shelf in NAFO Subareas 2 and 3 during 2006. NAFO SCR Doc. 07/20, Serial No. N5371, 15 pp.
- Hendry, R.M.** 2007. Environmental conditions in the Labrador Sea in 2006. NAFO SCR Doc. 07/46, Serial No. N5398, 8 pp.
- Maillet, G., and E. Colbourne.** 2007. Variations in the Labrador Current transport and zooplankton abundance on the NL Shelf. NAFO SCR Doc. 07/42, Serial No. N5394, 12 pp.
- Maillet, G.L., P. Pepin, S. Fraser, D. Lane and T. Shears.** 2007. Biological oceanographic conditions in NAFO Subareas 2 and 3 on the Newfoundland and Labrador Shelf during 2006. NAFO SCR Doc. 07/15, Serial No. N5362, 11 pp.
- Morgan, M.J., E.B. Colbourne and P.A. Shelton.** 2007. An examination of growth and condition of Div. 3NO cod at different environmental temperatures. NAFO SCR Doc. 07/24, Serial No. N5375, 23 pp.
- Petrie, B., R. G. Pettipas and W. M. Petrie.** 2007. Air temperature, sea ice and sea-surface temperature conditions off Eastern Canada during 2006. NAFO SCR Doc. 07/13, Serial No. N5360, 14 pp.
- Petrie, B., R. G. Pettipas, W. M. Petrie and V. V. Soukhovtsev.** 2007. Physical oceanographic conditions on the Scotian Shelf and in the eastern Gulf of Maine (NAFO areas 4V, W, X) during 2006. NAFO SCR Doc. 07/14, Serial No. N5361, 27 pp.
- Walsh, S. J., and E. Colbourne.** 2007. Investigating the effects of variation in surplus production, stock biomass, catch and climate on the Grand Bank yellowtail flounder population. NAFO SCR Doc. 07/43, Serial No. N5395, 22 pp.

Canadian Science Advisory Secretariat (CSAS) / Secrétariat canadien de consultation scientifique (SCCS)

Research Documents / Documents de recherche

- Colbourne, E. B., J. Craig, C. Fitzpatrick, D. Senciall, P. Stead and W. Bailey.** 2007. An assessment of the physical oceanographic environment on the Newfoundland and Labrador Shelf during 2006. DFO CSAS Res. Doc. 2007/30, 18 pp.
- Galbraith, P.S., D. Gilbert, C. Lafleur, P. Larouche, B. Pettigrew, J. Chassé, R.G. Pettipas and W.M. Petrie.** 2007. Physical oceanographic conditions in the Gulf of St. Lawrence in 2006. DFO CSAS Res. Doc. 2007/024, 56 pp.
- Harrison, G., D. Sameoto, J. Spry, K. Pauley, H. Maass, M. Kennedy, C. Porter and V. Soukhovtsev.** 2007. Optical, chemical and biological oceanographic conditions in the Maritimes region in 2006. DFO CSAS Res. Doc. 2007/050, 52 pp.
- Harvey, M., and L. Devine.** 2007. Oceanographic conditions in the Estuary and the Gulf of St. Lawrence during 2006: zooplankton. DFO CSAS Res. Doc. 2007/049, 36 pp.
- Pepin, P., G.L. Maillet, S. Fraser, D. Lane and T. Shears.** 2007. Biological and chemical oceanographic conditions on the Newfoundland and Labrador Shelf during 2006. DFO CSAS Res. Doc. 2007/042, 47 pp.
- Petrie, B., R. G. Pettipas, W. M. Petrie and V. V. Soukhovtsev.** 2007. Physical oceanographic conditions on the Scotian Shelf and in the Eastern Gulf of Maine during 2006. DFO CSAS Res. Doc 2007/023, 45 pp.

Science Advisory Reports / Rapports d'avis scientifiques

(All advisory reports are available in English and French / Tous les rapports d'avis sont disponibles en français et en anglais)

- DFO (Colbourne, E. B.).** 2007. 2006 State of the ocean: physical oceanographic conditions in the Newfoundland and Labrador Region. DFO CSAS Sci. Advis. Rep. 2007/025, 11 pp.
- DFO (Galbraith, P.S.).** 2007. 2006 State of the ocean: physical oceanographic conditions in the Gulf of St. Lawrence. DFO CSAS Sci. Advis. Rep. 2007/036, 12 pp.
- DFO (Harrison, G.).** 2007. 2006 State of the ocean: chemical and biological oceanographic conditions in the Gulf of Maine - Bay of Fundy and on the Scotian Shelf. DFO CSAS Sci. Advis. Rep. 2007/047, 16 pp.
- DFO (Pepin, P.).** 2007. 2006 State of the ocean: chemical and biological oceanographic conditions in the Newfoundland and Labrador region. DFO CSAS Sci. Advis. Rep. 2007/032, 8 pp.

Others / Autres

- Boessenkool, K. P., I. R. Hall, H. Elderfield and I. Yashayaev.** 2008. Deep ocean flow speed linked to NAO through Labrador Sea convection. PAGES (Past Global Changes) News, January 2008, 16(1): 32-33.
- Colbourne, E. B., M. Stein, M. Ribergaard, R. Hendry, B. Petrie and D. Mountain.** 2007. The 2006 NAFO annual ocean climate

status summary for the Northwest Atlantic. On line at <http://www.nafo.int/science/frames/ecosystem.html>

- Hendry, R.M., H. van Aken and I. Yashayaev.** 2007. Monitoring the ventilation of the Irminger and Labrador Seas. CLIVAR Exchanges, No. 40, pp. 25-27.